EFFECTS OF VITEXIN ON LEAD-INDUCED PREFRONTAL CORTICAL DAMAGE AND BEHAVIOURAL DEFICITS IN YOUNG MICE

AMEDU, NATHANIEL OHIEMI

(13/68LD002)

B.Sc. (MUN), M.Sc. (ILORIN)

A THESIS SUBMITTED TO THE DEPARTMENT OF ANATOMY, FACULTY OF BASIC MEDICAL SCIENCES, COLLEGE OF HEALTH SCIENCES, UNIVERSITY OF ILORIN, ILORIN, NIGERIA,

IN PARTIAL FULFILMENT OF THE REQUIREMENTS FOR THE AWARD OF DOCTOR OF PHILOSOPHY (Ph.D.) DEGREE IN ANATOMY.

JANUARY, 2021

CERTIFICATION

This is to certify that this thesis by AMEDU, Nathaniel Ohiemi (13/68LD002) has been read and approved as meeting the requirements of the Department of Anatomy, University of Ilorin, Ilorin, Nigeria, for the Award of Doctor of Philosophy (Ph.D.) degree in Anatomy.

---------- ----------
Dr. G. O. Omotoso (B.Sc., M.B; B.S., M.Sc., Ph.D.) DATE
(Supervisor)

---------- ----------
Dr. Misturah Y. Adana (M.B; B.S., M.Sc., Ph.D.) DATE
(Departmental Postgraduate Programmes Coordinator)

---------- ----------
Dr. G. O. Omotoso (B.Sc., M.B; B.S., M.Sc., Ph.D.) DATE
(Ag. Head of Department)

---------- ----------
Internal Examiner
DATE

---------- ----------
External Examiner DATE

DEDICATION

This work is dedicated to God and my parents.

DECLARATION

I, AMEDU Nathaniel Ohiemi, hereby declare that this thesis entitled "Effects of Vitexin on Lead-induced Prefrontal Cortical Damage and Behavioural Deficits in Young Mice", submitted by me is based on my actual and original work. Any materials obtained from other sources have been duly acknowledged. In addition, the research has been approved by the University of Ilorin Ethical Review Committee.

---------- ----------

AMEDU, Nathaniel Ohiemi
(13/68LD002)

Date

ACKNOWLEDGEMENTS

My profound gratitude goes to my teacher and supervisor, Dr G. O Omotoso whose valuable contributions, effort, support, understanding and intellectual guidance made this work a huge success. He will always be remembered for his contributions towards the successful completion of this programme.

I sincerely appreciate the Kogi State University Management and the Department of Anatomy, Kogi State University, Anyigba for giving me study leave and financial support needed for this programme. I specially appreciate Dr. A. Ajayi and Dr. O. D Omotoso for their encouragement, concern and assistance towards securing financial support.

My appreciation goes to the lecturers in the Department of Anatomy, University of Ilorin especially Prof. O.B. Akiola, Prof. M.S. Ajao, Dr. B.U Enaibe, Dr. A.O. Oyewopo, Dr. A.S Alabi, Dr. M.Y Adana, Dr. O.J Olajide, Dr. A. Imam, Miss F.S Lewu and Mrs. R. Jaji-Sulaimon for their contributions, intellectual stimulation and presence during my presentations.

In addition, I must not forget to thank the entire laboratory staff of the Central Research Laboratory and Diagnostic Centre, Tanke, Ilorin particularly; Dr. N. Emeka, Mr. I.T Gbadamosi, and Mr L. Arietarhire for explaining some biochemical laboratory procedures to me during the study.

Very importantly, my gratitude and sincere appreciation goes to my lovely parents Elder James and Mrs Sarah Amedu for their encouragement, support and prayers throughout the period of this programme and for guiding me into the path of intellectual pursuit. I specially thank my younger siblings: Emmanuel, Solomon, Christopher and David for their concern and moral support.

Finally**,** Special thanks to my friends: Mr S. Olorunnado, Mr. P. Idoko, Mr. E. Ogbonna, Mr. S. Abba, Mr. J. Momoh, Mr. J.A Adedeji, and Mr. D.E Babatunde.

Amedu, N.O

January, 2021

TABLE OF CONTENTS

LIST OF FIGURES

LIST OF TABLES

ABSTRACT

Lead (Pb) is a neurotoxicant that affects several brain regions including the prefrontal cortex (PFC) regardless of age or gender. Vitexin is a flavonoid that is extracted from plants and exhibits several properties. However, its effect on Pb-intoxicated subjects is unclear. The objectives of this study were to: (i) investigate changes in working memory; (ii) assess Lead concentration in the PFC; (iii) determine changes in oxidative stress markers of the PFC; (iv) evaluate cholinergic activities of the PFC; (v) assess the histomorphological changes of the PFC; and (vi) determine the expression of astrocytes and synaptophysin in the PFC.

Forty-two Balb/c mice of both sexes were divided on postnatal day (P) 21 into seven groups with the following treatment: A (control) normal saline; (B) Pb acetate 100 mg/kg body weight (bwt); (C) Vitexin 1 mg/kg bwt; (D) 100 mg/kg bwt of Pb acetate + 1 mg/kg bwt of Vitexin; (E) 100 mg/kg bwt of Pb acetate + 1 mg/kg bwt of Vitexin; (F) 1 mg/kg bwt of Vitexin 60 minutes before 100 mg/kg bwt of Pb acetate; (G) 1 mg/kg bwt of Vitexin 60 minutes after 100 mg/kg bwt of Pb. Behavioural tests were performed between P61 and P67. On P67, mice were sacrificed and the PFC of the brain was excised and fixed in 4% Paraformaldehyde for histomorphological investigations. Some of the PFC tissues excised were homogenised in 0.25 M sucrose solution. The supernatants obtained were used to test malondialdehyde (MDA), superoxide dismutase (SOD), glutathione peroxidase (GPx), and acetylcholinesterase (AChE) levels using colorimetric technique. Lead was quantified using direct spectrophotometric technique. Astrocytes and synaptophysin expression were assessed using immunohistochemical techniques. Data were analysed using one-way analysis of variance. A significant difference was defined at $P < 0.05$.

The findings of the study were that:

i. vitexin and Pb co-administration significantly ($P < 0.05$) improved working memory (30±2.5 s) when compared to Pb only administration (24±1.0 s);
ii. vitexin and Pb co-administration significantly ($P < 0.05$) lowers the concentration of Pb (4.0±0.36 µg/dl) when compared to Pb only administration (5.6±0.29 µg/dl);
iii. vitexin and Pb co-administration significantly ($P < 0.05$) decreased MDA activity (0.33±0.01 U/mg) and increased SOD (3.3±0.14 U/mg) and GPx (3.4±0.1 U/mg) activities; while Pb only administration significantly increased MDA activity (0.41±0.03 U/mg), and decreased SOD (1.2±0.23 µg/dl) and GPx (1.3±0.1 µg/dl) activities;
iv. vitexin and Pb co-administration significantly ($P < 0.05$) increased AChE level (0.058±0.004 U/mg) when compared to Pb only administration (0.036±0.003 U/mg);
v. vitexin and Pb co-administration prevented histomorphological damage thus leading to a significant ($P < 0.05$) increase in the number of neurons (184±2.3) in layer II-III of the PFC when compared with Pb only administration (85±2.9);
vi. vitexin and Pb co-administration significantly increased the expression of synaptophysin but not astrocytes when compared to Pb only administration.

The study concluded that vitexin protected the PFC from Lead-induced damage through the antioxidative pathway. The study recommended that vitexin be explored further as an agent that protects the PFC from Lead-induced neurodegeneration.

CHAPTER ONE

INTRODUCTION

1.1 Background to the Study

According to the World Health Organisation (2018), about 0.6% global burden of diseases is due to Lead (Pb) poisoning. Similarly, an estimate by the Institute for Health Metrics and Evaluation (IHME) in 2016, shows that Pb toxicity accounted for 540, 000 deaths and 13.9 million years of healthy life lost (disability-adjusted life years). The highest burden of healthy life lost due to Pb toxicity was found in low- and middle-income countries including Nigeria. The IHME also estimated that Pb exposure accounted for 63.8% of the global burden of idiopathic developmental and intellectual disability (WHO, 2018). In Nigeria, Pb exposure accounts for 7 - 25% of disease burden among children per year (Ogunseitan *et al.,* 2007). The disease burden due to Pb toxicity, costs the Nigerian health and education sectors approximately $0.38 – 1.15 billion (Ogunseitan *et al.,* 2007).

The sources and routes of Lead toxicity include inhalation of Lead particles during smelting, recycling, stripping of Lead paint, and gasoline. Lead exposure could also occur through ingestion of Lead-contaminated dust, water (via leaded pipes), food (via lead-glazed or lead-soldered containers) and traditional medicines (Flora *et al.,* 2012; von Stackelberg *et al.,* 2015; Wani *et al.,* 2015; WHO, 2018). Lately, exposure to certain types of unregulated cosmetics through the skin has been mentioned as a lesser route of exposure to Lead (Wani *et al.,* 2015).

In children, the primary source of Pb exposure is via Pb-containing or Pb-coated objects such as toys, pencils, and flakes from decaying Pb-containing paint (Wani *et al.,* 2015). Children are easily exposed due to their innate curiosity and their hand-to-mouth behaviour that frequently results in mouthing and swallowing of Pb contaminated substance (Flora *et al.,* 2012; WHO, 2018). During pregnancy, Pb stored in the bone of the mother overtime is released

into the blood and becomes a source of exposure to the developing foetus (von Stackelberg *et al.,* 2015). In Nigeria, the major sources of Pb exposure in children are Pb-contaminated water, dust from battery recycling and mining sites (Dooyema *et al.,* 2012; Bartrem *et al.,* 2014).

In the body, Pb is distributed to the brain, liver, kidney, and bones (Kim *et al.,* 2015). It accumulates primarily in the teeth and bones, which are sites for long-term storage of Pb (von Stackelberg *et al.*, 2015). As a cumulative toxicant, Pb affects multiple body systems in both humans and animals. It is particularly harmful to children because they absorb 4–5 times as much Pb ingested from any given source than adults (WHO, 2018).

The effect of Pb-induced toxicity on body systems and organs are widespread and varies according to dose of exposure, duration of exposure and other factors. In the brain, the effect of Pb-induced toxicity results in protein modifications, alteration in signalling pathways, enzyme level alterations, morphological changes, neurodegeneration, and behavioural deficits (Flora *et al.,* 2012; Sharma *et al.,* 2015; Wani *et al.,* 2015; von Stackelberg *et al.,* 2015). In children, the toxic effects of Pb is more overwhelming than in adults because of their developmental age which influences pharmacokinetics of Pb. The critical periods of structural and functional development are the greatest time of vulnerability to Pb toxicity in children (Flora *et al.,* 2012). Lead exposure in children results in neurobehavioral effects that persists into adulthood and often may not manifest until a later stage of development (Schwartz *et al.,* 1990; Liu *et al.,* 2013). Also, environmental Lead exposure in childhood affects intellectual function, language, visuospatial skills, motor skills, and mood (Mazumdar *et al.,* 2011; Mason *et al.,* 2014).

Human exposure to Pb is usually assessed through the measurement of blood lead level (BLL) (von Stackelberg *et al.,* 2015) in addition to measurement of hair and urine samples. Earlier human studies showed a connection between blood lead level of ≤7.5 μg/dl to decreased

intelligence and increased risk of cognitive deficits (Lanphear *et al.*, 2005; Jusko *et al.*, 2008; Sharma *et al.*, 2015; Wani *et al.*, 2015). Blood lead level (BLL) of 5 µg/dL once thought to be a "safe level" is now being associated with decreased intelligence, behavioural difficulties, and learning problems (Sobin *et al.*, 2015; WHO, 2018; Rădulescu and Lundgren, 2019). According to general agreement reached by researchers, no level of Pb exposure should be considered safe (Rădulescu and Lundgren, 2019). In view of this agreement and with new evidence, the blood levels at which morbidities occur has been reduced from 10 μg/dl to 2 μg/dl by the Centre for Disease Control (CDC) screening guideline (Rădulescu and Lundgren, 2019).

In order to prevent Pb-induced toxicity, a three-way preliminary strategy that includes: individual intervention, preventive medicine strategy, and public health strategy were suggested (Guidotti and Ragain, 2007). In addition to the preliminary strategies mentioned, nutrition also plays a vital role in the prevention of Pb- induced toxicity. This is because studies have shown that uptake of certain nutrients like mineral elements, vitamins, and flavonoids can offer protection against environmental Pb toxicity (Flora *et al.*, 2012). These nutrients, including flavonoids, have been reported to play a significant part in restoring the imbalance between pro-oxidants and anti-oxidants that arises because of oxidative stress.

Flavonoids have been listed as one of the nutrients that offers protection against Pb-induced toxicity (Flora *et al.*, 2012). Flavonoids are a group of natural secondary metabolites that have variable phenolic structures found in fruits, barks, roots, stems, and flowers of plants (Panche *et al.*, 2016). Flavonoids have been reported to limit neurodegeneration in diverse neurological diseases, including cognitive impairments (Arredondo *et al.*, 2015; Muralidhara, 2015). According to emerging evidence, dietary flavonoids and their metabolites cross the blood-brain barrier to exert multiple neuropharmacological actions, which include modulation of the innate architecture of the brain to impact intellectual function (Muralidhara, 2015). Crucial factors

that are involved in flavonoids being use as neuroprotective agents include; inducing synaptic plasticity, suppression of neuroinflammatory processes, promotion of cerebrovascular perfusion, and activation of adaptive cellular stress responses against oxidative stressors (Arredondo *et al.,* 2015; Muralidhara, 2015).

Vitexin (apigenin-8-C-glucoside) is a flavonoid that is extracted from various plants including pearl millet, hawthorn, pigeon pea, mung bean, mosses, Passiflora, bamboo, mimosa, wheat leaves, and chaste berry (He *et al.,* 2016). The known health benefits of Vitexin are anti-oxidative, anti-tumour, anti-viral, anti-inflammatory, anti-bacterial, anti-hypertensive, anti-nociceptive, anti-spasmodic, anti-diabetic, anti-depressant, neuroprotective and cognitive improving functions (Choi *et al.,* 2014; Hritcu *et al.,* 2017; Lima *et al.,* 2018; Nabavi *et al.,* 2018; Rosa *et al.,* 2016; Yang *et al.,* 2014; Zhu *et al.,* 2016). The contribution of Vitexin to neuroprotection is through counteracting targets that induces neurodegeneration such as redox imbalance, neuroinflammation, and abnormal protein aggregation (Lima *et al.,* 2018).

The mammalian prefrontal cortex (PFC) represents a large mass of frontal lobe of the cerebral cortex. This part comprises mainly the Brodmann area 46 (Afifi and Bergman, 2005). The general function of the PFC is to plan and direct motor, cognitive, affective, and social behaviour as it receives input from other cortical regions (Kolb *et al.,* 2012). Among other specific functions, PFC controls working memory, which refers to the neural functions for temporary storage and manipulation of information (Goldman-Rakic, 1995). The exposure of PFC to different environmental actions and agents such as stimuli, stress, drugs, toxins, hormones, and social experiences during development affect it in different ways (Kolb *et al.,* 2012).

Lesions in the prefrontal cortex can lead to impairment in executive functions like decision-making, prioritization, and planning (Afifi and Bergman, 2005). Injury to the dorsolateral

prefrontal cortex area results in impairment of working (short-term) memory, allocation of attention, and speed of processing. Injury to the ventromedial prefrontal cortex results in severe impairment of decision- making and emotion. Injury to the superior mesial area impacts emotion, motivation, and initiation of behaviour (Afifi and Bergman, 2005).

The PFC receives information about all sensory modalities as well as motivational and emotional states through its interconnections with association cortices of other lobes and with the hypothalamus, medial thalamus, and amygdala (Afifi and Bergman, 2005). Human PFC is more complicated in function than in simpler mammals such as rodents. However, in each mammalian order, there are standard functions that are required of PFC regardless of complexity (Kolb *et al.,* 2012). Early experiences changes PFC circuitry and behaviour in laboratory animals, such as rodents. These experiences are likely to have even more significant effects in a more complex PFC.

The nervous system in human begins development three weeks after fertilization; however, maturation of the cerebral cortex is not completed until after birth (Kolb *et al.,* 2012). The reason is that the development of the nervous system takes place via the interaction of several processes; some of them are completed before birth, while others continue into adulthood. For instance, the proliferation and migration of cells mostly occur during foetal development, while the formation of neuronal circuits, elimination of synapses, and other developments occur postnatally till adulthood (Tsujimoto, 2008).

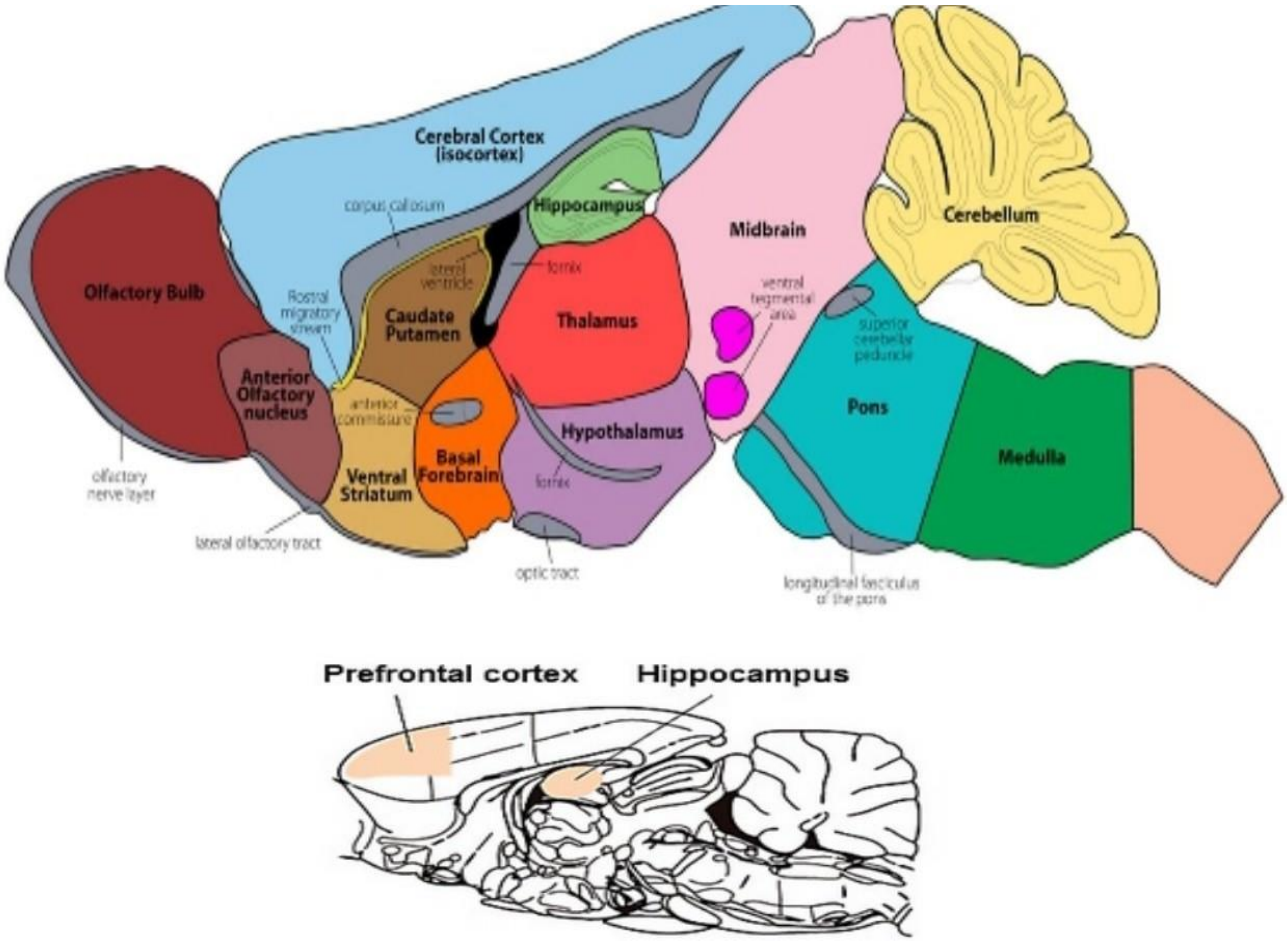

Figure 1.1: Schematic diagram of mouse brain with the location of the prefrontal cortex (Satsix, 2010)

Two critical features of cerebral development that are involve in modification of cortical organization are; Overproduction of dendritic spine, (Petanjek *et al.*, 2011) and the reversal of the over-produced spine starting from late childhood (puberty) until completion in the third decade of life (Kolb *et al.*, 2012). The overproduction of spines is highest in the PFC, which also has the slowest rate of synapse elimination (Elston *et al.*, 2009). This extraordinarily long period of synapse elimination in the PFC has implications on adult cognitive capacity (Petanjek *et al.*, 2011). The peak of synaptic density in humans is reached between 10 to 12 years of age, depending on the region of the cortex. The reason is because the synaptic density of the posterior region of the cerebral cortex peak sooner than the anterior (Kolb *et al.*, 2012).

Earlier argument pinpoints the period between early childhood to kindergarten as the time in which the PFC forms the underlying neural circuitry that will later underlie higher cognitive functions (Tsujimoto, 2008). The intellectual capacity in humans is not only region-specific but also changes with structural development from childhood through adolescence. For example, individuals with superior intelligence have a thinner PFC in early childhood, but the thickness of the PFC of these subjects increases rapidly with age, peaking at age 13. Also, in children, the variance in IQ measure is counted by the volumetric measure of the PFC while in adults, both density and thickness of the gray matter of the PFC significantly correlate with general intelligence (Tsujimoto, 2008).

Earlier paragraphs describe developmental events in the human cerebral cortex, including the PFC, the basic principles remain the same for other mammals, including common laboratory animals like mice. However, the timeline of mouse brain development is different from human (Table 1.1).

Table 1.1: Comparative timeline of brain development between rodents and human

Developmental milestones	Rodents	Human
Gestation (days)	18-21	270
The brain reaches 90–95% of adult weight.	Postnatal day 20-21	2–3 year old
Oligodendrocyte maturation state changes	Postnatal day 1–3	23–32 wk gestation
Establishment of the blood-brain barrier	Postnatal day 1–3	23–32 wk gestation
Peak brain growth spurt	Postnatal day 7-10	36–40 wk gestation
Peak in gliogenesis.	Postnatal day 7-10	36–40 wk gestation
Increasing axonal and dendritic density	Postnatal day 7-10	36–40 wk gestation
Peak in myelination rate.	Postnatal day 20-21	2–3 year old
Fractionation/specialization of prefrontal cortex neural networks (structural maturation)	Postnatal day 25–35	4–11 year old
Maximum volume of grey matter and cortical thickness.	Postnatal day 25–35	4–11 year old
Reduced synapse density, reaching a plateau at adult levels.	Postnatal day 35–49	12–18 year old
Refinement of cognitive-dependent circuitry.	Postnatal day 35–49	12–18 year old
Ongoing myelination, increasing white matter volume, and fractional anisotropy.		
Adult levels of synaptic density.	Postnatal day 60+	20 years +
Ongoing myelination and declining grey matter.	Postnatal day 60+	20 years +
Adult levels of neurotransmitters.	Postnatal day 60+	20 years +

Source: Semple *et al.*, 2013

The development of PFC is prone to various influences. Some of the well-established factors that affect PFC development include sensory or motor stimulation, stress, parent-infant relationship (including parental deprivation), and peer relationship. Other factors are exposure to heavy metals (such as Pb), infection, psychoactive drugs, and adult stimulants (Kolb *et al.*, 2012).

1.2 Rationale of the Study

Although some vitamins, flavonoids, and other natural products have been reported to have neuroprotective abilities against Pb-induced neurotoxicity, none has so far reported the role vitexin could play (either ameliorative or deteriorative) in Pb-induced behavioural deficits as well as degenerative changes seen in the cytoarchitecture of the prefrontal cortex. Also, none has so far reported sex-dependent actions of vitexin on working memory following acute Pb administration. More data is still needed on the toxic effect of Pb on the developing brain, particularly on the morphometric analysis of layers II and III of the prefrontal cortex that have been linked to higher cognitive functions. Furthermore, the mechanism of action utilized by both Pb and vitexin, needs to be further examined.

1.3 Aim of the Study

The aim of the study was to investigate the effect of acute Vitexin intervention against lead-induced neurotoxicity and cytoarchitectural changes in the prefrontal cortex of young mice.

1.4 Objectives of the Study

The specific objectives of the study were:

i. to investigate the effect of Vitexin on working memory, anxiety, depression, and motor behaviours in young mice before, during and after Pb- induced neurotoxicity;
ii. to assess blood lead level and some haematological components using haematological techniques after the administration of Pb and Vitexin;

iii. to determine the effect of Vitexin on the oxidative stress markers, acetylcholinesterase, Na^+/K^+ ATPase, and nitric oxide in the prefrontal cortex before, during and after Pb-induced neurotoxicity using biochemical techniques;

iv. to assess the role of Vitexin intervention on neuronal and histomorphological changes in the prefrontal cortex of young mice exposed to Pb, using routine histological, histochemical and immunohistochemical stains;

v. to carry out morphometric analysis of neuronal cells in layer 2/3 of the PFC following Pb and Vitexin administration using morphometric techniques.

1.5 Research questions

Can Vitexin intervention prevent lead-induced behavioural deficits and histomorphological changes in the prefrontal cortex of young mice? Can antioxidant activity of Vitexin prevent or ameliorate oxidative stress caused by Pb in mice? Does Vitexin have effect on blood as well as blood lead level in mice?

1.6 Hypothesis

Vitexin administration will prevent and ameliorate lead-induced neurotoxicity and histomorphological changes in the prefrontal cortex of young mice.

1.7 Significance of the Study

This study will provide additional knowledge on Vitexin that could lead to its adoption as a cheap, potent and natural therapy for the prevention or treatment of lead-induced neurotoxicity that causes intellectual disability in the future. It will provide basic information about sex-specific intellectual disability behaviours following Pb and Vitexin administration. Furthermore, the study will add to the existing body of knowledge on Pb-induced neurotoxicity in mice.

1.8 Scope of the Study

The study was strictly an *in vivo* study that involves the use of mice as the model of the study. The study was also limited to:

i. morphological study of the body, brain and PFC weight;
ii. analysis of blood Pb level and some selected haematological components;
iii. histomorphological analysis of the PFC using routine histological, histochemical and immunohistochemical stains that are relevant to the study;
iv. oxidative stress markers and some biochemical markers;
v. behavioural tests for working memory, motor, anxiety, and depression.

1.9 Limitation of the Study

This study could not demonstrate electrophysiological techniques that would have provided insights into electrical properties involved in higher intellectual functions, anxiety, and depression in mice exposed to Pb and Vitexin treatment due to financial constrain.

Secondly, this study could not demonstrate genetic analysis that would have provided insights into the level of expression of genes associated with intellectual functions, anxiety, and depression in mice exposed to Pb and Vitexin treatment.

CHAPTER TWO

LITERATURE REVIEW

2.1 Chemistry of Lead

Lead is a bluish-grey coloured heavy metal that is extracted from the earth's crust in form of ores (Abadin *et al.*, 2007). The chemical symbol of Lead is "Pb" while its atomic number and standard atomic weight are 82 and 207.2, respectively (Meija *et al.*, 2016). Lead is soft and malleable; also, it has a melting point of 327.46 °C and a boiling point of 1749 °C. Other physical properties of Pb are 11.34 g/cm^3 density; 4.77 kJ/mol heat of fusion; 179.5 kJ/mol heat of vapourisation; and 26.650 J/(mol·K) molar heat capacity (Abadin et al., 2007). Pb exists mainly in two oxidative states (which are +4 and +2). Pb^{2+} exists mainly in an ordinary environment, while Pb^{4+} is found under exceptional oxidizing conditions and in inorganic form. Although its occurrence is rare, metallic Pb exists at oxidation state 0 in nature (Abadin *et al.*, 2007).

2.1.1 Chemistry of Lead Acetate

Lead acetate [$Pb(CH_3COO)_2$], otherwise known as lead (II) acetate, lead diacetate, lead sugar, salt of Saturn, or Goulard's powder, is a white crystalline chemical compound with a sweet taste. Lead acetate is soluble in water and glycerol, and it is toxic (Abadin *et al.*, 2007). In the presence of water, lead acetate forms trihydrate [$Pb(CH_3COO)_2 \cdot 3H_2O$]. Lead acetate is white and solid in a physical state. It has a molecular weight of 325.28g, a density of 3.25 g/cm^3 at 20°C, and slightly acetic odour. Lead acetate has a pH range of 5.5-6.7 and melt at 75°C (Abadin *et al.*, 2007).

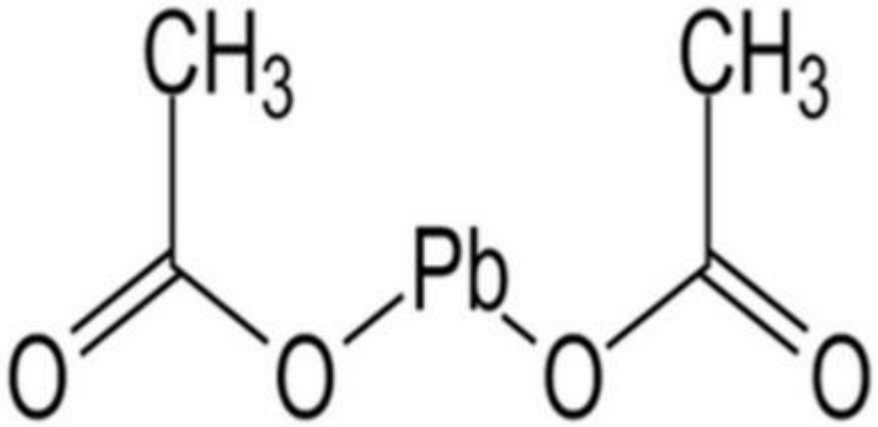

Figure 2.1: Chemical structure of lead acetate (Kabeer et al., 2019)

2.2 Uses of Lead

Lead acetate is used in cosmetics, for hair colouring, it is also use for medical purposes such as remedy for sore nipples and as treatment for poisonous ivy. In industries, Lead is used in the manufacture of several products such as paints, textile, mordants, firearms, ammunition, cable covers, ceramics, plastics, pipes, batteries, pigments, pencils, and toys (Flora *et al.,* 2012).

2.3 Pharmacokinetics of Lead

The common routes and sources of Pb exposure are through ingestion of lead-contaminated dust, water (via lead pipes), food (via lead-glazed or lead-soldered containers) and traditional medicines. Others are through inhalation of lead particles during smelting, recycling, stripping of lead paint, and gasoline (Flora *et al.,* 2012; von Stackelberg *et al.,* 2015). A lesser route of lead exposure is through the skin (dermal) via the use of lead contaminated cosmetics or injured skin (Wani *et al.,* 2015). Skin route of exposure account for about 1% of lead exposure (Kabeer *et al.,* 2019). During pregnancy, Pb stored in the bone of the mother overtime is released into the blood and becomes a source of exposure to the developing foetus (von Stackelberg *et al.,* 2015). Most of the lead absorbed through ingestion is accumulated in the blood and soft tissues. However chronic lead exposure is accumulated in bones and teeth overtime (von Stackelberg

et al., 2015; WHO, 2018). According to Rădulescu and Lundgren (2019), bones and teeth account for nearly 95% of lead in adult tissues, and nearly 70% in children. The lead accumulated in adult bone can replace Pb excreted, even long after exposure has ended because of slower turnover of Pb in adult bone.

The efficacy of Pb absorption via ingestion is dependent on food intake before exposure, since food consumption decreases absorption of water-soluble Pb and interactions with other elements in the diet (Rădulescu and Lundgren, 2019). Similarly, the effectiveness of absorption of water-soluble Pb is age-dependent, and substantially higher in children (4-5 times) than in adults (von Stackelberg *et al.,* 2015; WHO, 2018; Rădulescu and Lundgren, 2019). In rats, Pb absorption decrease substantially with increasing dose (Aungst *et al.,* 1981).

The distribution of Pb to organs such as the brain, kidney, liver, spleen, bones, and teeth is predominantly through blood plasma, which accounts for 1% of total blood lead level (Flora *et al.,* 2012). The systemic blood flow and soluble phosphate are important factors that promote lead distribution throughout the entire body (Sanders *et al.,* 2009). The estimated half-life of Pb in adult blood is shorter (30-40 days) when compared with those of children and pregnant women (Sanders *et al.,* 2009; Kabeer *et al.,* 2019). Due to poor metabolism of Pb in the body, excretion is low and often through the urine via the urinary tract. However, smaller quantities of Pb are excreted through sweat, saliva, fingernails, hair and gastrointestinal tract (Sanders *et al.,* 2009; Rădulescu and Lundgren, 2019).

In mice, plasma Pb clearance is faster in lactating mice when compared with non-lactating mice. Maternal milk is an extra route of Pb excretion in mice accounting for nearly 1/3 of the administered dose of plasma Pb excreted (Hallen *et al.,* 1996).

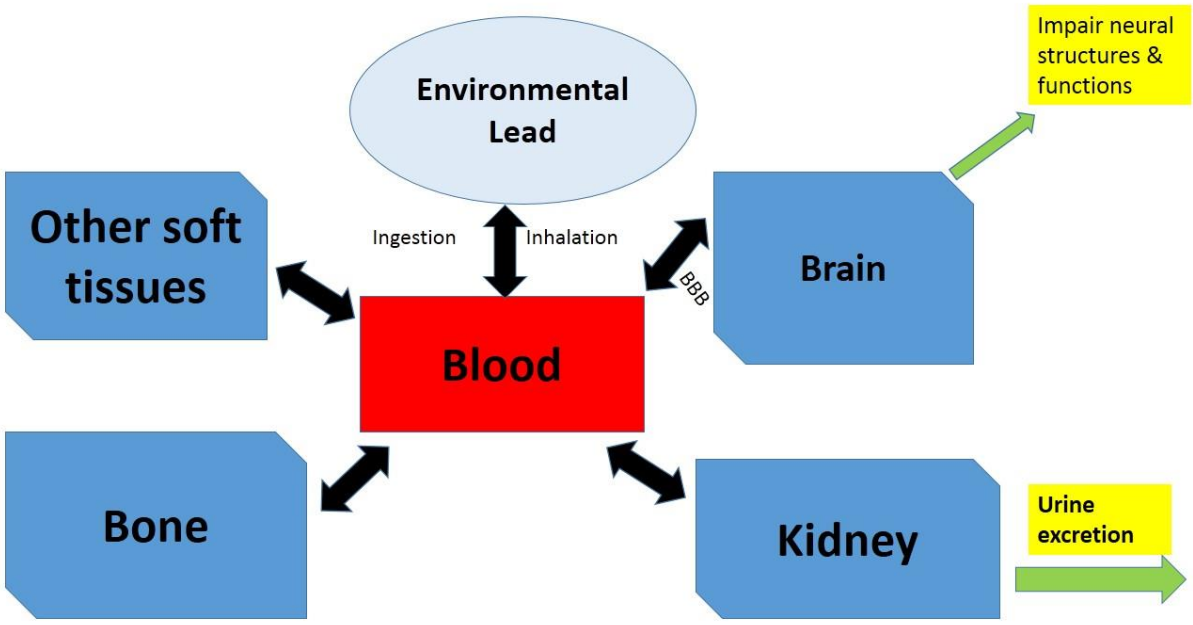

Figure 2.2: Illustrative diagram of Lead distribution in mammals

2.4 Mechanisms of Lead-induced neurotoxicity

The key aspects involved in Pb-induced neurotoxicity are oxidative stress, membrane bio-physics alterations, deregulation of cell signalling, and the impairment of neurotransmission (Sanders *et al.,* 2009). The ability of Pb to substitute for other polyvalent cations (such as Ca^{2+}) is one of the key mechanisms underlying its neurotoxicity. In the case of neurological deficits, after replacing calcium ions, Pb becomes competent to cross the blood-brain barrier (BBB) at an appreciable rate (Karri *et al.,* 2016). In the brain, Pb causes excessive generation of pro-oxidants (such as hydroperoxides, hydrogen peroxide, and single oxygen) and depletion of anti-oxidant reserves (such as superoxide dismutase, catalase, glutathione, glutathione peroxidase) (Flora *et al.,* 2012). The oxidative imbalance created between pro-oxidant and anti-oxidant reserves, eventually results in oxidative damage, which in turn disrupts neuronal signalling, neurotransmitter release and neurobehavioural deficits (von Stackelberg *et al.*, 2015). Enzymes like glutathione, which has functional sulfhydryl group binds with Pb and renders them inactive, thereby causing further impairment in oxidative balance. (Sanders *et al.*, 2009).

Another mechanism used by Pb^{2+} to potentiate its neurotoxic feature is by displacing Ca^{2+} bound to calmodulin (CaM) and activating calmodulin. The activation of calmodulin by Pb^{2+} results in protein phosphorylation altering cAMP messenger pathways; calcium homeostasis, and the multiplicity of calcium-mediated processes intrinsic to regular cellular activity (Schneider and Lidsky, 2003). Pb^{2+} activates protein kinase C (PKC), an important neurotransmitter that regulates long term neural excitation and learning memory. The activation of PKC induces genes that regulate the formation of the AP-1 transcriptional regulatory complex, this activation disrupts signalling mechanisms and cause impairment of memory (Nava-Ruiz *et al.*, 2012).

2.5 Lethal dose of Lead

The lethal dose (LD50), is a common dose estimate for toxicity test at which 50% of the group of test organisms (rat, mouse, or other species) are expected to die from derived maximum dose of the test substance. The acute oral toxicity (LD50) of Pb acetate in young rabbits is 1240 mg/kg body weight (Ahul *et al.,* 2018). The oral LD50 of Pb acetate in rats is 400 mg/kg body weight (Ashraf *et al.,* 2017) while intraperitoneal injection (i.p) in rats is 215 mg/kg body weight (Saxena *et al.,* 1984).

2.6 Pharmacodynamics of Lead

2.6.1 Effect of Lead on blood brain barrier

The blood brain barrier (BBB) is a physiological barrier formed by components of vascular, immune, metabolic and neural tissues to control the movement of ions, molecules, and cells between the blood and the brain (Daneman and Prat, 2015). Physically, astrocytes together with the cerebral micro-vascular endothelium, pericytes, neurons, and the extracellular matrix constitute a blood-brain-barrier (Sander *et al.,* 2009). The tendency of Pb to traverse the blood-brain barrier is due largely to its ability to substitute for calcium ions (Sander *et al.,* 2009). Also, the ability of Pb to mimic or mobilize calcium and PKC may well alter the behaviour of endothelial cells in the immature brain and disrupt the BBB (Goldstein, 1993). In the blood brain barrier of rats, Pb accumulation on the plasmalemma of the endotheliocyte endosurface could damage the close junctions and allow Pb between endotheliocytes (Ruan and Gu, 1999). According to Struzynska *et al.* (1997) lead also induces BBB dysfunction when administered in low doses in rats.

2.6.2 Effect of Lead on memory, anxiety, depression and motor behaviour in animal model

An investigation into the effect of co-exposure of lead, manganese and stress during early development in rats showed increase in anxiety level, reduced open-field activity and impaired

learning ability following Pb exposure (Sprowles *et al,* 2018). A study carried out to evaluate lead-induced memory disorder in adult Wistar rats by Moosavirad *et al.* (2016) revealed significant decline in learning and memory triggered by Pb acetate administration. Thangarajan *et al.* (2018) revealed that Pb acetate intoxication resulted in motor deficit and memory impairment. Furthermore, Zhai *et al.* (2018) revealed that Pb toxicity in mice resulted in learning and memory impairments.

Stangle *et al.,* (2007) designed an experiment to answer questions on early life exposure to Pb and treatment with succimer in a rat model. It was found that Pb exposure created long-term impairments in learning, attention, inhibitory control, and arousal regulation in rats. In a follow-up study to investigate the effect of Pb exposure at low level dose during prenatal and early postnatal period in rats, it was revealed that Pb triggered impaired memory retention in rats which persists into adulthood (Barkur *et al.,* 2011). The long-term consequences of early chronic Pb exposure on neuronal activity in male and female mice at low (30 ppm) and high (330 ppm) doses showed that the ventral hippocampus-medial prefrontal cortex (vHPC-mPFC) synapses are crucial for working memory in rodents (Tena *et al.,* 2019).

Lead exposure reduces locomotor and exploratory activities in rats after 50 mg/kg treatment for five days via intraperitoneal injection (Reckziegel *et al.,* 2011). The exposure of adult rats to 0.15% Pb acetate from gestational day 6 till the end of weaning significantly perturb locomotor activity and exploratory behaviour in rats (Chintapanti *et al.,* 2018). Flores-Montoya and Sobin (2015) investigated the effect of chronic low-level Pb on the exploratory activity (using unbaited nose poke task), exploratory ambulation (using open-field task), and motor coordination (using rotarod task) in pre-adolescent mice. It was found that increased blood Pb level predicted decrease in exploratory activity but did not affect open-field behaviour. Similarly, Flores-Montoya *et al.,* (2015) examined the sensitivity of a novel odour recognition

task (NODR) in pre-adolescent C57BL/6J mice chronically exposed to Pb acetate from birth until postnatal day 28. It was observed that higher blood Pb level increased olfactory recognition and decreased memory activity in male mice. In female mice this observation was made at lower but not at higher levels of Pb exposure.

Anderson *et al.,* (2016) assessed low-level Pb exposure on associative learning and memory in rats with influence of sex and developing time. It was revealed that irrespective of sex, developmental period, or level of Pb exposure, the rats acquired conditioned-unconditioned stimulus association during training. Furthermore, female rats (early and late postnatal period) exposure to Pb considerably impaired recall. On the other hand, male rats exposed to Pb during perinatal period had significant recall deficits.

An investigation to determine whether Pb exposure during pregnancy or lactation are related to depressive and anxiety- like symptoms in adult rats was done by Souza *et al.* (2005). It was observed that male rats displayed increased anxiety-like behaviour while female rats displayed depressive-like behaviour due to Pb exposure during pregnancy and lactation. Similarly, Soeiro *et al.* (2007) reported that 500 ppm of Pb induced anxiogenic effect in male mice while 50 and 500 ppm induced anti-depressant-like effect in both male and female mice. Their study investigated the effect of sub chronic Pb exposure on anxiety, depression, and aggressiveness in male and female Swiss mice from weaning (postnatal day 21) to adulthood (postnatal day 91 day).

In a study to assess the effect of Pb poisoning and antidepressant drug on the cerebral cortex of Wistar rats, Highab (2018) reported significant increase in the duration of immobility of rats in forced swim test (depression) for groups that received 100 mg/kg and 200 mg/kg of Pb acetate (for one week) when compared with the depressed control group. Additionally, rat activities in the open field test (OFT) were reduced as a result of Pb exposure. According to

Sansar *et al.* (2011), Pb acetate (0.5%) administration via drinking water (for three months) results in decrease locomotor activity.

2.6.3 Effect of Lead on blood parameters in animal model

Exposure of rats to 50 mg/kg of Pb for five days via intraperitoneal administration reduced blood delta-aminolevulinic acid dehydratase (ALA-D) activity (Reckziegel *et al.,* 2011). Acute Pb exposure gives rise to significant inhibition of delta-aminolevulinic acid dehydratase activity in the blood, and significantly reduce blood haemoglobin as well as red blood cells in rats (Flora *et al.,* 2007). Katavolos *et al.* (2007) evaluated haematologic and biochemical changes associated with blood Pb concentrations and found that platelet cell volume, haemoglobin concentration, and mean corpuscular haemoglobin concentration **(**MCHC) decreased significantly with increasing blood Pb concentration in avian species.

2.6.4 Effect of Lead on neuroimmune system in animal model

Sobin *et al.,* (2013) examined neuroimmune system of C57BL/6J mice exposed to low, high, or no Pb conditions from birth to postnatal day 28. Sobin *et al.,* (2013) observed that only interleukin-6 (IL6) was different between the groups, and the observation was dose-dependent. It was concluded that early chronic exposure to Pb disrupts microglia through damage, loss, or lack of proliferation of microglia in the developing brain of mice.

2.6.5 Effects of Lead on oxidative stress in animal model

The possible link between alterations in Pb acetate-induced oxidative damage and cognitive impairment in male C57BL/6 mice was investigated and found that Pb induces oxidative stress and decreased cortical antioxidant biomarkers (Zhang *et al.,* 2017). Similarly, Chintapanti *et al.,* (2018) observed that Pb acetate exposure from gestation day 6 till the end of weaning decreased antioxidant enzymes in the hippocampus, cerebrum, cerebellum, and medulla of the exposed rats. The assessment of oxidative stress in the hippocampus, cerebellum, and frontal

cortex of rat pups exposed to 0.2% Pb acetate during specific periods of early brain development revealed maximum oxidative stress during lactation and postnatal day 30 (Barkur and Bairy, 2015).

2.6.5.1 Malondialdehyde as a marker of oxidative stress

Malondialdehyde (MDA) is one of the end products of lipid peroxidation and a widely recognized oxidative stress marker (Ayala *et al.*, 2014, Tang *et al.*, 2019). Assessment of oxidative stress parameters in Pb occupationally exposed workers revealed unchanged malondialdehyde level suggesting that short-term exposure to lead will not affect malondialdehyde (Dobrakowski *et al.*, 2017). An investigation to determine whether Pb acetate could induce oxidative stress in mice, showed that, Pb acetate (100mg/kg body weight) significantly increased the levels of reactive oxygen species, malondialdehyde, and severely damage deoxyribonucleic acid (Xu *et al.*, 2008). Zhai *et al.* (2018) reported that Pb toxicity in mice triggered increase in malondialdehyde level of tissues and blood along with oxidative stress.

Gottipolu and Davuljigari (2014) examined Pb-induced oxidative stress in the cerebellum and hippocampus of rats' brain at postnatal day (PND) 21, 28, 35, and 60. It was revealed that malondialdehyde (MDA) level was increased in the cerebellum and hippocampus of Pb-exposed rats. This observation was more noticeable on postnatal day 35 than in other postnatal days. According to Reckziegel *et al.* (2011), brain lipid peroxidation and protein carbonyl levels were increased following Pb exposure. Similarly, Chintapanti *et al.* (2018) observed that 0.15% Pb acetate exposure in rats from gestation day 6 till the end of weaning period, increased the level of lipid peroxidation. When rats were exposed to 300 mg/kg body weight of Pb, there was significant increase in lipid peroxidation in the brain tissues (Antonio-García *et al.*, 2008).

2.6.5.2 Superoxide dismutase as an anti-oxidant marker of oxidative stress

Superoxide dismutase (SOD) is a first-line defence antioxidant enzyme that dismutate superoxide radicals into harmless molecules (Ighodaro and Akinloye, 2017). Acute Pb exposure promotes significant reduction in superoxide dismutase (SOD) in rats brain (Flora *et al.,* 2007). Assessment of oxidative stress parameters in short-term Pb exposed workers revealed unchanged superoxide dismutase level (Dobrakowski *et al.,* 2017). Similarly, in rat model of Pb-induced toxicity, antioxidants including SOD activity were not different from the control group following 300 mg/kg of Pb administration (Antonio-García *et al.*, 2008).

Early life exposure to Pb induces alterations in the mitochondrial antioxidant system of brain regions, which persist long after Pb exposure has stopped (Gottipolu and Davuljigari, 2014). In a study to examine Pb-induced oxidative stress in the cerebellum and hippocampus on postnatal day (PND) 21, 28, 35, and 60 in rats, it was observed that superoxide dismutase activity was generally reduced. This observation was more noticeable on postnatal day 35 than in other postnatal days (Gottipolu and Davuljigari, 2014). Similarly, assessment of Pb induced toxicity in mice revealed a decrease in superoxide dismutase activity in tissues of the brain and blood. (Zhai *et al.,* 2018).

2.6.5.3 Glutathione peroxidase as an anti-oxidant marker of oxidative stress

Glutathione peroxidase (GPx) is one of the first-line defence antioxidant enzyme that catalyses the reduction of hydrogen peroxide to water and oxygen as well as conversion of peroxide radicals to alcohol and oxygen (Ighodaro and Akinloye, 2017). Assessment of Pb-induced oxidative stress in the cerebellum and hippocampus of the brain on postnatal day (PND) 21, 28, 35, and 60 in rats, revealed reduction in glutathione peroxidase activity. The observation was more evident on postnatal day 35 (Gottipolu and Davuljigari, 2014).

According to Chintapanti *et al.* (2018), administration of Pb acetate (0.15%) from gestation day 6 until rats are wean, decreased glutathione activity level in the hippocampus, cerebrum, cerebellum, and medulla of rats brain.

2.6.5.4 Catalase as an anti-oxidant marker of oxidative stress

Catalase is an anti-oxidant enzyme that catalyzes the conversion of hydrogen peroxide to water and oxygen (Ighodaro and Akinloye, 2017). An assessment of oxidative stress in short-term Pb occupationally exposed workers revealed unaffected catalase level (Dobrakowski *et al.*, 2017). In rats, Pb-induced toxicity gives rise to decrease in catalase activity in the cerebellum and hippocampus of the brain on postnatal day (PND) 21, 28, 35, and 60 (Gottipolu and Davuljigari, 2014). Assessment of Pb induced toxicity in mice revealed a decrease in catalase activity in the tissues of the brain and blood. (Zhai *et al.*, 2018). In Pb-pretreated Swiss mice, the brain catalase activity showed significant reduction (Correa *et al.*, 2004).

2.6.6 Effect of Lead on acetylcholinesterase in animal model

Chintapanti *et al.* (2018) revealed that, Pb acetate (0.15 %) administration from perinatal till the end of weaning, reduced acetylcholinesterase activity in the hippocampus, cerebrum, cerebellum, and medulla of rats. The combination of Pb treatment and natural antioxidants during pregnancy and lactation in rat significantly decrease (35%) acetylcholinesterase activity.

2.6.7 Effect of Lead on synaptophysin in animal model

Early-life exposure to Pb alters synaptic proteins in mice hippocampus and significantly decrease synaptophysin expression and neuronal nitric oxide synthase (nNOS). Furthermore, Yu *et al.* (2016) concluded that alteration of synaptic proteins in the hippocampus due to Pb exposure in early life could play an important role in subsequent intellectual impairments in later ages.

2.6.8 Effect of Lead on Nitric oxide in animal model

Nitric oxide (NO) is a biological messenger known to be involved in brain development. The effect of Pb on NO production is manifested via the inhibition of the nitric oxide synthase (NOS) activity (Chetty *et al.,* 2001). Heydari *et al.* (2006) investigated the short-term (4 and 8 weeks) and sub chronic (12 weeks) effects of Pb treatment on the responsiveness of the vascular adrenergic system and the level of nitric oxide metabolites using male Sprague-Dawley rats. It was found that short-term Pb administration resulted in a significant reduction in serum nitric oxide levels while the sub chronic Pb administration reversed the trend.

2.6.9 Effect of Lead on brain histomorphology in animal models

Assessment of different Pb acetate doses (0, 50, 100, 150 or 200 mg/kg), time intervals, and mice strains showed deleterious dose-dependent effects on brain weight (Correa *et al.,* 2004). In an experiment to investigate the ultra-structural effects of Pb toxicity on rat brain, it was observed that cortical neurons were degenerated. Additionally, vascularization of cells, haemorrhage and degeneration of mitochondria as well as electron-dense inclusion bodies were discovered (Deveci, 2006). Mahmoud and Sayed (2016) investigated the histological changes in the cerebral cortex, hippocampus, and cerebellum of adult albino mice exposed to Pb acetate (20 and 40 mg/kg for seven days). It was discovered that Pb acetate caused disorganization of cell layers, neuronal loss, and degeneration as well as neuropil vacuolization.

According to Highab *et al.* (2018), seven days of Pb acetate administration (100 mg/kg and 200 mg/kg body weight), initiated degeneration of cortical pyramidal cells. Furthermore, pyknotic nuclei, neuronal chromatolysis, and reduction in stain intensity of some neuronal cells were observed. Similarly, a study to investigate the impact of Pb toxicity (25, 50 and l00 mg/kg i.p 7 days) on different intermediates of apoptotic signaling pathway in rats, revealed

significant increase in caspase 8 expression, Bax level, as well as Bax/Bcl-2 ratio at low dose (Ahmed *et al.,* 2013).

Lead acetate- induced toxicity, resulted in significant loss of neurons in the cortex, cerebellum, and hippocampus of rats. It also alters Bax/Bcl-2 expression, and increases cytochrome c release from the mitochondria (Thangarajan *et al.,* 2018). Barkur and Bairy (2016) revealed that, administration of Pb acetate (0.2%) during different periods of early brain development initiated significant damage to neurons of the hippocampus, amygdala, and cerebellum. It was concluded that the postnatal period of brain development was more vulnerable to Pb neurotoxicity compared to the prenatal period of brain development.

Assessment of glial and dopaminergic systems in adult male Wistar rats exposed to Pb acetate (0.5%) showed hypertrophic immunoreactive astrocytes in the frontal cortex, and other brain structures of Pb-treated animals. Furthermore, there was increased number of astrocyte cell bodies and processes in Pb-treated rats. It was concluded that prolonged Pb exposure induces astroglial changes that can compromise neuronal function and, subsequently, animal behaviour (Sansar *et al.*, 2011).

A study was done to investigate the effect of maternal Pb exposure on the expression of interleukin (IL) - 1β, IL- 6, and glial fibrillary acidic protein (GFAP) in the hippocampus of mice offspring. The result revealed increase expression of IL-1β, IL-6, and GFAP in Pb-exposed mice (Li *et al.*, 2015). Sobin *et al.* (2013) discovered that early life (from birth to postnatal day 28) chronic exposure to Pb, perturbed microglia cells via damage, loss, or lack of proliferation of microglia cells in developing brain.

Sun *et al.* (2014) investigated the morphological changes and amyloid precursor protein (APP) accumulation in the hippocampus of adult rats following Pb acetate exposure. It was observed

that mitochondrial degeneration, apoptosis, and abnormal synapses occurred in rats exposed to Pb. Furthermore, APP was increased significantly in the hippocampus of Pb- exposed rats.

2.6.10 Factors underlying sex-related differences in response to lead exposure

Structural, neurochemical, and neuroendocrinological differences in the brain are the underlying causes of sex differences associated with Pb -exposed outcome (Kokras and Dalla, 2014). The mammalian sexually dimorphic brain is influenced by self-regulating actions or interactions among, sex chromosomes, gonadal hormones, and epigenetic factors. Interaction of Pb with all these factors, as well as the mechanisms linking these variables, could differ considerably between the two sexes. These variables could result in sex bias in neurobehavioral or disease susceptibility caused by Pb exposure (Singh *et al.*, 2018).

2.7 Vitexin

Vitexin is a flavonoid that is extracted from various plants including pearl millet, hawthorn, pigeon pea, mung bean, mosses, Passiflora, bamboo, mimosa, wheat leaves, and chaste berry (He *et al.*, 2016). The known health benefits of Vitexin are anti-oxidative anti-tumor, anti-viral, anti-inflammatory, anti-bacterial, anti-hypertensive, anti-nociceptive, anti-spasmodic, anti-diabetic, anti-depressant, neuroprotective and cognitive improving functions (Choi *et al.*, 2014; Yang *et al.*, 2014; ; Rosa *et al.*, 2016; Zhu *et al.*, 2016; Hritcu *et al.*, 2017; Lima *et al.*, 2018; Nabavi *et al.*, 2018). The contribution of Vitexin to neuroprotection is through counteracting targets that induces neurodegeneration, such as redox imbalance, neuroinflammation, and abnormal protein aggregation (Lima *et al.*, 2018).

2.7.1 Properties of Vitexin

Vitexin is light yellow powder in appearance with chemical formula "$C_{21}H_{20}O_{10}$" and a molecular weight of 432.38 g/mol. It has a melting point of 203 - 204 °C and a boiling point of 1496.39 K. The critical pressure and critical volume of Vitexin are 45.16 Bar and 1033.5 cm^3/mol respectively (He *et al.*, 2016). The summary of the properties of Vitexin is shown in Table 2.1.

Table 2.1: Properties of Vitexin

Chemical formula	$C_{21}H_{20}O_{10}$
Molecular weight	**432.38 g/mol**
Appearance	**Light yellow powder**
Melting point	**203 to 204 °C**
Boiling point	**1496.39 K**
Critical Pressure	**45.16 Bar**
Critical volume	**1033.5 cm^3/mol**

Source: He *et al.* (2016)

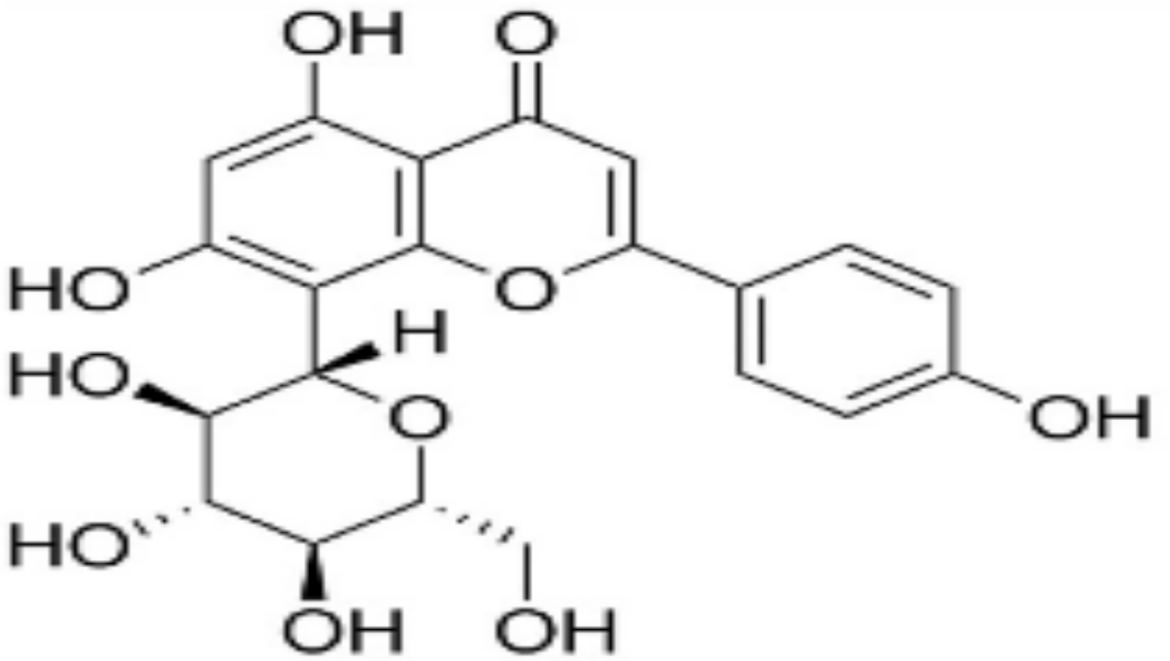

Figure 2.3: Chemical structure of Vitexin (He *et al.*, 2016)

2.7.2 Mechanism of action of Vitexin

Vitexin has seven hydroxyls that contributes to its bioactivity. In addition, Vitexin has o-di-hydroxyl structure in the ring (He *et al.*, 2016). These properties have proven to be potent contributor to its productive radical scavenging potential (He *et al.*, 2016). Vitexin inactivates and neutralizes reactive oxygen species (ROS) by high reactivity of the hydroxyl group against the reactive compound of the radical. In other words, the mechanisms of antioxidant action of Vitexin are through scavenging ROS and up-regulation of antioxidant defences of cells (Kumar and Pandey, 2013).

2.7.3 Pharmacokinetics of Vitexin

Vitexin can be administered intravenously, intraperitoneally, intramuscularly, and orally. When administered orally, Vitexin reaches the gastrointestinal tract, in the presence of gut microflora it is hydrolysed through deglycosylation and ring-opening of the heterocyclic C ring (He *et al.*, 2016). The product of this deglycosylation is aglycone, which undergo further cleavage and conversion resulting in the formation of 3-(4-hydroxyphenyl) propionic acid before absorption into the bloodstream (Panche *et al.*, 2016).

When Vitexin is administered intravenously, intraperitoneally or intramuscularly, it is absorbed rapidly into the blood serum and plasma with binding percentage of 97±3% and 85% respectively (He *et al.*, 2016). The rate and half-life of distribution, absorption, and elimination of vitexin administered orally is slower when compared with other routes of administration (He *et al.*, 2016). It also varies according to other factors such as body size and administered dose. After absorption, Vitexin is rapidly and widely distributed into various tissues including the brain where it enters through the blood brain barrier (Yin *et al.*, 2014). Although the exact mechanism used to transport Vitexin across the blood brain barrier is unclear, it is speculated that it uses polycyclic aromatic hydrocarbon (PAH) transporter or organic anion Transporter-

3 (Faria *et al.,* 2012). The half-life of elimination for orally administered Vitexin at 50 mg/kg in rats is $t_{1/2}$ = 6.37 (Yan *et al.,* 2013). The lethal dose 25 of Vitexin in mice via intraperitoneal injection is 1 mg/kg (Prabhakar *et al.,* 1981).

2.7.4 Pharmacodynamics of Vitexin

2.7.4.1 Effect of Vitexin on brain weight

In their bid to investigate the antioxidant effects of orientin and vitexin in D-galactose-aged mice, An *et al.* (2012) discovered that administration of Vitexin (8 weeks) at high, medium, and low doses significantly reduced brain weight when compared with the control. However, when Vitexin was compared with the model- aged mice group, there was a significant increase in brain weight.

2.7.4.2 Effect of Vitexin on learning and memory

Nurdiana *et al.* (2018) carried out a study to determine changes in behaviour, gyrification patterns, and brain oxidative stress markers in streptozotocin (STZ)-induced diabetic rats using *F. deltoidea* and vitexin treatments. It was observed that *F. deltoidea* extract and vitexin attenuated learning and memory impairment in diabetic rats, together with several clusters of improved gyrification.

The effect of Vitexin on scopolamine-induced memory impairment in rats was investigated by Abbasi *et al.* (2013). It was observed during retention tests that Vitexin (100 mM) without scopolamine significantly increased the step-through latencies compared to scopolamine. Furthermore, Vitexin (100 mM) significantly reversed the shorter step-through latencies caused by scopolamine. It was suggested that Vitexin has a potential role in enhancing memory retrieval through modulation of cholinergic receptors or other mechanisms.

In a bid to identify the flavonoids present in the stem bark extract of *Erythrina falcata* and to assess the effect of these flavonoids on conditioned fear memory, Oliveira *et al.* (2014) revealed that Vitexin found in *Erythrina falcata* improved the acquisition (retention) of fear memory but did not prevent the extinction of fear memory in rats.

2.7.4.3 Antioxidant effects of Vitexin

Nurdiana *et al.* (2018) reported that Vitexin treatments (oral) for eight weeks resulted in a significant increase in the superoxide dismutase (SOD) and glutathione peroxidase (GPX) values, in addition to a significant reduction of thiobarbituric acid reactive substances (TBARS). Similarly, An *et al.* (2012) observed that, Vitexin administration (20 mg/kg for eight weeks via intragastric) resulted in a rise of total antioxidant capacity, SOD, catalase, and GPx levels in the serum. Vitexin also increased the levels of SOD, catalase, GPx, Na^+/K^+ATP enzyme, and Ca^{2+}/Mg^{2+}ATP enzyme in the liver, kidneys, and brain (An *et al.,* 2012).

Furthermore, Lyu *et al.* (2018) reported that Vitexin pretreatment significantly caused a decrease in MDA level and increased SOD and GPx activities in sevoflurane-induced newborn rats. Malar *et al.* (2018) also found out that Vitexin inhibited the production of free radicals, and suppressed ROS mediated lipid peroxidation, protein oxidation, and loss of membrane potential. In the same study that involves neuroprotective activity of Vitexin against Abeta 25-35 induced toxicity in Neuro-2a cells, Vitexin modulated the expression of genes involved in antioxidant response mechanisms (Nrf-2, HO-1).

2.7.4.4 Vitexin as an Anti-depressant Agent

Naturally, isolated flavonoids such as Vitexin display an enormous number of biological activities, including antidepressant-like behavior (Guan and Liu, 2016; Hritcu *et al.,* 2017). In their bid to investigate the putative effect of Vitexin on the central nervous system, Can *et al.,* (2013) observed that Vitexin administration (10-30 mg/kg) significantly reduced immobility

time of the mice in both the tail-suspension and modified forced swim tests. Vitexin mediates antidepressant effect by increasing the catecholamine levels in the synaptic cleft as well as interactions with the serotonergic 5-HT_{1A}, noradrenergic α_2, and dopaminergic D_1, D_2, and D_3 receptors (Can *et al.*, 2013). Another possible mechanism of action of flavonoids including Vitexin as an antidepressant agent is via suppression of oxidative- nitroxative stress (Hritcu *et al.*, 2017). Additional mechanisms used by flavonoids to prevent advancement of depression include: prevention of mitochondrial membrane potential dissipation, agonizing GABA-benzodiazepine receptors interaction with κ-opioid receptors and kynurenine pathway (KP). Others are acetylcholinesterase activity regulation, maintaining brain plasticity, inhibition of L-arginine-NO, extracellular signal-related kinase (ERK) 1/2 and AKT phosphorylation pathways. Others include, modulation of intracellular calcium overload and K^+ channels; downregulation of cytochrome C (Cyt-C), Bax, caspases 3 and 9 expressions, in addition to upregulation of Bcl protein expression (Hritcu *et al.*, 2017).

2.7.4.5 Vitexin as an anxiolytic agent

Soulimani *et al.* (1997) assessed the effect of Lyophilised hydroalcoholic and aqueous extracts of Vitexin and other components of *Passiflora incarnata L.* (Passion-flower) on mice behaviour. At 400 mg/kg, the hydroalcoholic extract displayed anxiolytic characteristics in mice through the use of staircase test and light/dark box test. In contrast, 400 mg/kg of the aqueous extract showed sedative properties in mice through a decrease in steps climbed by the mice in the staircase test, and a decrease in locomotion in the free exploratory test.

2.7.4.6 Influence of Vitexin on motor activity

In the process of determining the ability of Vitexin to ameliorate the signs of nicotine sensitization in rats, Bedell *et al.* (2019) discovered that Vitexin (30 or 60 mg/kg) administration 30 minutes before nicotine (0.4 mg/kg), exhibited a level of locomotor activity

that is comparable to the vehicle-treated controls. It was suggested that Vitexin antagonizes the expression of nicotine locomotor sensitization in rats.

2.7.4.7 Anti-epilepsy action of Vitexin

Aseervatham *et al.* (2016) evaluated the effect of vitexin (10 mg/kg) and chlorogenic acid (CA) (5 mg/kg) on pilocarpine-induced (85 mg/kg) epileptic mice. The i.p administration of pilocarpine (85mg/kg) induced seizures in mice that were assessed by behavioural tests. Vitexin and CA significantly reduced the seizure. Additionally, Vitexin and CA selectively inhibited NMDAR, mGluR1, and mGlu5 expression. It was concluded that Vitexin and CA exerted antiepileptic and neuroprotective activity via the mechanism that involves suppressing glutamate receptors.

2.7.4.8 Effect of Vitexin on Alzheimer's disease

In an in vitro assay to determine anti-Alzheimer's disease potential of apigenin, vitexin and isovitexin using inhibitory activity against cholinesterases (both AChE and BChE) and BACE enzymes, Choi *et al.* (2014) found out that Vitexin showed slightly weaker inhibitory activity against AChE when compared to isovitexin. Vitexin also showed intense BChE inhibitory activity which was almost similar to isovitexin group. Furthermore, Choi *et al.* (2014) reported that vitexin exhibited weak inhibitory activity against BACE. It was concluded that apigenin, Vitexin, and isovitexin showed anti-Alzheimer's disease activities. Malar *et al.,* (2018) studied the neuroprotective activity of vitexin against Abeta 25-35 induced toxicity in Neuro-2a cells. It was found that Vitexin significantly inhibited the aggregation of Abeta 25-35. Pre-treatment of Neuro-2a cells with vitexin (50mM) before Abeta 25-35 toxicity significantly restored the cell viability when compared with only Abeta 25-35 treatment. It was suggested that vitexin gives neuroprotection to the Neuro-2a cells partly through augmenting the antioxidant mechanisms, maintaining lipid homeostasis and inhibiting apoptosis induced by Abeta

2.7.4.9 Effect of Vitexin on Parkinson's disease

Hu *et al.* (2018) investigated the neuroprotective effect of Vitexin on Parkinson's disease (PD) in *in vivo* (mice) and *in vitro* (SH-SY5Ycells) models. Hu *et al.* (2018) discovered from the pole and traction tests that Vitexin pretreatment prevented bradykinesia and improved the initial lesions caused by MPTP (1-methyl-4-phenyl-1,2,3,6-tetrahydropyridine) in mice PD model. It was further observed that Vitexin boosted the activation of PI3K and Akt as well as suppressed the ratio of Bax/Bcl-2 and caspase-3 activity in MPTP-treated mice. In *in vitro* model, Vitexin significantly improved parameters that were downregulated by MPP^+ treatment in SH-SY5Y cells, including phosphorylation of PI3K and Akt. It was concluded that Vitexin protected dopaminergic neurons against MPP^+/MPTP-induced neurotoxicity through the activation of the PI3K/Akt signaling pathway.

2.7.4.10 Influence of Vitexin against neuronal injury and apoptosis

An investigation into the protective effect of Vitexin against sevoflurane-induced neuronal apoptosis and the mechanisms underlying the protective effect in rats was done by Lyu *et al.* (2018). It was observed that pretreating with Vitexin significantly reduced neuronal apoptosis and inhibited caspase-3 activity, and BAX protein expression in sevoflurane-induced newborn rats. It was further revealed that treatment with Vitexin induced hypoxia-inducible factor 1α subunit (HIF-1α) and vascular endothelial growth factor (VEGF) protein expression. In addition, Vitexin curbed phosphorylated-p38 MAP kinase (p38) protein expression in the sevoflurane-induced newborn rats. The underlying mechanisms involved in their report were HIF-1α-, VEGF- and p38-associated signaling pathways.

Yang *et al.* (2014) investigated the neuroprotective effects of Vitexin on glutamate-induced excitotoxicity using primary cultured cortical neurons treated with N-methyl-D-aspartate receptor (NMDA). It was observed that pretreatment with Vitexin significantly prevented

NMDA-induced neuronal cell loss and reduced the number of apoptotic neurons. Also, pretreating with Vitexin reversed the up-regulation of NR2B-containing NMDA receptors and the intracellular Ca^{2+} overload caused by NMDA exposure. Furthermore, Vitexin significantly prevented neuronal apoptosis induced by NMDA exposure by regulating the balance between Bcl-2 and Bax expression as well as the cleavage of poly (ADP-ribose) polymerase and pro-caspase 3. It was concluded that Vitexin neuroprotective effects are through inhibiting the activities of NR2B-containing NMDA receptors and reducing the calcium influx in cultured cortical neurons.

Pre-treatment with Vitexin could suppress a pro-apoptotic signaling pathway in hypoxic-ischemic neuronal injury in neonates by inhibiting phosphorylation of Ca^{2+}/Calmodulin-dependent protein kinase II (Min *et al.,* 2017).

2.7.4.11 Anti-inflammatory action of Vitexin

Rosa *et al.* (2016) investigated cellular and molecular mechanisms that are involved in the acute anti-inflammatory effect of Vitexin with regards to neutrophil recruitment and macrophages activation using *in vivo* and *in vitro* techniques. Vitexin was found to effectively reduce leukocyte migration *in vivo* at all doses tested. It also reduced TNF-α, IL-1β, and NO releases in the peritoneal cavity of LPS-challenged mice. Furthermore, Vitexin was found to have regulated transcriptional factors for pro-inflammatory mediators, reducing the expression of p-p38, p-ERK1/2, and p-JNK in LPS-elicited cells. It was concluded that inhibition of neutrophil migration and pro-inflammatory mediators released, contributed to the anti-inflammatory activity of Vitexin. Similarly, Jiang *et al.* (2018) reported that vitexin mitigated the secretion of pro-inflammatory cytokine interleukin (IL)-6; tumor necrosis factor-alpha (TNF-α); and increased anti-inflammatory cytokine (IL-10) production to ameliorate middle cerebral artery occluded (MCAO)-induced inflammation.

2.7.4.12 Anti-nociceptive action of Vitexin

Zhu *et al.* (2016) studied the anti-nociceptive effects of Vitexin in a mouse model of postoperative pain. Interaction between vitexin and acetaminophen was examined using the Isobolographical analysis method. The results showed that acute Vitexin administration (3–10 mg/kg, i.p.) in a dose-dependent manner relieved hyperalgesia from 1 to 3 days when compared to 4 days in a mechanical hyperalgesia model. The pre-treatment of vitexin before surgery had no preventive value. It was concluded that Vitexin utilises behaviour-specific anti-nociception against postoperative pain through opioid receptors and GABA A receptors.

2.7.4.13 Influence of Vitexin on stroke

Jiang *et al.,* (2018) explored the role of Vitexin (2 mg/Kg i.v) in middle cerebral artery occlusion (MCAO)-induced ischemic stroke in rats. It was found that Vitexin significantly decreased the MCAO-induced brain infarction. Vitexin also reversed the abnormal protein levels of Caspase-3, Bcl-2-associated X protein (Bax), antigen identified by a monoclonal antibody (Ki-67), and B cell lymphoma 2 (Bcl-2) in MCAO model rats. Jiang *et al.* (2018) further revealed that vitexin improved MCAO-induced oxidative injury by reducing the levels of lactate dehydrogenase (LDH), malondialdehyde (MDA) and nitric oxide (NO). It was concluded that Vitexin suppresses autophagy dysfunction and attenuates MCAO-induced cerebral ischemic stroke through the mTOR/Ulk1 pathway.

2.7.4.14 Effect of Vitexin on hypoxia-ischaemia brain injury

Min *et al.,* (2015) tested their hypothesis, which states that treatment with Vitexin would protect against hypoxia-ischaemia (HI) brain injury in newborn rat pups when subjected to unilateral carotid artery ligation and 2.5 h of hypoxia (8% O2 at 37 °C). Min *et al.* (2015) observed that Vitexin, administered 5 min after hypoxia-ischaemia, showed neuroprotection by decreasing infarct volume that was assessed at 48 h post-hypoxia-ischaemia. However,

Vitexin administered 3 h after hypoxia-ischaemia showed no neuroprotection as neuronal cell death, blood-brain barrier (BBB) integrity, brain edema, HIF-1α, and VEGF protein levels were assessed. At 45 mg/kg, Vitexin ameliorated brain edema, BBB disruption, and neuronal cell death. Min *et al.* (2015) also evaluated the long-term effects of Vitexin on brain atrophy and neurobehavioral tests. It was discovered that Vitexin protected the brain against ipsilateral loss and improved neurobehavioral outcomes. Min *et al.* (2015) concluded that early use of Vitexin will inhibit HIF-1α and provide acute to long-term neuroprotection in the developing brain after neonatal hypoxia-ischaemia injury.

Similarly, Min *et al.* (2017) suggested that pretreatment with Vitexin could suppress a pro-apoptotic signaling pathway in hypoxic-ischemic neuronal injury in neonates by inhibiting phosphorylation of Ca^{2+}/Calmodulin-dependent protein kinase II. Furthermore, Vitexin pretreatment reduced brain infarct volume (in a dose-dependent manner) and reduced the number of TUNEL-positive cells as well as brain atrophy. Min *et al.* (2017) revealed that pretreatment with Vitexin increased the Bcl-2/Bax protein ratio, decreased phosphorylation of Ca^{2+}/Calmodulin-dependent protein kinase II, NF-κB, and cleaved caspase-3 protein expression 24 hours after injury.

2.8 The prefrontal cortex

The prefrontal cortex (PFC) occupies 29% of the cerebral cortex in humans, and it participates in several higher cognitive functions, such as thinking, reasoning, planning, and decision-making (Funahashi, 2017). It is because of this that the prefrontal cortex is believed to be an essential brain area for examining the origin of human intelligence and creativity. In comparison with other association cortices, the prefrontal cortex takes a longer time to mature (Fuster, 2008). The PFC is not one homogeneous cortical region, but a combination of

structural and functional distinct prefrontal areas in rodents and other phylogenetic species including human (Schubert *et al.*, 2015).

2.8.1 Functional anatomy and connections of the prefrontal cortex of mouse brain

The basis of anatomical features of mouse PFC can be divided into the dorsomedial PFC, ventro-medial PFC, and orbitofrontal PFC (Franklin and Chudasama, 2012).

2.8.1.1 The dorsomedial prefrontal cortex of mouse

The dorsomedial PFC comprises the dorsal anterior cingulate (Cg1) and the secondary motor area (M2). In mice, the anatomical division of the dorsal anterior cingulate cortex has not been systematically explored (Van De Werd *et al.*, 2010; Franklin and Chudasama, 2012; Van De Werd and Uylings, 2014; Schubert *et al.*, 2015). The dorsomedial PFC receives afferent input from sensory and parietal regions of the cortex. These afferents enable the dorsomedial PFC to respond to conditions that require immediate attention and respond with appropriate actions. It also receives afferents from the posterior agranular insular region, the retrosplenial cortex, as well as the ventral tegmental dopamine neurons (Van De Werd *et al.*, 2010; Franklin and Chudasama, 2012). There are also inputs from multisensory afferents to M2 dorsally, and limbic afferents to the ventral extent of the dorsal anterior cingulate. Together, M2 and the dorsal anterior cingulate projects to the motor cortex and dorsolateral striatum (Franklin and Chudasama, 2012). Lesions in mouse dorsal anterior cingulate reduces behavioural responses (such as licking, flinching), noxious stimuli, pain-induced behaviour, and social behaviours.

2.8.1.2 The ventromedial prefrontal cortex of mouse

The ventromedial prefrontal cortex comprises prelimbic (PrL) and infralimbic (IL) cortex, which are deeply interconnected. The ventromedial PFC has widespread connections with the amygdala, temporal lobe, and the anterior, medial, and ventral regions of the striatum (Van De Werd *et al.*, 2010; Franklin and Chudasama, 2012; Van De Werd and Uylings, 2014; Schubert

et al., 2015). It also has connections with the perirhinal, entorhinal and piriform cortex in addition to prominent afferent input from the CA1 field of the hippocampus and adjacent subiculum.

The infralimbic (IL) cortex is involve in modulating affective and autonomic functions. The IL cortex distributes efferent to the parabrachial nucleus, the lateral preoptic areas, central nucleus of the amygdala, the shell of the nucleus accumbens, and the posterior hypothalamus. The PrL sends few efferent projections mainly to the cognitive or limbic structures such as the striatum, the basolateral nucleus of the amygdala, the core of the nucleus accumbens, the orbitofrontal cortex and the raphe nuclei of the brainstem (Van De Werd *et al.*, 2010; Franklin and Chudasama, 2012). Lesions of the ventromedial PFC (including PrL and IL) in mice leads to emotional and cognitive disturbances (especially disturbances in incentive learning and working) (Franklin and Chudasama, 2012; Van De Werd and Uylings, 2014).

2.8.1.3 The orbitofrontal cortex of mouse

The orbitofrontal cortex (OFC) in mice, lies on the ventral half of the medial cortical surface near the tip of the frontal pole of the cerebral hemisphere (Schubert *et al.*, 2015). Laterally it extends to the dorsal part of the rhinal sulcus and caudal to where the frontal pole and olfactory peduncle unite. The medial orbital (MO) area lies rostral to the prelimbic (PrL) cortex on the medial wall. Additionally, OFC includes the dorsal and ventral agranular insular areas, which lie on the lateral surface of the brain above the rhinal fissure (Franklin and Chudasama, 2012; Van De Werd and Uylings, 2014).

The OFC region receives sensory afferents from M2 (secondary motor area), parietal cortex, the perirhinal cortex as well as the secondary visual area. The OFC has a reciprocal connection with the basolateral nucleus of the amygdala and also directs outputs to the motor system through the striatum. The efferent projections of the OFC are to the nucleus accumbens

(Franklin and Chudasama, 2012). Due to OFC connections with the limbic structures, it is believed to be involved in affective and motivational aspects of behaviour. In rodents, including mice, lesion to the OFC leads to inflexible and inappropriate response to reversal learning tasks (Franklin and Chudasama, 2012).

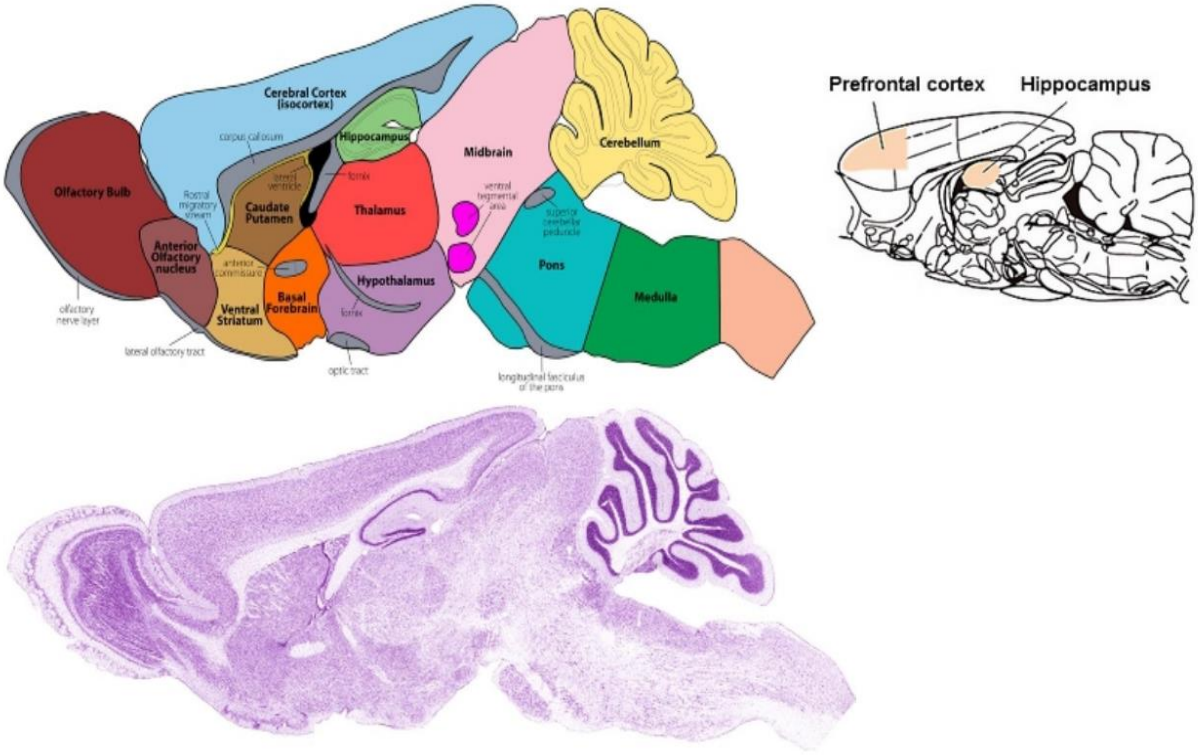

Figure 2.4: Schematic diagrams of the mouse brain in sagittal view (Satsix, 2010)

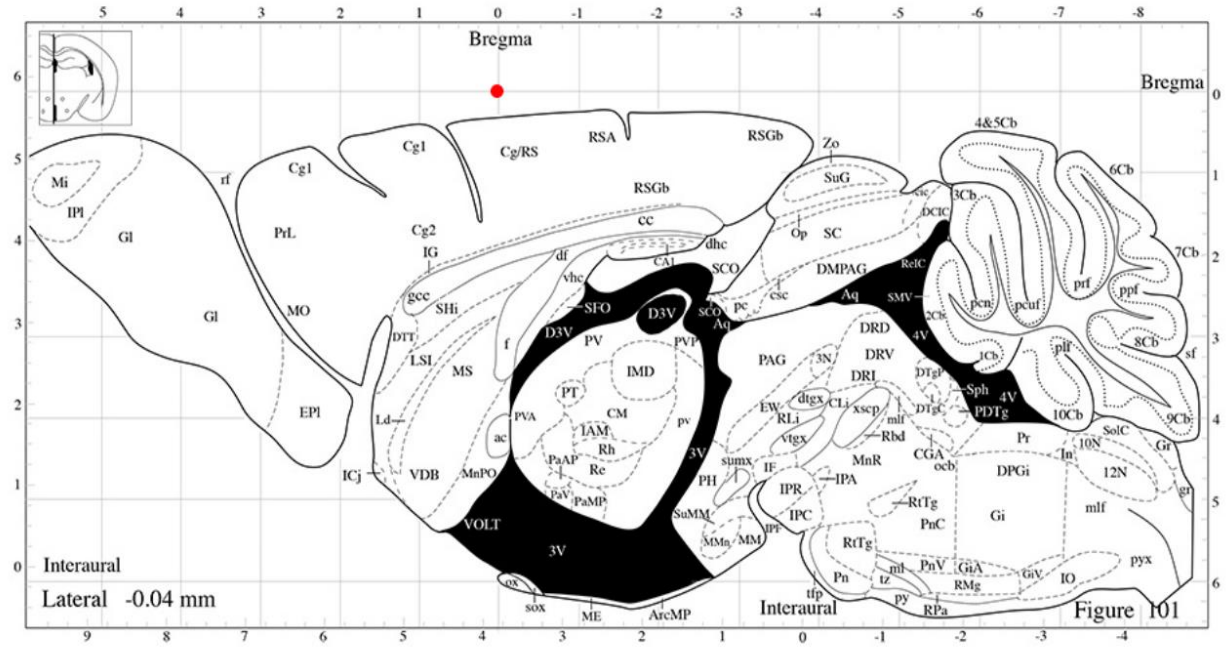

Figure 2.5: Sagittal view of mouse brain in stereotaxic coordinates (Paxinos and Franklin, 2007)

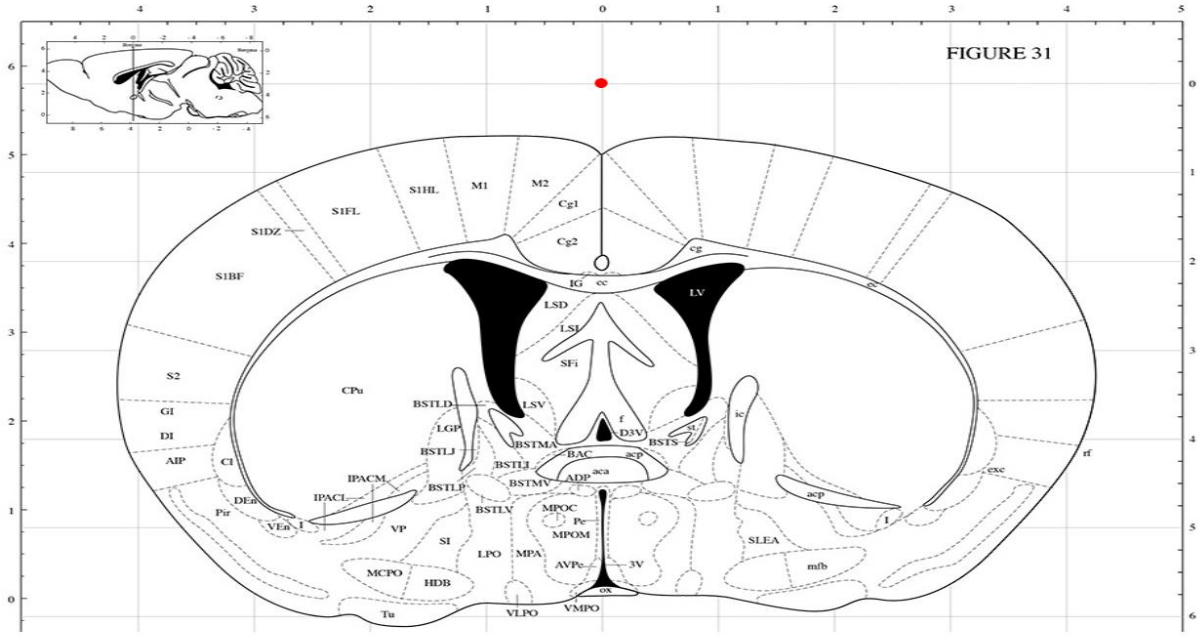

Figure 2.6: Coronal view of mouse brain in stereotaxic coordinates (Paxinos and Franklin, 2007)

2.8.2 Molecular basis of prefrontal cortical development in rodents

Rodents have proven to be excellent model in the study of genes involved in the development of the prefrontal cortex (PFC). Different genes have be identified as key participants in the induction of prefrontal cortical boundaries, intrinsic patterning, proliferation and migration of neurons (pyramidal) of the PFC. Furthermore, some genes have also been associated with migration of GABAergic interneurons towards the PFC, axon guidance, target selection, synapse formation and PFC connectivity formation (Schubert *et al.*, 2015). Table 2.2, shows genes involve in the PFC development in rodents.

2.8.3 Postnatal development of rodent prefrontal cortex

On postnatal day 1 (PND 1), four laminae can be distinguished in the developing cortex. The future layer I is relatively thin. The cortical plate (CP), comprising of radially oriented, undifferentiated cells, is located underneath this future layer I. In the PFC, the cortical plate is considerably thinner than in the dorsolateral cortex. The remaining part of the cortex, deep to the cortical plate, at this age is formed from the subplate layer. The subplate contains fewer cells and many relatively mature neurons than the cortical plate, along with many migrating neurons. The undifferentiated cells in the cortical plate are characterized by their radial orientation and pale, round nuclei with little cytoplasm. At the end of the first week, all cortical layers except layers II and III had been formed (Van Eden and Uylings, 1985; van Eden *et al.*, 1990).

Table 2.2: Genes associated with prefrontal cortical development

Gene	Role in PFC development
Induction of prefrontal boundaries	
FGF17	Fgf17 is secreted by the rostral patterning centre (RSC) and is involved in the induction of prefrontal boundaries
SHH	Shh is secreted by the VSC and regulates the expression of Fgf8, which is involved in the induction of prefrontal
Proliferation and migration of PFC neurons	
FGF2	Fgf2 has an important role in the production of glutamatergic pyramidal neurons in the (pre)frontal cortex.
FGFR1	Fgfr1 is required for the proper number of glutamatergic pyramidal neurons in the frontal cortex.
FGFR2	Fgfr2 is involved in generating excitatory glutamatergic neurons in the mPFC.
Migration of GABAergic interneurons into the PFC	
DLX2	Dlx2 controls interneurons migration toward frontal forebrain.
GAD1	Gad1 regulates the migration of GABA-ergic interneurons to the PFC.
Axon guidance, target selection and synapse formation of PFC neurons	
ERBB4	Erbb4 regulates dendritic spine formation and density of PV+ interneurons in the PFC.
EIF4E	*Eif4e* has a role in synaptic function, dendritic spine density and synaptic plasticity of PFC neurons.
FMR1	*Fmr1* functions in synaptogenesis of dendritic spines of PFC neurons
GRID1	Grid1 has a role in synaptogenesis of PFC neurons.
NRP2	Nrp2 is involved in regulating axon guidance of PFC neurons.
RELN	Reln is involved in regulating spine density and network formation.
MECP2	MeCP2 plays a critical role in the regulation of GABAergic transmission and cortical excitability of PFC pyramidal.
PFC connectivity	
DCC	DCC influences the prefrontal maturation and network formation with the dopaminergic midbrain.
DISC1	Disc1 KD is associated with dendritic abnormalities and affected cAMP signalling and hampers the mesocortical dopaminergic network formation.
CDK5/P35	knockout mice display improper mesolimbic circuitry of the PFC.
MAPT	Mutations in MAPT are associated with altered functional connectivity in the human PFC.
SEMA6A	Loss of *Sema6a* causes prefrontal loss of connectivity.
5-HTT	5-HTT is involved in proper raphe-prefrontal network formation.

Source: Schubert *et al.*, 2015

On PND 6, the primordial granular layer IV could be seen at the deepest part of the cortical plate in the dorsolateral cortex. The presence of the future layer IV gives the cortical plate a trilaminar appearance in this part of the cortex. In the PFC, the cortical plate has a bilaminar appearance. This bilaminar appearance, enables a proper distinction to be made between the future PFC and the dorsolateral cortex for the first time. The cells of the future layers II and III have not yet entirely differentiated at this time within the medial PFC, but within the cortical plate, an upper cortical plate can be identified by densely packed immature cells, and a lower cortical plate with fewer immature cells. While layer V at this time remain underdeveloped, layers VIa and b, are now more advanced in their development (Van Eden and Uylings, 1985).

Starting from PND 6 until PND 10, the development of the PFC is characterised by the maturation of the superficial layers II and III. On PND10, the cells in the cortical plate have matured, and layers II and III can be identified. Also, layer V of the medial PFC at this time has further differentiated. Beginning from PND10, the adult cytoarchitectonic pattern of the different subareas of the PFC can progressively be recognised (Van Eden and Uylings, 1985; van Eden *et al.,* 1990).

On PND 14, layer II and layer III are more distinct and have developed most of the regional characteristics that are found in adult cortex. In the medial PFC, layer V is still comparatively thin, while layer VIa is comparatively broad. Starting from PND 14 until PND 18, the middle and upper sublayers of layer V reach their adult appearance in the medial PFC (Van Eden and Uylings, 1985). The cortical layers in all subareas of the medial PFC reach the same comparative thickness as in adult PFC on PND 24.

Beginning from PND 18 until PND 30, the laminar pattern of the PFC does not have significant change (Van Eden and Uylings, 1985). Commencing from PND 30 until PND 90, the

developing PFC in rodents is characterise by gradual distribution of cells over the entire width of the cortex, rendering the lamination less noticeable (Van Eden and Uylings, 1985).

The development of the prelimbic area of the PFC on PND 6 is characterise by trilamination of the primordium of layer V. Initially (on PND 6), densely packed large cells occupy the upper sublayer of layer V but on PND 10, these cells occupy the entire width of layer V, and the trilaminar character changes into adult-like appearance. The lower sublayer of layer V cannot be distinguished on PND 10, however the first indication of trilaminar formation in layer VIa is visible at this age (Van Eden and Uylings, 1985).

The transition from the dorsal anterior cingulate area to the prelimbic area as observed on PND 6, is characterised by a change in the appearance of the future layer V, which is more homogeneous in the dorsal anterior cingulate area than the prelimbic area. The distinct lower sublayer is absent and the large, darkly staining, pyramid-like cell somata are distributed throughout the layer. The relative width of the cortical layers between PND 6 and 10 remained the same in this region (Van Eden and Uylings, 1985; van Eden *et al.,* 1990). As development progresses (on PND 10), the homogenous nature of layer V of the dorsal anterior cingulate area disappear. In place of homogeneity of this layer, the cells become more densely packed in the margin than in the rest of the layer, where fewer pyramidal cell somata are found. Layer VIa at this age, remain homogeneous and separate from layer VIb by a thin strip that lack cells.

On PND 14, layer III is less dense in the prelimbic area than in the dorsal anterior cingulate area. The deeper sublayer of layer V is less dense than the central sublayer, while the middle sublayer of layer VIa is clearly visible on PND 14. Furthermore, layer I of the prelimbic area, grow wider and reaches adult thickness by PND 18 (Van Eden and Uylings, 1985). Additionally, the cells layer V of the dorsal anterior cingulate area are well distributed by PND

14, thus giving the area adult characteristics. At this age, layers VIa, and VIb now have the main adult characteristics in this region (Van Eden and Uylings, 1985).

The relative width of the cortical layers of the medial precentral area between PND 6 and 10 remain similar. Some darkly stained cells found on PND 6 within the upper sublayer of layer V disappear on PND 10. The cell density of the lower sublayer of layer V decreased (when compared to upper sublayer). These changes in layer V, gives the medial precentral area a less heterogeneous appearance on PND 10. On PND 14 of the development of the medial precentral area, most of the neurons of layer V still reside predominantly in the upper part of this layer, which indicates that the development of laminar has not been fully completed in this area (van Eden *et al.,* 1990).

The development of the orbitofrontal PFC can be distinguished from the dorsolateral cortex on PND 6. In the dorsal agranular insular area, layer V is comparatively broad to either ventral area or the dorsolateral cortex. The large and darkly stain cells which are unique features of this layer, at this age, are seen only irregularly in this area of the cortex (Van Eden & Uylings, 1985). The ventral agranular insular area already has some of the characteristics of the adult. However, the relative width of the layers is quite different. For instance, the lower sublayer of layer V is broader than in the adult, but is almost devoid of cells, whereas the middle sublayer is relatively thin and contains some darkly staining pyramid-like somata. These examples also serve as features that best demarcate the border between the dorsal and ventral agranular insular area in layer V (Van Eden and Uylings, 1985; van Eden *et al.,* 1990).

Layer VIa of the orbitofrontal PFC increase in lamination as development progresses on the dorsal agranular insular area. Layer VIa is separated from layer VIb by a thin lamina. In the ventral agranular insular area, the sublayer of layer V adjacent to layer VIa contains some medium-size, pale-staining cells. Layers VIa and VIb of the ventral agranular insular area are

much denser than the dorsal agranular insular area, with the claustral cells scattered among the layers. In the orbitofrontal PFC, the relative size of the cortical layers does not change after PND 14, but layer VIa becomes more fused with the claustral cells (Van Eden and Uylings, 1985).

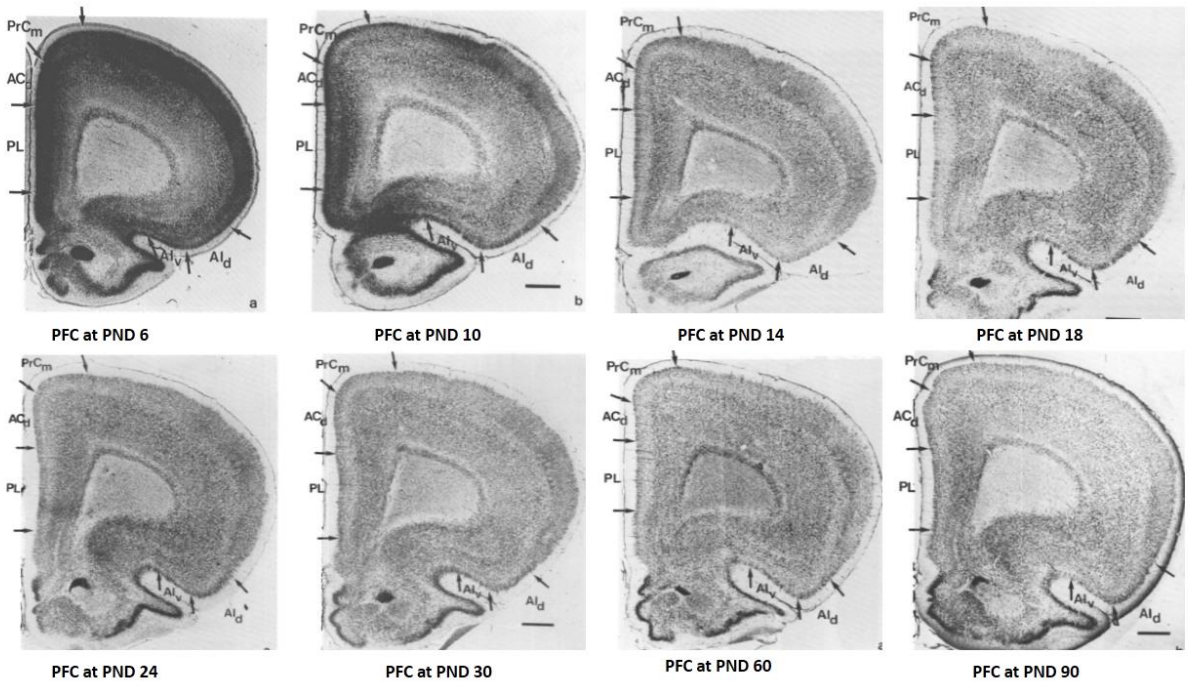

Figure 2.7: Stages of postnatal development of rodent PFC.

PFC= prefrontal cortex; PND= postnatal day; AId1= Dorsal agranular insular area, dorsal part; ACd= Dorsal anterior cingulate cortex; PL= Prelimbic area; Prcm= medial precentral area (Van Eden and Uylings, 1985).

2.8.4 Morphological and functional characterisation of pyramidal neurons in young mice

A study to determine the morphological and functional characterisation of pyramidal neurons in mouse mPFC during the first postnatal month of development was done by Kroon *et al.,* (2019). The study also correspond to the known critical periods of synapse and neuron formation in mouse sensory neocortex. The study revealed that similar maturation profiles of dendritic morphology and intrinsic properties of pyramidal neurons exist in both deep and superficial layers. Furthermore, the balance of synaptic excitation and inhibition differs in a layer-specific pattern from postnatal week 1-4 (Kroon *et al.,* 2019).

2.8.5 Adult layers of prefrontal cortex in mouse

The PFC in mouse has six cortical layers categorised as layer I to VI. Layers II-III are difficult to delineate in mice (Narayanan *et al.,* 2017). According to Defelipe, (2011), the total cortical thickness in mouse is 1210 µm. Also, the number of neurons counted were 364; while the number of synapses formed were 7673503 (asymmetric synapses 84%; symmetric synapses 16% with 21081 number of synapse per neuron). Defelipe (2011), further revealed that layer I had 3 neurons (with 535257 synapses); layer II-III had 81 neurons (with 1438740 synapses); and layer IV had 93 neurons (with 1810662 synapses). Furthermore, Layer V had 48 neurons (with 1326180 synapses), while layer VI had 138 neurons (with 2567317 synapses).

2.8.6 Prefrontal cortical connections involving Layer II/III and V neurons

PFC micro-circuitry involving Layer II/III and V neurons provide insights into the mechanism involved in higher cognitive functions using generalized Volterra model (GVM) in non-human primates (Song *et al.* 2012). In a bid to understand the organization of intrinsic connections that play essential role in cognitive information processing in the prefrontal association cortex, Kritzer and Goldman-Rakic (1995), discovered that intrinsic connections differ from the local circuits of the corresponding layers of the primary visual cortex. It was suggested that the

unique intrinsic wiring of the prefrontal cortex might be associated with its specialized cognitive and mnemonic functions.

2.8.7 Working memory in human studies

The working memory is used to designate a distinct temporary active storage mechanism that is used to achieve a variety of cognitive activities, including thinking, reasoning, judging, decision-making, and language comprehension (Funahashi, 2017). Furthermore, working memory was defined by Miyake and Shah (1999) as the mechanisms or processes that participate in the control, regulation, and active maintenance of task-relevant information in the service of complex cognition, including novel and familiar skilled tasks. Similarly, working memory was described as a tool that permits humans to understand and mentally represent their immediate environment, retain information about their experience, support the acquisition of new knowledge, solve problems as well as act on current goals (Funahashi, 2017). According to Kieras *et al.* (1999), working memory incorporates the entire temporary stored codes, knowledge representations, and procedures where information is maintained, updated, and applied for performing perceptual-motor and cognitive tasks.

Working memory at times is distinguished from short-term memory, as short-term memory refers to the simple temporary storage of information, while working memory refers to both the storage and manipulation of information (Funahashi, 2017).

2.8.8 Working memory in animal studies

Working memory in animal studies has been described as a memory system that retains information that is essential for only one trial and not for subsequent trials. On the other hand, "reference memory" in animals is considered to be a memory that is useful in performing many trials in an experiment that could last for several weeks or months (Funahashi, 2017). Tasks in working memory requires cue information for animal model and may change from trial to trial.

Examples of working memory tasks that require spatial information such are the delayed-response task and the delayed-alternation task. Others include delayed matching-to-sample task and the delayed non-matching-to-sample task (Funahashi, 2017).

Table 2.3: Summary of behavioural features and the comparative timeline of emergence between rodent and human

Behavioral phenotype	Rodents	Human
Weaning, increased activity levels and sociability.	Postnatal day 20-21	2–3 years old
Increasing working memory.	Postnatal day 20-21	2–3 years old
Increased sociability.	Postnatal day 25–35	4-11 years old
Further development of working memory and inhibitory control.	Postnatal day 25–35	4-11 years old
Adolescent-type behaviors including sociability, risk-taking, impulsivity.	Postnatal day 35-49	12-18 year old
The onset of sexual maturity.	Postnatal day 35-49	12-18 year old
Increased cognitive control capacities.	Postnatal day 35-49	12-18 year old
The emergence of adult-type behaviours, such as reduced risk-taking, reduced impulsivity, and increased parental tendencies.	Postnatal day 60 and above	20 years and above

Source: Semple *et al.*, 2013

CHAPTER THREE

MATERIALS AND METHODS

3.1 Ethical approval

The approval for this research was given by the University of Ilorin Ethical Review Committee (UERC) with approval number UERC/ASN/2018/1257.

3.2 Animal handling and grouping

Forty-Two (42) postnatal day 14 (PND 14) old albino mice comprising of thirty-six males and six females were accommodated in plastic cages (22.22 cm × 36.83 cm× 13.97 cm) at the Animal House of the Central Research Laboratory, University of Ilorin, Ilorin, Nigeria. The mice were acclimatized for seven days on a 12 h light/dark cycle at room temperature and had unrestricted access to food and water throughout the experiment. The mice were maintained under the National Institute of Health guide for the care and use of laboratory animals (NRC Publication, 2008).

After seven days of acclimatization, the mice were categorised into seven groups of six animals.

Group A: the control group;

Group B: Pb acetate group;

Group C: Vitexin only group;

Group D: Pb acetate plus Vitexin (Male) group; (this group was created to test sexual dimorphism in the experiment)

Group E: Pb acetate plus Vitexin (Female) group (this group was created to test sexual dimorphism in the experiment);

Group F: Vitexin pre-treated plus Pb acetate group;

Group G: Pb acetate plus Vitexin post-treated group.

3.3 Preparation of treatment solutions

On each day of administration, 10 mg of Vitexin (98% HPLC purity, CAS Number 3681-93-4) purchased from Sigma Aldrich (St Louis, MO, USA) was dissolved in 1ml of normal saline (NaCl, 0.9%) before treatment. Also, the Pb acetate solution was prepared by dissolving 500 mg of Pb in 1 mL of normal saline before taking the required dose of 100 mg/kg bwt for treatment. The quantity of Vitexin and Pb acetate dissolved in normal saline were based on the pilot study carried out earlier in the research. The LD_{50} of Vitexin from the pilot study of this research was 1.90 mg/kg bwt (i.p) while the LD_{50} of Pb acetate was 174 mg/kg bwt (oral).

3.3.1 Administration of treatment

The administration of treatment began on postnatal day 21 and ended on postnatal day 34 (14 days of administration). The rationale for choosing this period and duration of administration was because it coincides with the period of increasing development of working memory, inhibitory control and other behavioural developments (Semple *et al.,* 2013). Furthermore, the period corresponds to the timeline of fractionation and specialization of prefrontal cortex including cortical thickness in rodents (Semple *et al.,* 2013). The doses administered in the study were based on the outcome of the pilot study carried out earlier.

- Control group (Group A) was administered 0.2 ml normal saline for 14 days via oral gavage;
- Pb group (Group B) received 100 mg/kg bwt of Pb acetate through oral gavage for 14 days;

- Vitexin group (Group C) received 1 mg/kg bwt of Vitexin via intraperitoneal (i.p) injection for 14 days;
- Pb+Vitexin male group (Group D) received concurrent administration of 100 mg/kg bwt of Pb acetate (via oral gavage) + 1 mg/kg bwt of Vitexin (via i.p) for 14 days;
- Pb+Vitexin female group (Group E) received concurrent administration of 100 mg/kg bwt of Pb (via oral gavage) + 1 mg/kg bwt of Vitexin (via i.p) for 14 days.
- Vitexin + Pb group (Group F) received 1 mg/kg bwt of Vitexin (via i.p) 1 hour before the administration of 100 mg/kg bwt of Pb (via oral gavage) for 14 days.
- Pb + Vitexin group (Group G) received 1 mg/kg bwt of Vitexin (via i.p) 1 hour after the administration of 100 mg/kg bwt of Pb (via oral gavage) for 14 days.

3.4 Body weight measurement

The body weight of the mice were measured weekly (every Saturday) from postnatal day 21 until the termination of the experiment using a weighing scale (Adventurer Pro-AV313, OHAUS corp., USA).

3.5 Neurobehavioural tests

The behavioural tests began twenty-five days (PND 61) after the end of administration. The rationale for starting the tests on postnatal day 61 was because it marks the period of emergence of adult-type behaviours in rodents (Semple *et al.,* 2013). Furthermore, different days for each test was chosen to reduce stress on the mice which may in turn influence the results.

3.5.1 Barnes maze test

This test for spatial learning memory was done 25 days after the end of administration (PND 61), according to the modified method of Rosenfeld and Ferguson (2014). In this test, a circular table with 15 holes around the circumference, was placed in a lighted room. Fourteen of these holes open directly to the floor, but a single hole leads to a dark drop box that the animal can

hide. Initially (trials), the mice were placed in the centre of the table and were led to the drop box. Subsequently, the mice were allowed to locate the drop box on their own, starting from the centre of the table. All the mice had a total of four trials before the final test. The time between each trial and test was 10 minutes. The test was recorded using a video camera attached to a computer. The record of the number of incorrect holes visited before the correct hole was taken. Also, the time it took the animals to find the correct hole was recorded in addition to the search pattern used by each mouse.

3.5.2 Novel object recognition (NOR) test

This test was carried out 26 days after the end of administration (PND 62) according to the modified method described by Huang and Hsueh (2014). The apparatus for this test comprise a wooden box (of dimension 40 cm x 40 cm x 40 cm), coloured plastic ping pong balls (1 pink and 2 green), and a video camera for recording. The first 15 minutes of the test was for habituation, which involves the mouse being placed in the wooden box for acclimatization. After the habituation, the test began by placing two identical coloured (green) balls before the mice for 45 minutes (for exploration). After that, one pink ball (novel object) and one green ball (old object which the mouse has explored before) were placed in the box before introducing the mouse. While the test was ongoing, the mouse activity was recorded with a camera. At the end of the test, the time spent on the old object, and the novel (new) object were calculated. Also, the percentage preference for the new object was calculated. This same procedure was repeated for all the remaining mice.

$$\% \text{ preference for new object} = \frac{\text{Time use to explore new object}}{\text{Total exploration time for objects}} \times \frac{100}{1}$$

3.5.3 Y-maze test

The Y maze test measures spatial working and reference memory by making use of a rodent's natural exploratory instincts. This test was done according to the modified technique described by Kraeuter *et al.* (2019). The Y-maze consists of three opaque coloured arms of equal length interconnected at 120^0. The arms were labelled A, B, and C.

1. In the test, a mouse was placed in the maze and allowed to explore undisturbed for 8 minutes while the camera was recording.
2. The test includes two sessions. The first session measures working memory in mouse by scoring the number of alternations the mouse made.
3. An entry occurs when all four limbs of the mouse are within an arm while an alternation is described as consecutive entries into all three arms (without going into the same arm twice in a row).
4. At the end of the test, video analysis was carried out. The number of arm entries and alternations were recorded in other to calculate the percentage alternation. This procedure was repeated with each of the remaining mice.
5. A high percentage alternation was taken as good working memory as this indicates that the mouse has recall of the arm already visited.

$$\% \text{ alternation} = \frac{\text{Number of alternations}}{\text{Total number of arm entries}} \times \frac{100}{1}$$

3.5.4 Tail suspension test

On PND 63, this test for depression was carried out using a modified procedure described previously by Can *et al.* (2012). The apparatus for this test include: an aluminium suspension bar (1 cm. height X 1 cm. width x 60 cm. length), a climb stopper, a tape for suspension of mouse tail, and a camera positioned on a support structure close to the bar. The animals were

brought to the testing room and acclimatized for 60 minutes. Before attaching the tails of the mice with a tape to the horizontal bar, a climb stopper (Clear hollow cylinder of 4 cm length, 1.6 cm outside diameter, 1.3 cm inside diameter, 1.5 grams) was placed around their tails. The mice were suspended such that the distance between the nose of each mouse and the apparatus floor is 20-25 cm. The moment their tails were suspended, the video recording began, and it ran for 6 minutes. After three trials, the mice were returned to their home cage and the apparatus sterilized. Video analysis was done, and the following parameters were calculated for each group: Total mobility time and total immobility time. The longer immobility time indicates depressive behaviour.

3.5.5 Elevated plus maze test

This test for anxiety behaviour was conducted on PND 64 according to the modified method of Komada *et al.* (2008).

1. The test apparatus was made of wooden materials with a plus (+) shape that comprises of two open arms (25 x 5 x 0.5 cm) across from each other and perpendicular to two closed arms (25 x 5 x 16 cm) with a centre platform (5 x 5 x 0.5 cm). The open arms had a small (0.5 cm) wall to decrease the number of falls, whereas the closed arms had a high (16 cm) wall to enclose the arm.
2. Before the test commenced, the mice were transferred to the behaviour test room for acclimatization.
3. In this test, a mouse was placed in the central area of the maze with its head directed towards a closed arm.
4. The mouse was allowed to move freely within the maze for 5 minutes. Each mouse had one trial before the main test.
5. The test was recorded using video camera for subsequent analysis.

6. The number of entries in each arm and the time spent in the open arms were recorded. The measurements served as an index of anxiety-like behaviour.
7. After each test, all arms and the central area of the maze were cleaned with alcohol.

Calculations:

- % Time spent in open arm = $\frac{\text{Time in open arms}}{\text{Total time in both arms}} \times \frac{100}{1}$

- % Open arm entries = $\frac{\text{Number of open arm entries}}{\text{Total number of entries in both arms}} \times \frac{100}{1}$

3.5.6 Open field test (OFT)

The modified method of Seibenhener and Wooten (2015) was used for this test on PND 65. Although this test is use at times for locomotion test, it was used in this study to test anxiety behaviour.

1. The main apparatus for the test was a white-coated wooden box measuring 1m x 1m x 1m. The floor of the box was gridded (8× 8 cm) into quadrants such that it had an inner part and an outer part (towards the box wall).
2. The chamber was wiped with 95% ethanol before and after subsequent tests.
3. A video camera was suspended over the apparatus to record the activity for subsequent analysis.
4. The mice were brought into the testing room 30 minutes before the test began for acclimatization.
5. With the tail gently grasped, a single mouse was placed in the middle of the open field maze while concurrently starting the video recorder.
6. The animal was allowed to move freely and uninterrupted throughout the respective quadrants or zones of the maze (inner and outer) for a single 10 minutes period.
7. At the end of the test period, the mouse was gently returned to its home cage.

8. Before cleaning the maze for the next test, faecal boli pellets were visually counted and manually recorded for further analysis.
9. The procedure was repeated for the remaining mice.
10. Video analysis of the time spent in the inner and outer zones were later computed.

3.5.7 Hanging tests with two limbs

The test was carried out according to the modified procedure of Aartsma-Rus and van Putten (2014) on PND 66. This test was carried out to ascertain decision making ability relating to motor and balancing behaviours. The apparatus comprise of a 2 mm thick metallic wire with 55 cm width secured between two vertical stands. The distance between the metallic wire and soft bedding underneath was 37 cm. In the test, the mouse was handled via the tail and allowed to grasp the 2 mm thick metallic wire with the two forepaws only. After that, timing with a stopwatch commenced until the mouse fell off the wire. The record of hanging time was taken. The same process was repeated for all the mice with each mouse given a maximum of three trials before mean hanging time was calculated.

3.5.8 Footprint test

On PND 67, the test was carried out using modified protocols described by Carter *et al.* (2001), and Meng *et al.* (2007). The apparatus for the test was an open-top runway with an enclosed cage that opens at both ends. The runway length was 60 cm long, and the width was 11 cm. Furthermore, the open-top runway was flanked by two walls (12 cm high) on each side. In other to obtain footprints, mouse front and hind paws were coated with non-toxic red and blue inks respectively and was allowed to walk down the narrow runway covered with white paper. Each mouse had a total of three trials. Once the footprints had dried, the following parameters were measured with the aid of a pencil and a measuring ruler: base width, overlap width,

forelimb stride length, and hind limb stride length. The mean of each parameter was then calculated for each group.

3.6 Animal sacrifice, sample collection and analysis

On PND 68, the mice were anaesthetized with an intraperitoneal injection of ketamine (50 mg/kg).

3.6.1 Blood collection

After anaesthetizing the mice, blood was collected using a modified procedure described by Parasuraman *et al.* (2010). In this technique, thoracotomy was performed on the animals, and blood samples were collected from the ventricle of the heart using 23 G needles and syringes. Blood samples collected in EDTA (ethylenediamine tetraacetic acid) bottles were immediately kept in ice before analysis.

3.6.2 Blood Lead level (BLL) test

Part of the blood samples collected was used to test the level of Pb using microwave dissolution technique (De-Souza *et al.*, 2005). The Pb concentration was determined by atomic absorption spectrophotometry (De- Souza *et al.*, 2005).

3.6.3 Haematology test

The remaining blood samples collected were used to evaluate haematological parameters using the auto haematology analyser (Model: AJ-3125, Seattle, USA). The parameters analysed include red blood cell (RBC) count, haemoglobin concentration (Hb), red cell distribution width (RDW), Platelet (PLT) count, Procalcitonin (PCT) level, and white blood cell (WBC) count.

3.7 Biochemical analysis

3.7.1 Preparation of brain samples for biochemical analysis

After collection of blood was completed, the mice were subsequently decapitated, and their brains excised. The excised brains were weighed using a sensitive weighing scale (Model: EHA251, Hangzhou, China). After that, the prefrontal cortices (PFC) were also excised between coordinates 1.8 to 3.1 mm anterior to the bregma. The excised PFC tissues were washed with phosphate buffer saline (PBS). The tissues were then homogenized with ice-cold 0.25 M sucrose in a Teflon Potter–Elvehjem homogenizer (PRO200, Hamburg, Germany). The homogenate was centrifuged at 12, 000 × g (relative centrifugal force) for 10 minutes at 4 °C. The supernatant was then decanted and subsequently used for measuring biochemical activities.

3.7.2 Determination of malondialdehyde level in the prefrontal cortex

Malondialdehyde (MDA) is a lipid peroxidation marker measured using MDA assay kit obtained from Sigma Aldrich (Catalog Number: MAK085; MO, USA). MDA level was monitored using thiobarbituric acid reacting substances (TBARS) assay. To generate MDA-thiobarbituric acid (TBA) adduct, 600 µL of TBA reagent was added into each vial containing 200 µL standard and 200 µL sample. The solution was incubated at 95^0C for one hour and cooled to room temperature in an ice bath for 10 minutes. For higher sensitivity, 300 µL of butanol and 100 µL of 5 M NaCl were added to each tube and vortex vigorously. The solution was centrifuged at 4,000 × g (relative centrifugal force) for 10 min. The upper layer was decanted into another tube while butanol was evaporated. The residue containing the MDA-TBA adduct was dissolved in 200 µL of water and then transferred into a 96 well plate using a pipette where absorbance was measured at 532 nm (Pomierny-Chamioło *et al.,* 2013).

3.7.3 Determination of Superoxide dismutase level in the prefrontal cortex

In brief, superoxide dismutase (SOD) standard (Abcam: ab65354) and sample solutions were prepared and 10 µl of each of the two solutions were added to each of the microwell plate. 200 µl of diluted radical detector was then added to all the wells. Thereafter, 20 µl of xanthine oxidase was added to all the wells to initiate reaction and 20 µl of buffer was added to blank well. The microwell plate was gently shaken for few seconds to allow for proper mixing and the incubated for 30 minutes at room temperature. Absorbance was read at 450 nm using visible spectrophotometer (Model: 721, Axiom medical Ltd, UK) (Ukeda *et al.,* 1999).

3.7.4 Determination of glutathione peroxidase level in the prefrontal cortex

In this reaction, glutathione peroxidase (GPx) reduces cumene hydroperoxide (Abcam: ab102530) while oxidizing GSH to GSSG. The generated GSSG is then reduced to GSH with the consumption of NADPH by glutathione reductase (GR). The decrease of NADPH (which was quickly measured at 340 nm) is proportional to GPx activity (Popović *et al.,* 2019).

In brief, 20 µl of the samples were added to 96-well plate. 0, 20, 40, 60, 80, and 100 µl of 1 mM NADPH standard were then added to 96-well plate in duplicate to generate 0, 20, 40, 60, 80, and 100 nmol/well. The final volume was brought to 100 µl with assay buffer. NADPH was measured at 340 nm. 40 µl of the reaction mixture was added to each test sample and incubated for 15 minutes to deplete GSSG. 10 µl of cumene hydroperoxide solution was then added to start GPx reaction. The first measurement at T1 (340 nm) was done. The reaction was incubated at 25 °C for 5 min before the second reading was done at T2 (340 nm) (Popović *et al.,* 2019).

3.7.5 Determination of Catalase level in the prefrontal cortex

In this test, catalase (Abcam: ab83464) first reacts with H_2O_2 to produce water and oxygen. The unconverted H_2O_2 reacts with the Oxi Red probe (in DMSO) to produce a product that can be measured. In this reaction, 50 µl of samples were added to each well, and volume adjusted to 78 µl with assay buffer. Also, sample high control (HC) was prepared with 50 µl of the sample in separate wells while adjusting the volume to 78 µl. 10 µl of stop solution was then added to the sample HC before it was mixed and incubated at 25°C for 5 min. 0, 2, 4, 6, 8, and 10 µl of 1 mM H_2O_2 solution were added into 96-well plate to generate 0, 2, 4, 6, 8, 10 nmol/well H_2O_2. 12 µl of 1 mM H_2O_2 was then added to each well of tissue samples and the HC sample before incubating at 25°C for 30 min. 50 µl of the developer mix was then added to each test samples, control, and standard while mixing. Incubation was done at 25°C for 10 min. Optical density (OD) was measured at 230 nm. A unit of catalase activity was defined as μmol of H_2O_2 decomposed (Popović *et al.*, 2017).

3.7.6 Determination of Nitric oxide level in the prefrontal cortex

In this assay, nitrate was converted to nitrite by utilizing nitrate reductase. Griess reagents (abcam: ab65328) then converted nitrite to a deep purple azo compound. The amount of the azochromophore accurately reflects the level of nitric oxide in the samples. The setup had three reaction wells i.e., nitrate standard wells (85 µL standard dilutions), sample wells (50 µL samples adjusted to 85 µL/well with assay buffer) and blank wells (50 µL adjusted to 85 µL/well with Assay Buffer samples). 5 µL of nitrate reductase and enzyme cofactor was added to both standard wells and sample wells, while 115 µL of assay buffer was added to blank wells. The samples were incubated at room temperature for 1 hour to convert nitrate to nitrite. 5 µL enhancer was then added to standard and sample wells only. Incubation was done at room temperature for 10 min. 50 µL of griess reagents were added to standard and sample wells. Optical density (OD) was measured at 540nm (Ricart-Jané *et al.*, 2002).

3.7.7 Determination of acetylcholinesterase activity

The specific activity of AChE was determined, as described by Ellman *et al.,* (1961). The reaction mixture contained 3 mL of 0.1 M phosphate buffer (pH 8), 20 µL of 0.075 M acetylcholine iodide, and 100 µL of 0.01 M 5, 5-dithiobis-2-nitrobenzoic acid. The reaction was initiated with the addition of 100 µL of tissue homogenate sample. The mixture was incubated for 30 minutes at room temperature, and the colour absorbance was measured at 412 nm.

3.7.8 Determination of Na^+/K^+-ATPase activity

Na^+/K^+-ATPase activity was assayed according to the method described by Noske *et al.* (2010). In this method, reaction mixtures were Media I (containing 30 mM imidazole-HCl, 130 mM NaCl, 20 mM KCl, 4 mM $MgCl_2$), and Media II (containing 30 mM imidazole-HCl, 4 mM $MgCl_2$, and 1 mM ouabain) at pH 7.4. The reaction was incubated at 37°C for 10 minutes. The enzyme activity was stopped by the addition of 100 µl of 20% sodium dodecylsulfate. The Na^+-K^+-ATPase activity was calculated as difference in inorganic phosphate (Pi) content between media (I) and (II) expressed in nmol/min.

3.8 Histological and histochemical techniques

On PND 68, the mice for histological and histochemical studies were anaesthetised with an intraperitoneal injection of ketamine (50 mg/kg). The process of anaesthetising was followed by transcardiac perfusion with 4% paraformaldehyde (4% PFA) in phosphate buffer saline (PBS) using the method described by Gage *et al.* (2012). The mice were subsequently decapitated, and their brains excised before weighing on a sensitive weighing scale (Model: EHA251, Hangzhou, China). The prefrontal cortex was excised from each mouse brain between stereotaxic coordinates of 1.8 to 3.1 mm anterior to the bregma, before post-fixing in 4% PFA for twenty-four (24) hours.

Tissue processing was carried out using the facilities at the Histopathology Unit of the University of Ilorin Teaching Hospital, Ilorin, Nigeria. The reagents and procedures used for tissue processing have been stated in Appendix II of this thesis.

3.8.1 Staining procedures

Staining procedures were carried out using the facilities at the Histopathology Unit of the National Hospital, Abuja, Nigeria. The reagents and procedures used for staining have been stated in Appendix III of this thesis.

3.8.1.1 Haematoxylin and Eosin staining technique

This technique was carried out in order to show the histoarchitecture and general outline of the prefrontal cortical cells. The technique was carried out based on the report of Bancroft and Gamble (2008), and outlined in Appendix III of this thesis.

3.8.1.2 Cresyl fast violet staining technique

This technique was carried out in order to reveal Nissl staining of the prefrontal cortex. This stain was also used for morphological analysis of the cells. The technique was carried out based on the report of Bancroft and Gamble (2008), and outlined in Appendix III of this thesis.

3.8.1.3 Congo red staining technique (Highman)

The reason behind the use of this technique was to demonstrate the presence amyloid protein expression. The technique was carried out in line with the description of Bancroft and Gamble (2008), and outlined in Appendix III of this thesis.

3.8.1.4 Bielschowsky's silver staining technique

This technique was carried out in order to reveal senile plaques in the prefrontal cortex. The technique was carried out based on the report of Bancroft and Gamble (2008), and outlined in Appendix III of this thesis.

3.8.1.5 Glial fibrillary acidic protein (GFAP) staining technique

The demonstration of immunoreactive (ir) astrocytes was the reason behind the use of this technique. This technique was carried out according to the report of Olajide and Akinola (2016), and outlined in Appendix III of this thesis.

3.8.1.6 Synaptophysin staining technique

This technique was carried out according to the description of Lentz *et al.* (2005), to demonstrate synaptophysin protein expression. The procedures involve in this technique have been outlined in Appendix III of this thesis.

3.8.1.7 Protein-53 staining technique

This technique was carried out to demonstrate the expression of protein-53 (p53) in the prefrontal cortex. The technique was carried out based on the report of Hafez and Tahoun (2011), and outlined in Appendix III of this thesis.

3.8.2 Photomicrography

Stained tissue sections were viewed under a light binocular microscope (Olympus Model: XSZ-107BN, New Jersey, USA) attached to a camera (amscope MD500, CA, USA.) and a computer. The window view used was 767 × 575 µm at a scale bar of 180µm or 45µm. Six visual fields from each of the tissues were photographed.

3.8.3 Morphometric analysis

Sections for morphometric analysis were taken three sections apart, while six visual fields of the tissues were photographed in each section for analysis. Image J (1.52r) software (NIH, USA) with various plugins was used to analyse the following parameters:

3.8.3.1 Cell count

Cell count for normal and degenerating neurons was done at 767 × 575 µm counter window with a scale bar of 180 µm.

3.8.3.2 Neuronal length, Soma length, and Intercellular distance

Neuronal length, soma length, and intercellular distance were measured using Image J (1.52r) software at a scale of 3.4 pixel/µm with the results expressed in µm.

3.8.3.3 Cross-sectional area of neurons

The cross-sectional area of normal neurons was measured using Image J (1.52r) software at a scale of 3.4 pixel/µm, and the result expressed in μm^2.

3.9 Statistical analysis

All statistical analyses and graph fitting were performed using Graph Pad Prism (version 5.0, La Jolla, CA). The Significant difference between groups was determined using one-way analysis of variance (ANOVA) followed by Tukey's *post-hoc* test or two-way ANOVA followed by Bonferroni *post-hoc* test. Data were expressed as mean ± SEM (standard error of mean) while statistical significance was defined at $p < 0.05$.

CHAPTER FOUR

RESULTS

4.1 Physical observation

4.1.1 Body weight changes

The result of body weight of mice (Table 4.1), shows general progressive weight gain ($p < 0.05$) as the mice grew older in the control and Pb+Vitexin treated groups. In the Pb treated group, the body weight of the mice was not different, from PND 42 until PND 68. Furthermore, from PND 63 until PND 68, the body weights of mice in Pb+Vitexin (Female), Vitexin pre-treated, and Vitexin post-treated groups were not different ($p > 0.05$). When comparisons were made between each group on postnatal days that body weights of mice were measured, no significant difference ($p > 0.05$) was found.

Table 4.1: Body weight of animals

Group/PND	PND 21	PND 28	PND 35	PND 42	PND 56	PND 63	PND 68
Control (g)	16.9±0.5	19.2±0.3[a]	24.9±0.7[a b]	27.6±0.4[a b c]	25.6±0.4[a b c]	30.0±0.4[a b c d e]	32.1±0.4[a b c d e]
Lead (g)	16.8±0.8	20.0±0.4[a]	24.6±0.8[a b]	28.8±0.3[a b c]	28.7±0.4[a b c]	28.6±0.43[a b c]	29.2±0.4[a b c]
Vitexin (g)	16.9±0.1	20.2±0.3[a]	25.3±0.5[a b]	28.7±0.3[a b c]	29.4±0.5[a b c]	30.4±0.5[a b c d]	29.9±0.5[a b c]
Pb+Vitexin (M) (g)	16.2±0.4	21.2±0.4[a]	26.7±0.8[a b]	28.8±0.4[a b c]	28.7±0.4[a b c]	29.3±0.4[a b c]	30.1±0.4[a b c]
Pb+Vitexin (F) (g)	16.6±0.3	20.6±0.2[a]	25.8±0.4[a b]	26.6±0.5[a b]	27.2±0.6[a b]	29.1±0.6[a b c]	29.6±0.6[a b c]
Vitexin pre-treated (g)	16.5±0.4	20.5±0.4[a]	24.6±0.4[a b]	27.5±0.9[a b c]	27.9±0.4[a b c]	29.6±0.4[a b c]	29.4±0.4[a b c]
Vitexin post-treated (g)	16.9±0.4	20.2±0.3[a]	24.4±0.4[a b]	26.4±0.3[a b]	27.0±0.3[a b c]	29.3±0.3[a b c]	29.7±0.2[a b c d]

Legends: PND= Postnatal day; F= female; Male= male; g= gramme; [a] Significant difference with PND 21 ($p < 0.05$); [b] Significant difference with PND 28 ($p < 0.05$); [c] Significant difference with PND 35 ($p < 0.05$); [d] Significant difference with PND 42 ($p < 0.05$); [e] Significant difference with PND 56 ($p < 0.05$). Data are presented as Mean± SEM.

4.1.2 Brain and prefrontal cortical weight changes

The result of brain weight (Table 4.2), showed that all the treated groups were not significantly different ($p > 0.05$) from the control group when comparisons were made. When Pb treated group was compared with Pb + Vitexin (M), and Pb +Vitexin (F) groups, no significant difference ($p > 0.05$) was found in the brain weight of mice. Similarly, when Pb treated group was compared with Vitexin pre-treated, and Vitexin post-treated groups, no significant difference ($p > 0.05$) was found in the brain weight of mice. Furthermore, no significant brain weight difference ($p > 0.05$) was found when Pb + Vitexin (M) and Pb +Vitexin (F) treated groups were compared. The brain weight comparison made between Vitexin pre-treated and Vitexin post-treated groups showed no significant difference ($p > 0.05$).

The prefrontal cortex (PFC) weight (Table 4.2) was significantly low ($P<0.05$) in Pb treated group (0.036±0.003 g) and Pb +Vitexin (F) treated group (0.057±0.008 g) when compared with the control group (0.083±0.001 g). There was no significant difference ($p > 0.05$) in PFC weight in groups administered Vitexin only, Pb + Vitexin (M), Vitexin pre-treated; and Vitexin post-treated when comparisons were made with the control group ($p > 0.05$). Similarly, the PFC weight between Pb + Vitexin (M) group and Pb +Vitexin (F) treated group was not significantly different ($p > 0.05$), neither was there difference between Vitexin pre-treated; and Vitexin post-treated groups ($p > 0.05$). However, the PFC weights of mice in Pb + Vitexin (M); Vitexin pre-treated and Vitexin post-treated groups (0.067±0.03 g; 0.07±0.06 g and 0.067±0.003 g respectively) were significantly high ($p<0.05$) when compared with Pb treated group (0.036±0.003 g).

The ratio of brain weight to PFC weight (Table 4.2) in Pb treated group (11:1) was significantly higher ($P<0.05$) when compared with the control group (5:1). Likewise, the ratio of brain weight to PFC weight in Pb treated group (11:1) appeared significantly high ($p<0.05$) when

comparison was made between Pb and Vitexin (M); Pb +Vitexin (F); Vitexin pre-treated and Vitexin post-treated groups (6:1; 7.5:1; 5.9:1 and 6.3:1 respectively). There was no significant difference ($p > 0.05$) in brain weight to PFC weight ratio when comparison was made between the control group and all the treated groups (except Pub treated group).

Table 4.2: Whole brain and prefrontal cortical weight

Weight	Control	Lead (Pb)	Vitexin	Pb + Vitexin (M) (concurrent)	Pb + Vitexin (F) (concurrent)	Vitexin Pre-treated	Vitexin Post-treated
Brain(g)	0.42±0.01	0.40±0.006	0.41±0.009	0.40±0.008	0.43±0.009	0.41±0.006	0.42±0.008
PFC (g)	0.083±0.001	0.036±0.003[a]	0.073±0.002[b]	0.067±0.03[b]	0.057±0.008a	0.07±0.06[b]	0.067±0.003[b]
B-P Ratio	5:1[b]	11:1[a]	5.6:1[b]	6:1[b]	7.5:1[b]	5.9:1[b]	6.3:1[b]

Legends: PFC = Prefrontal cortex; B-P Ratio= Brain weight to PFC weight Ratio; g=gramme; F= female; M= male; [a] Statistical different with Control ($p < 0.05$); [b] Statistical different with Pb ($p < 0.05$); Data are presented as mean± SEM.

4.2 Blood lead level and changes in haematological parameters

In Table 4.3, the blood lead levels (BLL) in all the experimental groups except Vitexin treated group (1.7±0.13 µg/dl) were significantly higher ($p<0.05$) than the control group (1.3±0.13 µg/dl). When BLL in Pb treated group (5.6±0.29 µg/dl) was compared with Pb + Vitexin (M); Pb +Vitexin (F); Vitexin pre-treated and Vitexin post-treated groups (4.2±0.27 µg/dl; 4.2±0.3 µg/dl; 4.3±0.4 µg/dl and 4.0±0.36 µg/dl respectively), no statistically significant difference ($p>0.05$) was seen. However, BLL in mice was significantly higher ($p<0.05$) in Vitexin pre-treated and Vitexin post-treated groups (4.3±0.4 µg/dl and 4.0±0.36 µg/dl respectively) when compared with Vitexin only treated group (1.7±0.13 µg/dl). Similarly, Pb + Vitexin (M) and Pb + Vitexin (F) treated groups (4.2±0.27 µg/dl and 4.2±0.3 µg/dl respectively) had significantly high level of BLL when compared with Vitexin treated group (1.7±0.13). Additionally, no significant difference ($p>0.05$) in BLL was observed between Pb + Vitexin (M) treated group (4.2±0.27 µg/dl) and Pb + Vitexin (F) treated group (4.2±0.3 µg/dl) neither was there any significant difference ($p>0.05$) between Vitexin pre-treated (4.3±0.4 µg/dl) and Vitexin post-treated groups (4.0±0.36 µg/dl).

The number of red blood cell (RBC) in Pb treated group (5.4±0.6 $\times 10^6$/µl) was significantly low ($p<0.05$) when compared with the control group (7.1±0.07 $\times 10^6$/µl), as well as Vitexin pre-treated group (6.9±0.5 $\times 10^6$/µl). There was no significant difference ($p>0.05$) in the number of RBC when all experimental groups with the exception of Pb treated group was compared with the control group (7.1±0.07 $\times 10^6$/µl). Similarly, no significant difference ($p>0.05$) in RBC was found when comparison was made between Pb + Vitexin (M) (6.5±0.3 $\times 10^6$/µl) and Pb + Vitexin (F) (6.4±0.4 $\times 10^6$/µl), neither was there any difference ($p>0.05$) in RBC when Vitexin pre-treated group (6.9±0.5 $\times 10^6$/µl) and Vitexin post-treated group (6.9±0.7 $\times 10^6$/µl) was compared (Table 4.3).

In Table 4.3, the number of white blood cells (WBCs) were not significantly different ($p > 0.05$) between the experimental groups and the control group (12.4±1.8 $\times 10^3/\mu l$) when comparisons were made.

The platelets count (Table 4.3) in Pb treated group, Vitexin pre-treated group and Vitexin post-treated group (297±45 $\times 10^3/\mu l$; 327.7±18 $\times 10^3/\mu l$ and 300.8±60 $\times 10^3/\mu l$ respectively) were significantly low ($p<0.05$) when compared with the control group (486.7±67). In contrast, platelets count in Vitexin only, Pb + Vitexin (M) treated, and Pb + Vitexin (F) treated groups (412.3±16 $\times 10^3/\mu l$; 430.7±50 $\times 10^3/\mu l$; and 472.3±48 $\times 10^3/\mu l$ respectively) were not significantly different ($p > 0.05$) when comparison were made with the control group (486.7±67 $\times 10^3/\mu l$). Furthermore, platelets count in Pb + Vitexin (M), and Pb + Vitexin (F) treated groups (430.7±50 $\times 10^3/\mu l$; and 472.3±48 $\times 10^3/\mu l$ respectively) was not different ($p > 0.05$) when comparison was made neither was there any statistical significant difference ($p > 0.05$) between Vitexin pre-treated group (327.7±18 $\times 10^3/\mu l$) and Vitexin post-treated group (300.8±60 $\times 10^3/\mu l$).

The haemoglobin level (Table 4.3) in Pb treated group (8.8±1.3 g/dl) was significantly low ($p<0.05$) when compared with the control group (13.6±0.2 g/dl). Similarly, the level of haemoglobin in Pb treated group (8.8±1.3 g/dl) was significantly low ($p<0.05$) when compared with Pb + Vitexin (M) treated (12.5±0.7 g/dl); Pb + Vitexin (F) treated (12.8±1.2 g/dl); Vitexin pre-treated (12.03±2 g/dl); and Vitexin post-treated (13.8±0.6 g/dl) groups. Furthermore, the haemoglobin level in Vitexin only treated group, Pb + Vitexin (M) group; Pb + Vitexin (F) group; Vitexin pre-treated group; and Vitexin post-treated group were not significantly different ($p > 0.05$) from the control group.

In Table 4.3, the red cell distribution width (RDW) in Pb treated group, Vitexin only treated group, Pb + Vitexin (M) treated group and Vitexin pre-treated group (16.9±0.8 fL; 17.5±1 fL;

17.9±0.4 fL; and 17.07±2 fL respectively) were significantly lower ($p<0.05$) than the control group (20.9±0.1 fL). Similarly, RDW within Pb + Vitexin (F) group (19.5±1 fL) and Vitexin post-treated group (19.9±0.7 fL) were significantly high ($p<0.05$) when compared with Pb treated group (16.9±0.8 fL). On the other hand, the RDW within Vitexin only treated group, Pb + Vitexin (M) treated group; Pb + Vitexin (F) treated group; Vitexin pre-treated group; and Vitexin post-treated group was not significantly different ($p>0.05$).

The procalcitonin levels (Table 4.3) in Pb treated group, Vitexin pre-treated group; and Vitexin post-treated group (0.36±0.03 ng/ml; 0.36±0.03 ng/ml and 0.30±0.01 ng/ml respectively) were significantly higher ($p<0.05$) than the control group (0.19±0.03 ng/ml) when comparisons were made. On the contrary, the levels of procalcitonin in Vitexin only treated group, Pb + Vitexin (M) treated group, and Pb + Vitexin (F) treated group were not significantly different ($p>0.05$) from the control group. Similarly, no significant difference ($p>0.05$) was found when Pb treated group was compared with Vitexin pre-treated and Vitexin post-treated groups. Furthermore, no significant difference ($p>0.05$) was found between Pb + Vitexin (M) treated and Pb + Vitexin (F) treated groups; neither was there any difference ($p>0.05$) between Vitexin pre-treated group and Vitexin post-treated group.

Table 4.3: Mean values of haematological parameters and Lead level

Parameters	Control	Lead (Pb)	Vitexin	Pb +Vitexin (M)	Pb + Vitexin (F)	Vitexin Pre-treated	Vitexin Post-treated
BLL (µg/dl)	1.3±0.13	5.6±0.29$^{a\ c\ d}$	1.7±0.13$^{b\ d}$	4.2±0.27$^{a\ c}$	4.2±0.3$^{a\ c}$	4.3±0.4$^{a\ c}$	4.0±0.36$^{a\ c}$
RBC ($\times10^6$/µl)	7.1±0.07	5.4±0.6^{a}	7.5±0.2$^{b\ d}$	6.5±0.3	6.4±0.4	6.9±0.5^{b}	6.9±0.7
WBC ($\times10^3$/µl)	12.4±1.8	11.9±1.0	12.6±1.7	12.0±1.3	12.2±1.5	12.1±2.2	12.4±1.7
PLT ($\times10^3$/µl)	486.7±67	297±45^{a}	412.3±16^{b}	430.7±50^{b}	472.3±48^{b}	327.7±18^{a}	300.8±60^{a}
Hb (g/dl)	13.6±0.2	8.8±1.3^{a}	13.5± 1.6^{b}	12.5±0.7^{b}	12.8†±1.2	12.03±2^{b}	13.8±0.6^{b}
RDW (fL)	20.9±0.1	16.9±0.8^{a}	17.5±1^{a}	17.9±0.4^{a}	19.5±1^{b}	17.07±2^{a}	19.9±0.7^{b}
PCT (ng/ml)	0.19±0.03	0.36±0.03^{a}	0.25±0.02^{b}	0.28±0.01	0.27±0.02	0.36±0.03^{a}	0.30±0.01^{a}

Data are presented as mean± SEM. ^{a} significantly different from control ($p < 0.05$); ^{b} significantly different from Pb treated group ($p < 0.05$); ^{c} significantly different from Vitexin only treated group ($p < 0.05$); ^{d} significantly different from Vitexin post-treated group ($p < 0.05$). Red blood cell count (RBC), haemoglobin (Hb), red cell distribution width (RDW), Platelets (PLT), Procalcitonin (PCT), and blood lead level (BLL).

4.3 Biochemical observation

4.3.1 Changes in oxidative stress markers

4.3.1.1 Changes in malondialdehyde level

In Figure 4.1, malondialdehyde (MDA) level in Pb treated group (0.41±0.03 U/mg) was significantly high ($p<0.05$) when compared with the control group (0.29±0.001 U/mg). Similarly, the level of MDA in Pb treated group (0.41±0.03 U/mg) was significantly high ($p<0.05$) when compared with Pb + Vitexin (M), Vitexin pre-treated, and Vitexin post-treated groups (0.3±0.03 U/mg; 0.29±0.01 U/mg; and 0.31±0.01 U/mg respectively). The MDA level in all the experimental groups (with exception of Pb treated group) were not significantly different ($p>0.05$) from the control group. Similarly, no significant difference ($p>0.05$) was found when comparison was made between Vitexin treated, Pb + Vitexin (M) treated and Pb +Vitexin (F) treated groups. Furthermore, the level of MDA was not significantly different ($p>0.05$) between Vitexin pre-treated, and Vitexin post-treated groups.

Malondialdehyde level

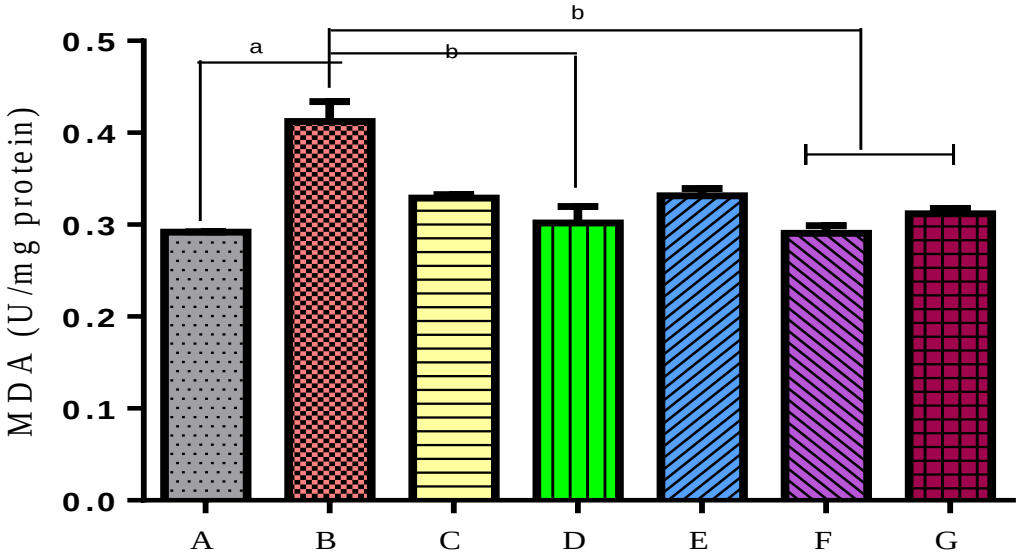

Figure 4.1: Changes in malondialdehyde level of the PFC.

The coloured bars represent levels of malondialdehyde (MDA) in each group (A-G) of the experiment. The horizontal lines with superscript alphabets joining directly with the vertical lines above the groups, indicates significant difference in the level of MDA between groups connected by the horizontal lines. [a] represent significant difference in the level of MDA between B and A. [b] represent significant difference in the level of MDA in C, E and G when compared with B.

Keys: A= Control; B = Lead (Pb); C =Vitexin; D = Pb+Vitexin (Male); E= Pb+Vitexin (Female); F =Pre-treated with vitexin; G =Post-treated with vitexin.

4.3.1.2 Changes in superoxide dismutase level

The superoxide dismutase (SOD) level (Figure 4.2) in Pb treated group (1.2±0.23 U/mg) was significantly low ($p<0.05$) when compared with the control group (3.6±0.18 U/mg). Similarly, the level of SOD in Pb treated group (1.2±0.23 U/mg) was significantly low ($p<0.05$) when compared with Vitexin only, Pb + Vitexin (M), and Vitexin pre-treated groups (2.9±0.21 U/mg; 3.3±0.14 U/mg; and 3.0±0.1 U/mg respectively). Equally, the SOD level in Vitexin post-treated group (1.8±0.21 U/mg) was significantly low ($p<0.05$) when compared with the control group (3.6±0.18 U/mg). When the levels of SOD in Vitexin only treated, Pb + Vitexin (M) treated and Vitexin pre-treated groups were compared with the control group, no significant difference ($p>0.05$) was found. Furthermore, the level of SOD in Pb + Vitexin (M) treated group (3.3±0.14 U/mg) was significantly higher ($p>0.05$) than Pb + Vitexin (F) treated (2.4±0.21 U/mg) group. Also, SOD level in Vitexin pre-treated group (3.0±0.1 U/mg) was significantly higher ($p>0.05$) than Vitexin post-treated group (1.8±0.21 U/mg) when comparison was made. On the other hand, no significant difference ($p>0.05$) was found between the Pb treated group and Vitexin post-treated group neither was there a significant difference ($p>0.05$) within Vitexin only treated, Pb + Vitexin (M), and Vitexin pre-treated groups when comparisons were made.

Superoxide dismutase level

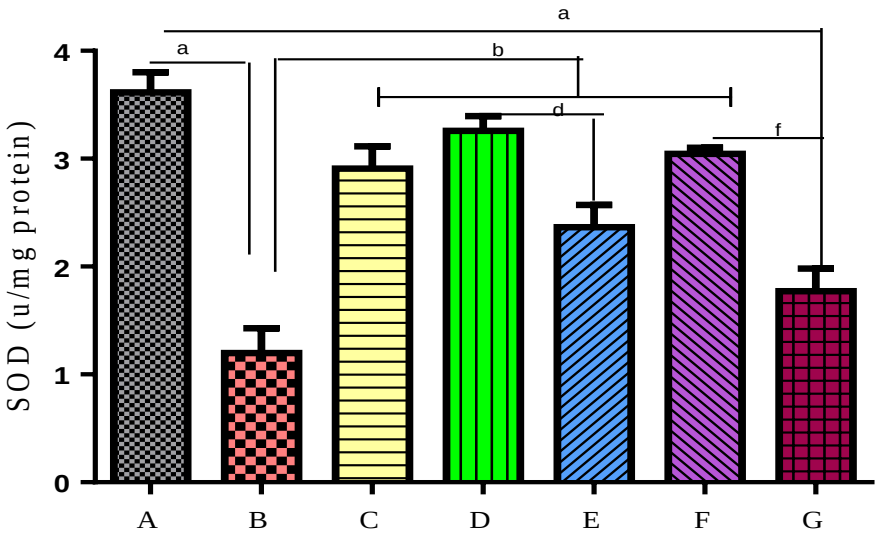

Figure 4.2: Changes in superoxide dismutase level of the PFC.

The coloured bars represent levels of superoxide dismutase (SOD) in each group (A-G) of the experiment. The horizontal lines with superscript alphabets joining directly with the vertical lines above the groups, indicates significant difference in the level of SOD between groups connected by the horizontal lines. [a] represent significant difference in the level of SOD between B, G and A. [b] represent significant difference in the level of SOD in C, D and F when compared with B. [d] represent significant difference in the level of SOD between E and D. [f] represent significant difference in the level of SOD between G and F

Keys: A= Control; B = Lead (Pb); C =Vitexin; D = Pb+Vitexin (Male); E= Pb+Vitexin (Female); F =Pre-treated with vitexin; G =Post-treated with vitexin.

4.3.1.2 Changes in glutathione peroxidase level

In Figure 4.3, glutathione peroxidase (GPx) level in all the treated groups with exception of Vitexin pre-treated group (3.4±0.1 U/mg) was significantly low ($p<0.05$) when compared with the control group (3.9±0.22 U/mg). Similarly, the GPx level in Pb treated group (1.3±0.1 U/mg) was significantly low ($p<0.05$) when compared with Pb + Vitexin (M) treated group (2.8±0.2 U/mg) and Pb + Vitexin (F) treated group (2.4±0.04 U/mg). Additionally, the GPx level in Pb treated group (1.3±0.1 U/mg) was significantly low ($p<0.05$) when compared with Vitexin pre-treated (3.4±0.1 U/mg) and Vitexin post-treated (2.7±0.1 U/mg) groups. The level of GPx in Vitexin only treated group (3.1±0.3) was not significantly different ($p >0.05$) from Pb + Vitexin (M) treated (2.8±0.2 U/mg) and Pb + Vitexin (F) treated (2.4±0.04 U/mg) groups; Neither was there any significant difference ($p >0.05$) when GPx in Vitexin only treated group (3.1±0.3) was compared with Vitexin pre-treated (3.4±0.1 U/mg) and Vitexin post-treated (2.7±0.1 U/mg) groups. Likewise, no significant difference ($p >0.05$) was found between Pb +Vitexin (M) group (2.8±0.2 U/mg) and Pb + Vitexin (F) group (2.4±0.04 U/mg) neither was there any significant difference ($p >0.05$) between Vitexin pre-treated group (3.4±0.1 U/mg) and Vitexin post-treated group (2.7±0.1 U/mg).

Glutathione peroxidase level

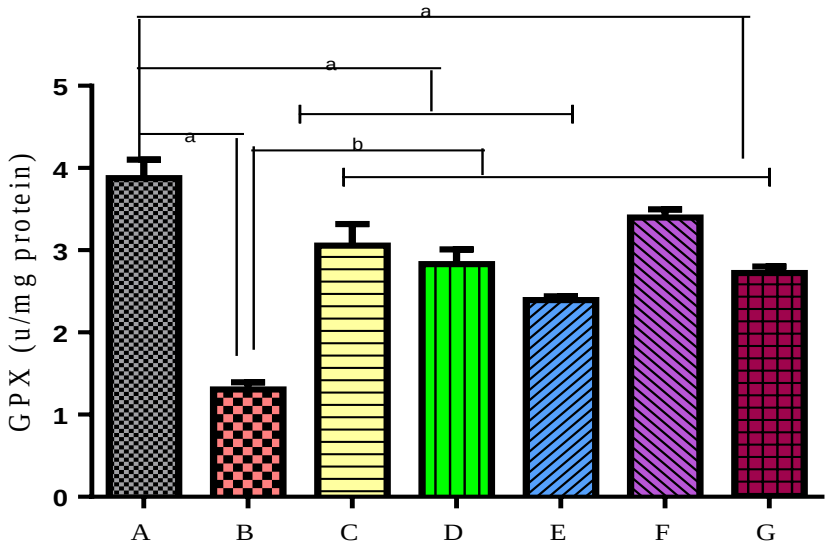

Figure 4.3: Changes in glutathione peroxidase level of the PFC.

The coloured bars represent levels of glutathione peroxidase (GPX) in each group (A-G) of the experiment. The horizontal lines with superscript alphabets joining directly with the vertical lines above the groups, indicates significant difference in the level of GPX between groups connected by the horizontal lines. [a] represent significant difference in the level of GPX in B, C, D & G when compared with A. [b] represent significant difference in the level of GPX in C-G when compared B.

Keys: A= Control; B = Lead (Pb); C =Vitexin; D = Pb+Vitexin (Male); E= Pb+Vitexin (Female); F =Pre-treated with vitexin; G =Post-treated with vitexin.

4.3.1.3 Changes in catalase level

Catalase level (Figure 4.4) in all the treated groups with exception of Vitexin pre-treated group (114±5.1 µmol H_2O_2/g) was significantly low ($p<0.05$) when compared with the control group (153±14 µmol H_2O_2/g). Catalase level in Pb treated group (54±9 µmol H_2O_2/g) was significantly low ($p<0.05$) when compared with Pb + Vitexin (F) group (114±5.1 µmol H_2O_2/g). However, the level of catalase in Pb treated group (54±9 µmol H_2O_2/g) was not significantly different ($p >0.05$) when compared with Pb + Vitexin (M), Vitexin pre-treated and Vitexin post-treated groups. Similarly, no significant difference ($p >0.05$) was found between Pb + Vitexin (M) group and Pb + Vitexin (F) group neither was there a significant difference ($p>0.05$) between Vitexin pre-treated group (93±3.5 µmol H_2O_2/g) and Vitexin post-treated group (91±9.4 µmol H_2O_2/g).

Catalase level

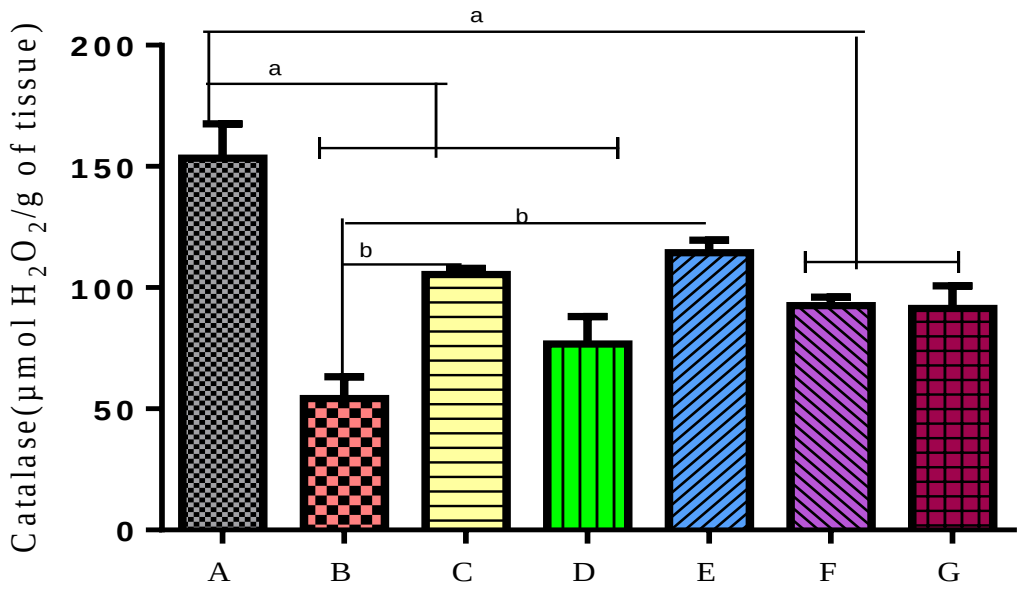

Figure 4.4: Changes in catalase level of the PFC.

The coloured bars represent levels of glutathione peroxidase catalase in each group (A-G) of the experiment. The horizontal lines with superscript alphabets joining directly with the vertical lines above the groups, indicates significant difference in the level of catalase between groups connected by the horizontal lines. [a] represent significant difference in the level of catalase in B, C, D, F, & G when compared with A. [b] represent significant difference in the level of catalase in C and E when compared B.

Keys: A= Control; B = Lead (Pb); C =Vitexin; D = Pb+Vitexin (Male); E= Pb+Vitexin (Female); F =Pre-treated with vitexin; G =Post-treated with vitexin.

4.3.2 Changes in sodium/ potassium ATPase enzyme

The Na^+/K^+ ATPase (Figure 4.5) level in Pb treated group (0.99±0.02 ngip/min/mg) was significantly low ($p<0.05$) when compared with the control group (1.2±0.07 ngip/min/mg). However, the levels of the enzyme in Vitexin only, Pb + Vitexin (M), and Pb + Vitexin (F) treated groups were not significantly different ($p>0.05$) with the control group. Similarly, the level of the enzyme in Vitexin pre-treated group and Vitexin post-treated group were not significantly different ($p>0.05$) with the control group. Furthermore, the level of Na^+/K^+ ATPase in all the treated groups including the Pb treated group was not significantly different ($p>0.05$) when comparisons were made among the treated groups.

Sodium/ Potassium ATPase level

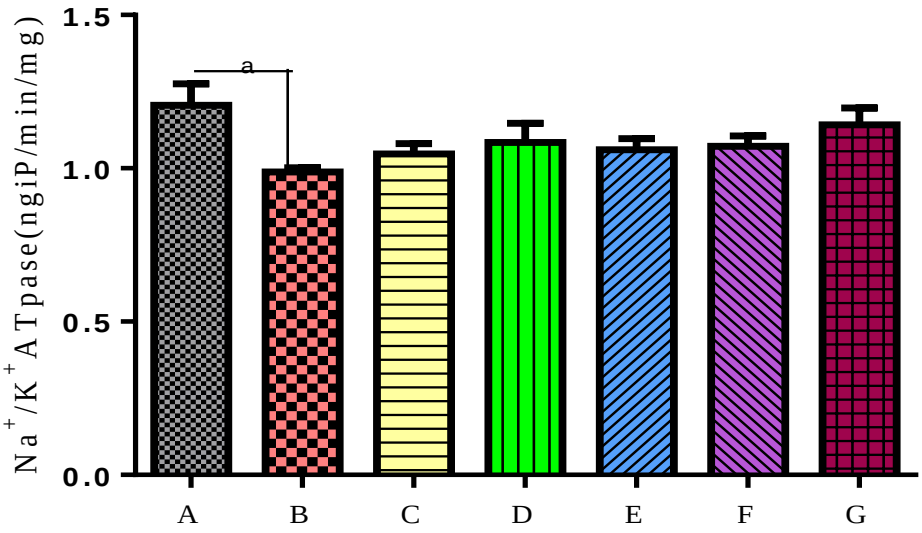

Figure 4.5: Variations in sodium/ potassium ATPase level of the PFC.

The coloured bars represent levels of sodium/ potassium ATPase (Na^+/K^+ ATPase) in each group (A-G) of the experiment. The horizontal line with superscript alphabet joining directly with the vertical line above the group, indicates significant difference in the level of Na^+/K^+ ATPase between groups connected by the horizontal line. [a] represent significant difference in the level of Na^+/K^+ ATPase between B and A.

Keys: A= Control; B = Lead (Pb); C =Vitexin; D = Pb+Vitexin (Male); E= Pb+Vitexin (Female); F =Pre-treated with vitexin; G =Post-treated with vitexin.

4.3.3 Changes in acetylcholinesterase level

In Figure 4.6, the level of acetylcholinesterase (AChE) in Pb treated group (0.036±0.003 U/min/mg) was significantly low ($p<0.05$) when compared with the control group (0.071±0.005 U/min/mg). Similarly, AChE level in Pb treated group (0.036±0.003 U/min/mg) was significantly low ($p<0.05$) when compared with Pb + Vitexin (M) group (0.058±0.004 U/min/mg), Pb + Vitexin (F) group (0.071±0.004 U/min/mg), Vitexin pre-treated group (0.095±0.005 U/min/mg) and Vitexin post-treated group (0.068±0.004 U/min/mg). Furthermore, the level of AChE was significantly low ($p<0.05$) when Vitexin post-treated group (0.068±0.004 U/min/mg) was compared with Vitexin pre-treated group (0.095±0.005 U/min/mg). Likewise, the level of the enzyme in Vitexin only treated group (0.086±0.004 U/min/mg) was significantly low ($p<0.05$) when compared with Vitexin pre-treated group (0.095±0.005 U/min/mg). Conversely, the levels of AChE in Vitexin only treated group, Pb + Vitexin (M) group, Pb + Vitexin (F) group, and Vitexin post-treated group were not significantly different ($p>0.05$) when compared with the control group. Also, AChE level in Pb + Vitexin (M) group was not significantly different ($p>0.05$) when compared with Pb + Vitexin (F) group.

Acetylcholinesterase level

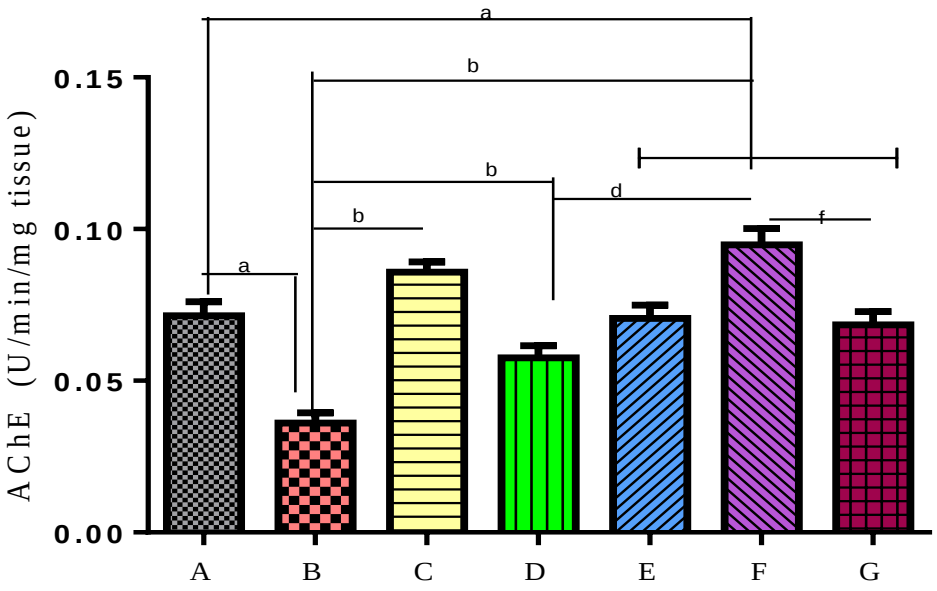

Figure 4.6: Variations in acetylcholinesterase level of the PFC.

The coloured bars represent levels of acetylcholinesterase (AChE) in each group (A-G) of the experiment. The horizontal lines with superscript alphabets joining directly with the vertical lines above the groups, indicates significant difference in the level of AChE between groups connected by the horizontal lines. [a] represent significant difference in the level of AChE in B and F when compared with A. [b] represent significant difference in the level of AChE in C-G when compared with B. [d] represent significant difference in the level of AChE between F and D. [f] represent significant difference in the level of AChE between G and F

Keys: A= Control; B = Lead (Pb); C =Vitexin; D = Pb+Vitexin (Male); E= Pb+Vitexin (Female); F =Pre-treated with vitexin; G =Post-treated with vitexin.

4.3.4 Changes in nitric oxide level

The levels of nitric oxide (Figure 4.7) in all the treated groups were significantly low ($p<0.05$) when compared with the control group (53±4.1 mg/dl). In Pb treated group (6.6±3.4 mg/dl), the level of nitric oxide (NO) was significantly low ($p<0.05$) when compared with Pb + Vitexin (M), Pb + Vitexin (F), and Vitexin pre-treated groups (27±1.7 mg/dl; 29±0.93 mg/dl; and 24±3.7 mg/dl respectively). Conversely, the level of NO in Pb treated group was not significantly different ($p >0.05$) when compared with Vitexin post-treated group. Also, no significant difference ($p >0.05$) was found between Pb + Vitexin (M) group and Pb + Vitexin (F) group; neither was there a significant difference between Vitexin pre-treated and Vitexin post-treated groups when comparisons were made. Nevertheless, the level of NO in Pb + Vitexin (F) group (29±0.93 mg/dl) was significantly high ($p<0.05$) when compared with either Vitexin pre-treated group (24±3.7 mg/dl) or Vitexin post-treated group (12±5.4 mg/dl).

Nitric oxide level

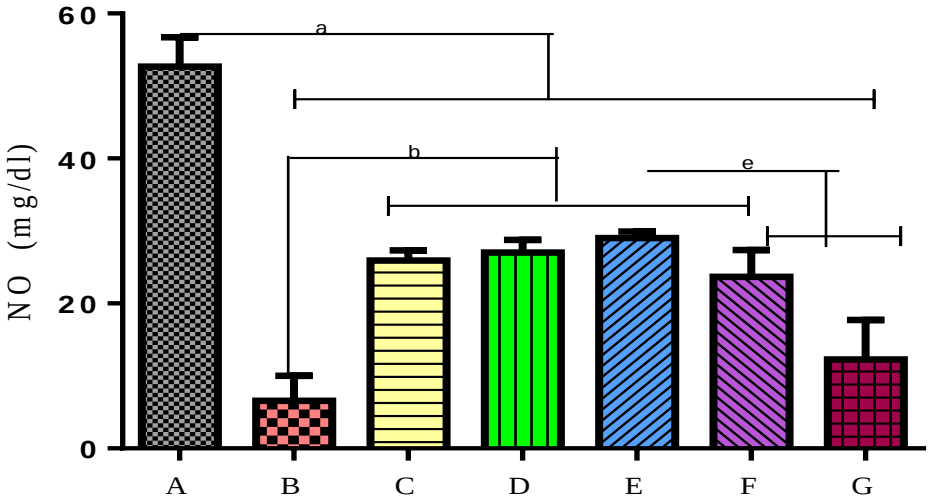

Figure 4.7: Variations in nitric oxide level of the PFC.

The coloured bars represent levels of nitric oxide (NO) in each group (A-G) of the experiment. The horizontal lines with superscript alphabets joining directly with the vertical lines above the groups, indicates significant difference in the level of NO between groups connected by the horizontal lines. [a] represent significant difference in the level of NO in B-G when compared with A. [b] represent significant difference in the level of NO in C-F when compared with B. [e] represent significant difference in the level of NO in F & G when compared with E.

Keys: A= Control; B = Lead (Pb); C =Vitexin; D = Pb+Vitexin (Male); E= Pb+Vitexin (Female); F =Pre-treated with vitexin; G =Post-treated with vitexin.

4.4 Neurobehavioural observation

4.4.1 Changes in working memory

4.4.1.1 Barnes maze test

The result of the Barnes maze test (Figure 4.8) showed that during the first and second trials (Figure 4.8 A & B), the mice in all the groups showed the same ($p > 0.05$) latency to locate the dropbox. However, at the third trial (Figure 4.8 C), Pb treated group (102±3.8 s) showed longer ($p < 0.05$) latency when compared with Vitexin treated group (74±5.9 s). Also, during the third trial (Figure 4.8 C), the latency to locate the dropbox was not significantly different ($p > 0.05$) when the treated groups were compared with the control group. At the fourth trial (Figure 4.8 D), Pb treated group (92±3.8 s) showed longer ($p < 0.05$) latency when compared with the control group (63±4.5 s). Similarly, at the fourth trial (Figure 4.8 D), Pb treated group (92±3.8 s) showed longer ($p < 0.05$) latency when compared with Pb + Vitexin (F), Vitexin pre-treated and Vitexin post-treated groups (60±3.7 s; 65±6.8 s; and 66±4.8s respectively). Conversely, all the treated groups (except Pb treated group) showed no significant difference ($p > 0.05$) when compared with the control group at the fourth trial (Figure 4.8 D).

During the main test (Figure 4.8 E), the mice in all the treated groups (except Pb treated group) showed no significant difference ($p > 0.05$) in latency to locate the drop box when compared with the control group (53±5.4s). On the other hand, mice in the Pb treated group (82±3.8 s) showed longer ($p < 0.05$) latency to locate the drop box when compared with Pb + vitexin (M) group (63±3.0 s) and Pb +Vitexin (F) group (58±2.9 s). Similarly, mice in Pb treated group (82±3.8 s) showed longer ($p < 0.05$) latency to locate the drop box when compared with Vitexin pre-treated group (62±5.2s) and Vitexin post-treated group (60±4.1s). Furthermore, there was no significant difference ($p > 0.05$) between all the treated groups (except Pb treated group) when comparisons were made (Figure 4.8 E).

The number of incorrect holes visited by the mice (Figure 4.8 F) in the Pb treated group (7.8±0.31) were significantly high ($p<0.05$) when compared with mice in the control group (5.3±0.49). Similarly, mice in Pb treated group visited more ($p<0.05$) in-corrected holes when compared with mice in Pb + vitexin (F) group, Vitexin pre-treated, and Vitexin post-treated groups (6.2±031; 6.3±0.42; and 6.2±0.31 respectively).

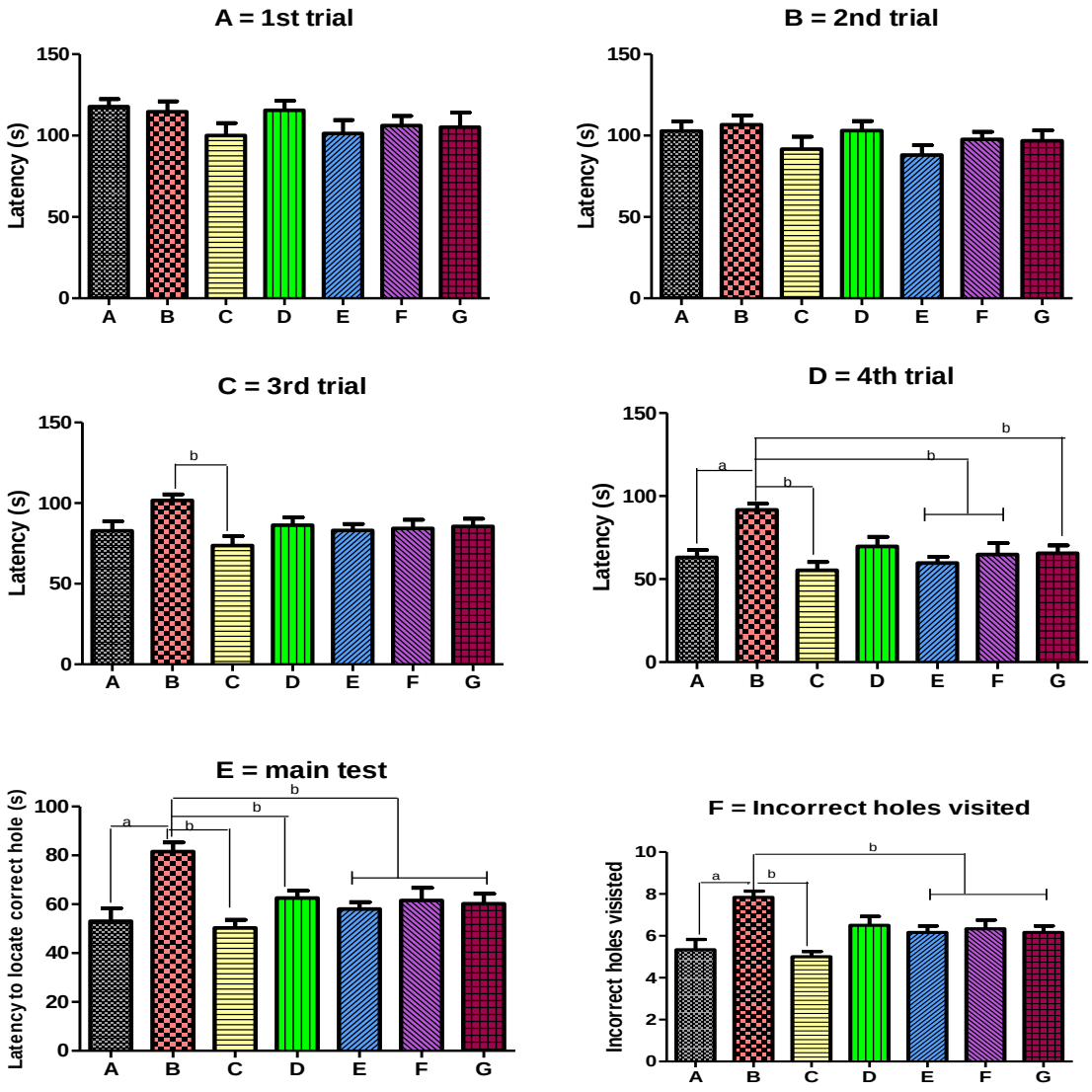

Figure 4.8: (A-F): Barnes maze test.

This figure represent changes in learning and working memory according to 1st trial (A), 2nd trial (B), 3rd trial (C) & 4th trials (D); as well as main test with incorrect holes visited (E-F). The coloured bars represent each group (A-G) of the experiment. The horizontal lines with superscript alphabets joining directly with the vertical lines above the groups, indicates significant difference between groups connected by the horizontal lines. [a] represent groups that are significantly different from A; [b] represent groups that are significantly different from B.

Keys: A= Control; B = Lead (Pb); C =Vitexin; D = Pb+Vitexin (Male); E= Pb+Vitexin (Female); F =Pre-treated with vitexin; G =Post-treated with vitexin.

4.4.1.2 Novel object recognition test

In Figure 4.9 A, mice in Pb treated group (32±3.3 s), spent longer ($p<0.05$) time observing old objects when compared with the control group (15±2.6 s) as well as Vitexin group (18±1.3 s). However, mice in Vitexin group, Pb + Vitexin (M) group, and Pb +Vitexin (F) group spent almost the same time ($p >0.05$) observing old objects when compared with the control group (15±2.6 s). Additionally, mice in Vitexin pre-treated group, and Vitexin post-treated group spent almost the same time ($p >0.05$) observing old objects when compared with the control group. Furthermore, the time spent observing old object by mice in all the treated groups (except Pb treated group) was not significantly different ($p >0.05$) when comparisons were made between the treated groups.

When new and old objects were presented to the mice (Figure 4.9 B & C), Pb treated group (24±1.0 s) mice, spent significantly short ($p<0.05$) time exploring the new object when compared with the control group (45±2.9 s) mice. Although mice in other treated groups (except Vitexin treated group) explored the new object longer than mice in Pb treated group (24±1.0 s), the difference were not significant ($p >0.05$). Furthermore, there was no significant difference ($p >0.05$) in time spent observing the new object by mice in all the treated groups (except Pb treated group) when comparisons were made between the groups.

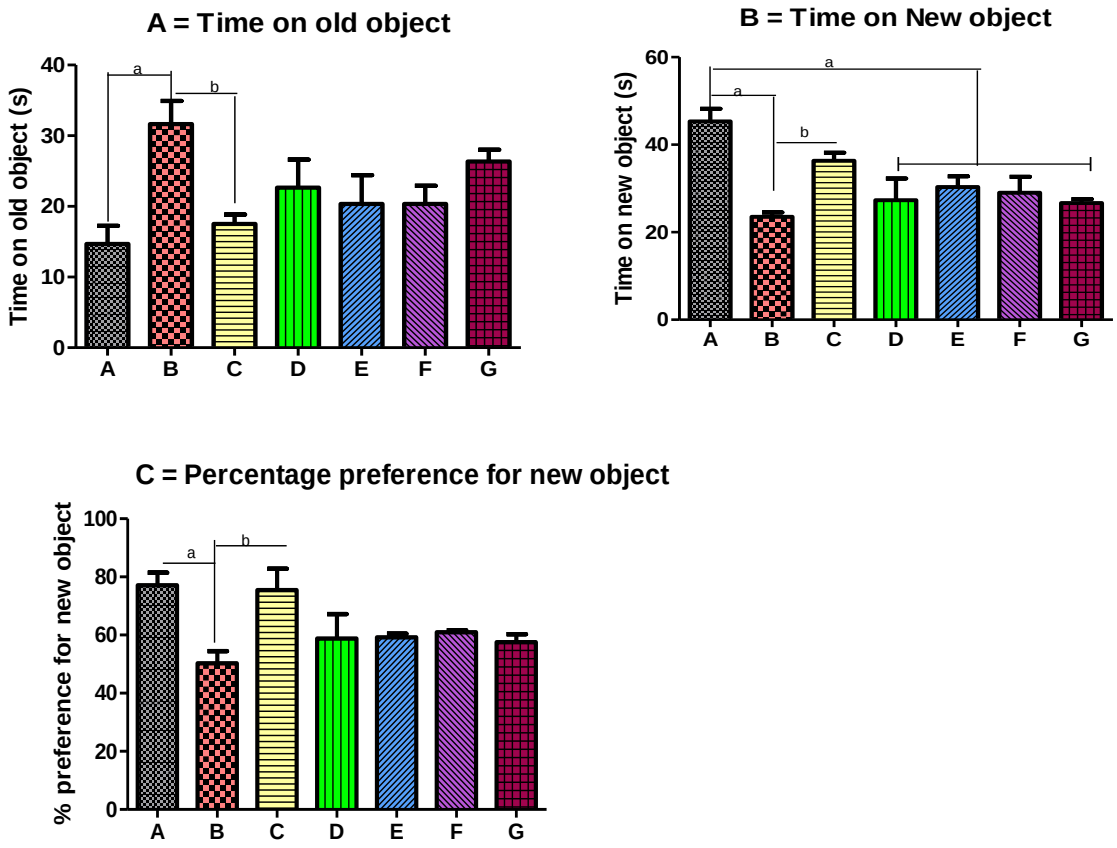

Figure 4.9: (A-C): Novel object recognition test.

This figure represent changes in learning and working memory according to time spent on old object (A), time spent on new object (B) and percentage preference for new object (C). The coloured bars represent each group (A-G) of the experiment. The horizontal lines with superscript alphabets joining directly with the vertical lines above the groups, indicates significant difference between groups connected by the horizontal lines. [a] represent groups that are significantly different from A; [b] represent groups that are significantly different from B.

Keys: A= Control; B = Lead (Pb); C =Vitexin; D = Pb+Vitexin (Male); E= Pb+Vitexin (Female); F =Pre-treated with vitexin; G =Post-treated with vitexin.

4.4.1.3 Y- maze test

The result from Y- maze test (Figure 4.10), showed that mice in Pb treated group (29±4.9 %) had significantly low ($p<0.05$) percentage alternation when compared with the control group (60±3.2 %). Similarly, mice in Pb treated group (29±4.9 %) also had significantly low ($p<0.05$) percentage alternation when compared with Vitexin group, Pb + Vitexin (M) group, and Pb + Vitexin (F) group (53±2.1 %; 52±5.0 %; and 51±5.9 % respectively). Conversely, the percentage alternation of mice in Pb treated group was not significantly different ($p >0.05$) when compared with Vitexin pre-treated and Vitexin post-treated groups. Likewise, percentage alternation in all the treated groups (except Pb treated group) were not significantly different ($p >0.05$) when compared with the control group (60±3.2 %). Furthermore, there was no significant difference ($p>0.05$) in percentage alternation between all the treated groups (except Pb treated group) when comparisons were made.

Y- maze test

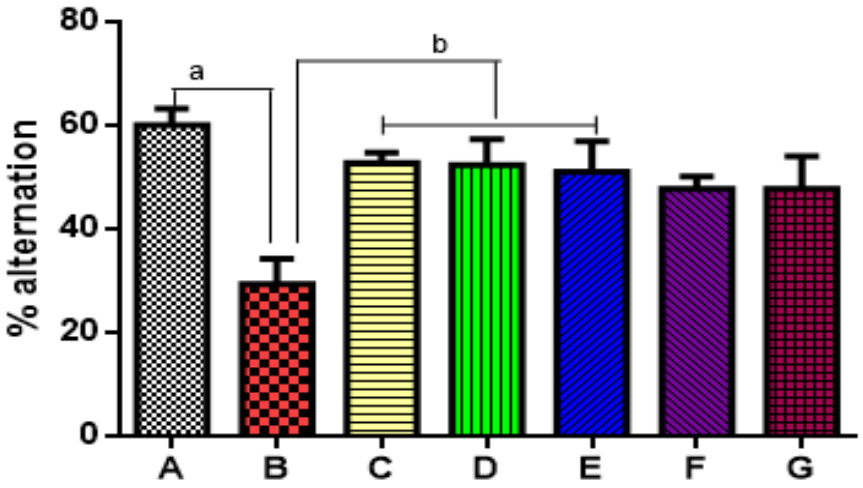

Figure 4.10: Y-maze test.

This figure represent changes in learning and working memory according to percentage alternation made by mice in various groups. The coloured bars represent each group (A-G) of the experiment. The horizontal lines with superscript alphabets joining directly with the vertical lines above the groups, indicates significant difference between groups connected by the horizontal lines. [a] represent group that has significantly different percentage alternation from A; [b] represent groups (C, D & E) that have significantly different percentage alternation from B.

Keys: A= Control; B = Lead (Pb); C =Vitexin; D = Pb+Vitexin (Male); E= Pb+Vitexin (Female); F =Pre-treated with vitexin; G =Post-treated with vitexin.

4.4.2 Changes in depression-like behaviour

4.4.2.1 Tail suspension test

The immobility time (Figure 4.11) of mice in Pb treated group (193±2.1 s) was significantly longer ($p<0.05$) than the control group (147±17 s). Similarly, the immobility time of mice in Pb treated group (193±2.1 s) was significantly longer ($p<0.05$) than mice in Pb + Vitexin (M), and Pb + Vitexin (F) groups (166±3.4 s and 164±2.2 s respectively). In addition, mice in Pb treated group (193±2.1 s) had significantly longer ($p<0.05$) immobility time when compared with Vitexin pre-treated and Vitexin post-treated groups (168±3.1 s; and 158±4.6 s respectively). In contrast, mice in Vitexin group (105±1.6 s) showed significantly shorter ($p<0.05$) immobility time when compared with the control group (147±17 s). Also, mice in Vitexin group (105±1.6 s) showed significantly shorter ($p<0.05$) immobility time when compared with Pb + Vitexin (M), and Pb + Vitexin (F) groups (166±3.4 s and 164±2.2 s respectively). Likewise, the immobility time of mice in Vitexin group (105±1.6 s) was significantly shorter ($p<0.05$) than mice in Vitexin pre-treated and Vitexin post-treated groups (168±3.1 s; and 158±4.6 s respectively). When Pb + Vitexin (M), Pb + Vitexin (F), Vitexin pre-treated and Vitexin post-treated groups were compared with the control group, no significant difference ($p>0.05$) in immobility time of mice was found. Furthermore, the immobility time of mice (Figure 4.11) in Pb + Vitexin (M), Pb + Vitexin (F), Vitexin pre-treated and Vitexin post-treated groups were not statistically different ($p>0.05$) when comparisons were made between those groups.

Tail suspension test

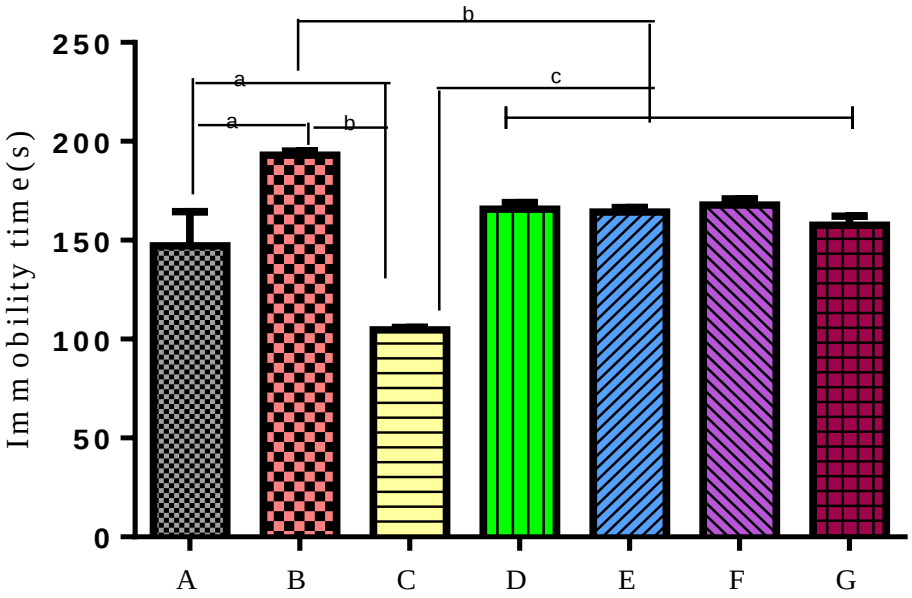

Figure 4.11: Tail suspension test.

The figure represent changes in depressive behaviour according to variation in immobility time of mice in various groups. The coloured bars represent each group (A-G) of the experiment. The horizontal lines with superscript alphabets joining directly with the vertical lines above the groups, indicates significant difference between groups connected by the horizontal lines. [a] represent groups (B and C) that have significantly different immobility time from A; [b] represent groups (C-G) that have significantly different immobility time from B. [c] represent groups (D-G) that have significantly different immobility time from B.

Keys: A= Control; B = Lead (Pb); C =Vitexin; D = Pb+Vitexin (Male); E= Pb+Vitexin (Female); F =Pre-treated with vitexin; G =Post-treated with vitexin.

4.4.3 Changes in anxiety-like behaviour

4.4.3.1 Elevated plus-maze test

The percentage open arm entries (Figure 4.12) by mice in Pb treated group, Vitexin pre-treated and Vitexin post-treated groups (23±2.7 %; 27±0.77 %; and 27±0.32 % respectively) were significantly lower ($p<0.05$) than the control group (43±2.3 %). In contrast, the percentage open arm entries by mice in Vitexin group, Pb + Vitexin (M), and Pb + Vitexin (F) groups were not statistically different from the control group (43±2.3 %) when comparisons were made. Although there was an increase in percentage open arm entry by mice in Pb + Vitexin (M), and Pb + Vitexin (F) groups (when compared with Pb treated group), the results were not significant ($p >0.05$). Likewise, when the percentage open arm entries were compared between the treated groups (except Pb treated group), no significant difference ($p>0.05$) was found.

Elevated plus maze

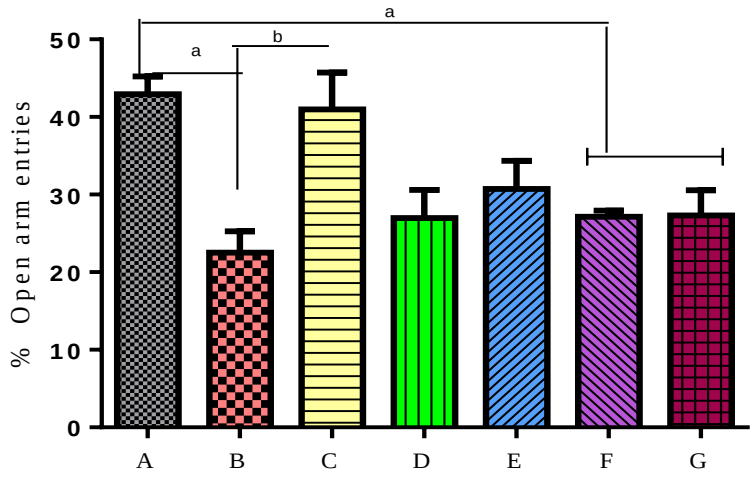

Figure 4.12: Elevated plus test.

The figure represent changes in anxiety behaviour based on the variation of open arm entries by mice in various groups. The coloured bars represent each group (A-G) of the experiment. The horizontal lines with superscript alphabets joining directly with the vertical lines above the groups, indicates significant difference between groups connected by the horizontal lines. [a] represent groups (B, F and G) that have significantly different open arm entries from A; [b] represent group (C) that has significantly different open arm entry from B.

Keys: A= Control; B = Lead (Pb); C =Vitexin; D = Pb+Vitexin (Male); E= Pb+Vitexin (Female); F =Pre-treated with vitexin; G =Post-treated with vitexin.

4.4.3.2 Open field test

In Figure 4.13 (the open field test), the mice in Pb treated group (69±6.6 s) spent less ($p<0.05$) time within the inner zone of the test box when compared with the control group (133±14 s). Although the mice in Pb + Vitexin (M), and Pb + Vitexin (F) groups spent more time in the inner zone of the box than mice in the Pb treated group, the difference was not statistically significant ($p >0.05$) neither was there any significant difference ($p >0.05$) when Vitexin pre-treated and Vitexin post-treated groups were compared with the Pb treated group. Furthermore, when all the treated groups (except Pb treated group) were compared with the control group, no significant difference ($p >0.05$) was found. In contrast, mice in Vitexin group (154±13 s) spent more time ($p<0.05$) within the inner zone of the test box than mice in Pb + Vitexin (M), Pb + Vitexin (F) and Vitexin post-treated groups (101±6.7 s; 93±12 s; and 101±7.9 s respectively). Furthermore, there was no significant difference ($p>0.05$) in time spent within the inner zone by mice of the Pb + Vitexin (M) group, and Pb + Vitexin (F) group neither was there a significant difference ($p>0.05$) between Vitexin pre-treated and Vitexin post-treated groups.

Open field test: Time in inner zone

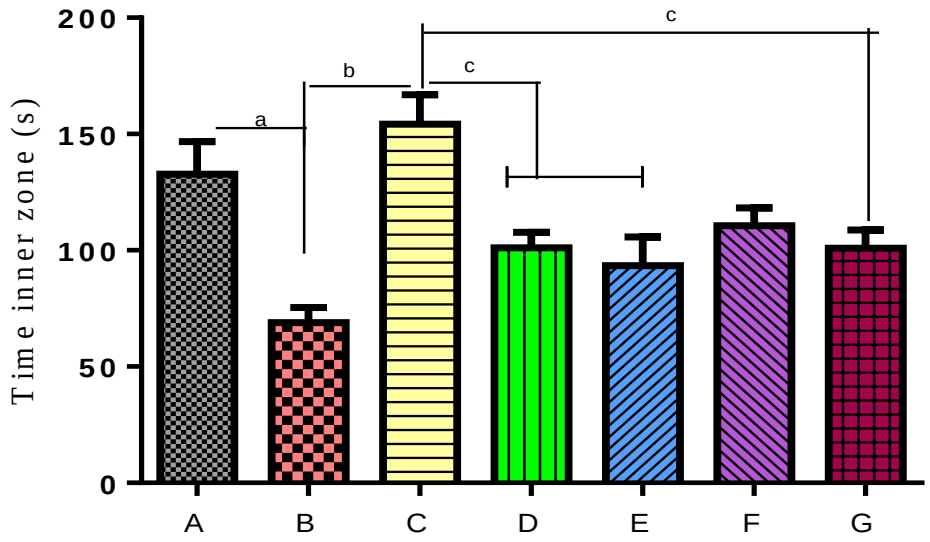

Figure 4.13: **Open field test.**

The figure represent changes in anxiety behaviour based on variation in time spent within the inner zone of the test box by mice in various groups. The coloured bars represent each group (A-G) of the experiment. The horizontal lines with superscript alphabets joining directly with the vertical lines above the groups, indicates significant difference between groups connected by the horizontal lines. [a] represent group (B) that spent significantly short time in the inner zone when compared with A; [b] represent group (C) that spent significantly long time in the inner zone when compared with B. [c] represent groups (D, E and G) that spent significantly short time in the inner zone when compared with C.

Keys: A= Control; B = Lead (Pb); C =Vitexin; D = Pb + Vitexin (M); E= Pb + Vitexin (Female); F =Pre-treated with vitexin; G =Post-treated with vitexin.

4.4.4 Alterations in motor behaviour

4.4.4.1 Hanging test

The result from the hanging test (Figure 4.14) shows that, mice in all the treated groups displayed shorter ($p<0.05$) latency to fall when compared with the control group (650±21 s). Similarly, the mice in Vitexin group (349±17 s) showed significantly short ($p<0.05$) latency to fall when compared with mice in Pb + Vitexin (M) and Pb +Vitexin (F) groups (457±28 s and 464±28 s respectively). In contrast, the latency to fall by mice in Vitexin group (349±17 s) was not significantly different ($p >0.05$) when compared with Vitexin pre-treated (437±17 s) and Vitexin post-treated (408±18 s) groups. Similarly, the latency to fall by mice in Pb treated group (506±25 s) was not significantly different ($p >0.05$) when compared with mice in Pb + Vitexin (M) and Pb +Vitexin (F) groups (457±28 s and 464±28 s respectively). Furthermore, the latency to fall by mice in Pb treated group (506±25 s) was not significantly different ($p >0.05$) when compared with mice in Vitexin pre-treated (437±17 s) and Vitexin post-treated (408±18 s) groups.

Hanging test

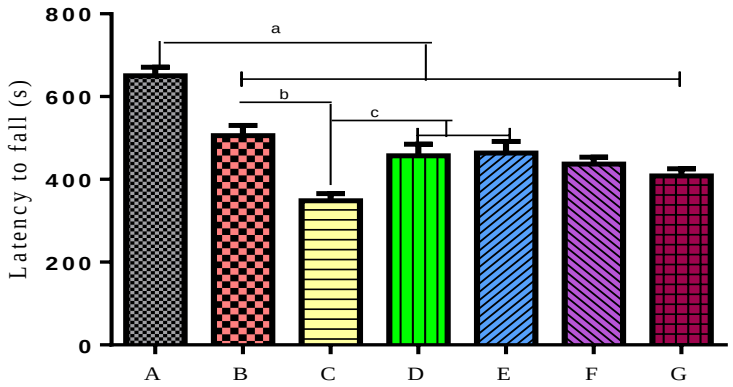

Figure 4.14: Hanging test.

The figure represent changes in motor behaviour based on the latency to fall by mice in various groups. The coloured bars represent each group (A-G) of the experiment. The horizontal lines with superscript alphabets joining directly with the vertical lines above the groups, indicates significant difference between groups connected by the horizontal lines. [a] represent groups (B-G) that have significantly short latency to fall when compared with A; [b] represent group (C) that has significantly short latency to fall when compared with B. [c] represent groups (D and E) that have significantly long latency to fall when compared with C.

Keys: A= Control; B = Lead (Pb); C =Vitexin; D = Pb + Vitexin (M); E= Pb + Vitexin (Female); F =Pre-treated with vitexin; G =Post-treated with vitexin.

4.4.4.2 Footprint test

The results of the footprint test (Figure 4.15 A) shows that, stride length of mice in Pb treated group (3.8±0.27 cm) and Pb + Vitexin (M) group (4.1±0.30 cm) were significantly shorter ($p<0.05$) when compared with the control group (5.4±0.31 cm). On the other hand, the stride length of mice in Vitexin group and Pb + Vitexin (F) group were not significantly different ($p>0.05$) with the control group. Similarly, the stride length of mice in Vitexin pre-treated group and Vitexin post-treated group were not significantly different ($p>0.05$) with the control group. Furthermore, the stride length of mice compared between the treated groups was not significantly different ($p>0.05$) when comparisons were made.

The base width (Figure 4.15 B) of mice foot in all the treated groups were significantly narrow ($p<0.05$) when compared with mice in the control group (2.0±0.15 cm). However, when the base width of mice foot in Vitexin post-treated group (1.7±0.092 cm) was compared with the control group (2.0±0.15), no significant difference ($p>0.05$) was found. Also, the comparison of base width of mice foot between the treated groups did not show any significant difference ($p>0.05$).

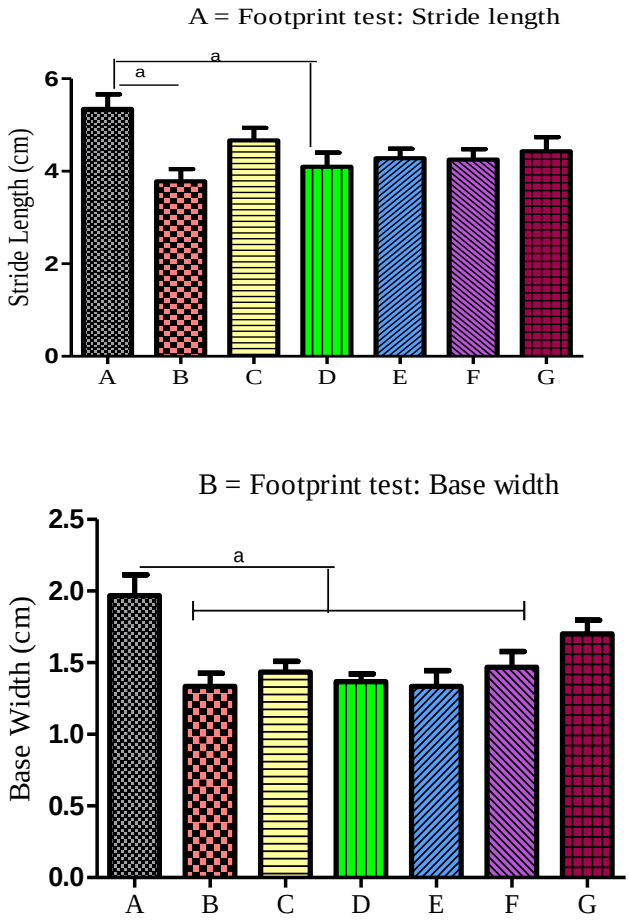

Figure 4.15A & B: Footprint test

The figure represent changes in locomotor behaviour in mice, based on the stride length (4.15 A) and base width (4.15 B) among mice in various groups. The coloured bars represent each group (A-G) of the experiment. The horizontal lines with superscript alphabets joining directly with the vertical lines above the groups, indicates significant difference between groups connected by the horizontal lines. For stride length (4.15A), [a] represent groups (B & D) that have significantly short stride lengths when compared with A. For base width (4.15 B), [a] represent groups (B-F) that have significantly short base width when compared with A.

Keys: A= Control; B = Lead (Pb); C =Vitexin; D = Pb + Vitexin (M); E= Pb + Vitexin (Female); F =Pre-treated with vitexin; G =Post-treated with vitexin.

4.5 Qualitative Analysis

4.5.1 Histological observation of the prefrontal cortex

4.5.1.1 Expression of prefrontal cortical layers using Haematoxylin and Eosin stain

The representative photomicrographs of Haematoxylin and Eosin (H & E) stain, shows the control group (Figure 4.16 A) with good cortical delineation of layers (with layer 1 very distinct). In Pb treated group (Figure 4.16 B), layer 1 (L1) was thinner, while other layers were not distinct. Vitexin group (Figure 4.16 C) presented similar cytoarchitecture and arrangement to the control group. In Pb + Vitexin (M) group (Figure 4.16 D), layers I & II were not distinct; however, Pb + Vitexin (F) group ((Figure 4.16 E) showed distinctly clear layers I-III with layer I thicker than the other layers. In Vitexin pre-treated group (Figure 4.16 F), layers II-III were distinct and clear, but layer I was not. In the photomicrograph of Vitexin post-treated group (Figure 4.16 G), layers I-III were distinct, but other layers were not distinct enough for identification.

Figure 4.16A-G: Representative photomicrographs of H&E stain in mice prefrontal cortex (Scale bar 180 µm). The control group (A), showed good cortical delineation of layers (L1-L3). In Pb treated group (B), layer 1 (L1) was thinner, while other layers were not distinct. Vitexin group (C) presented similar cytoarchitecture and arrangement to the control group. In Pb + Vitexin (M) group (D), layers I-II (L1-L2) were not distinct; however, Pb + Vitexin (F) group (E) showed distinctly clear layers I-III (L1-L3) with layer I (L1) thicker than the other layers. In Vitexin pre-treated group (F), layers II-III (L2-L3) were distinct and clear, but layer I (L1) was not. In the photomicrograph of Vitexin post-treated (G), layers I-III (L1-L3) were distinct, but other layers were not distinct enough for identification.

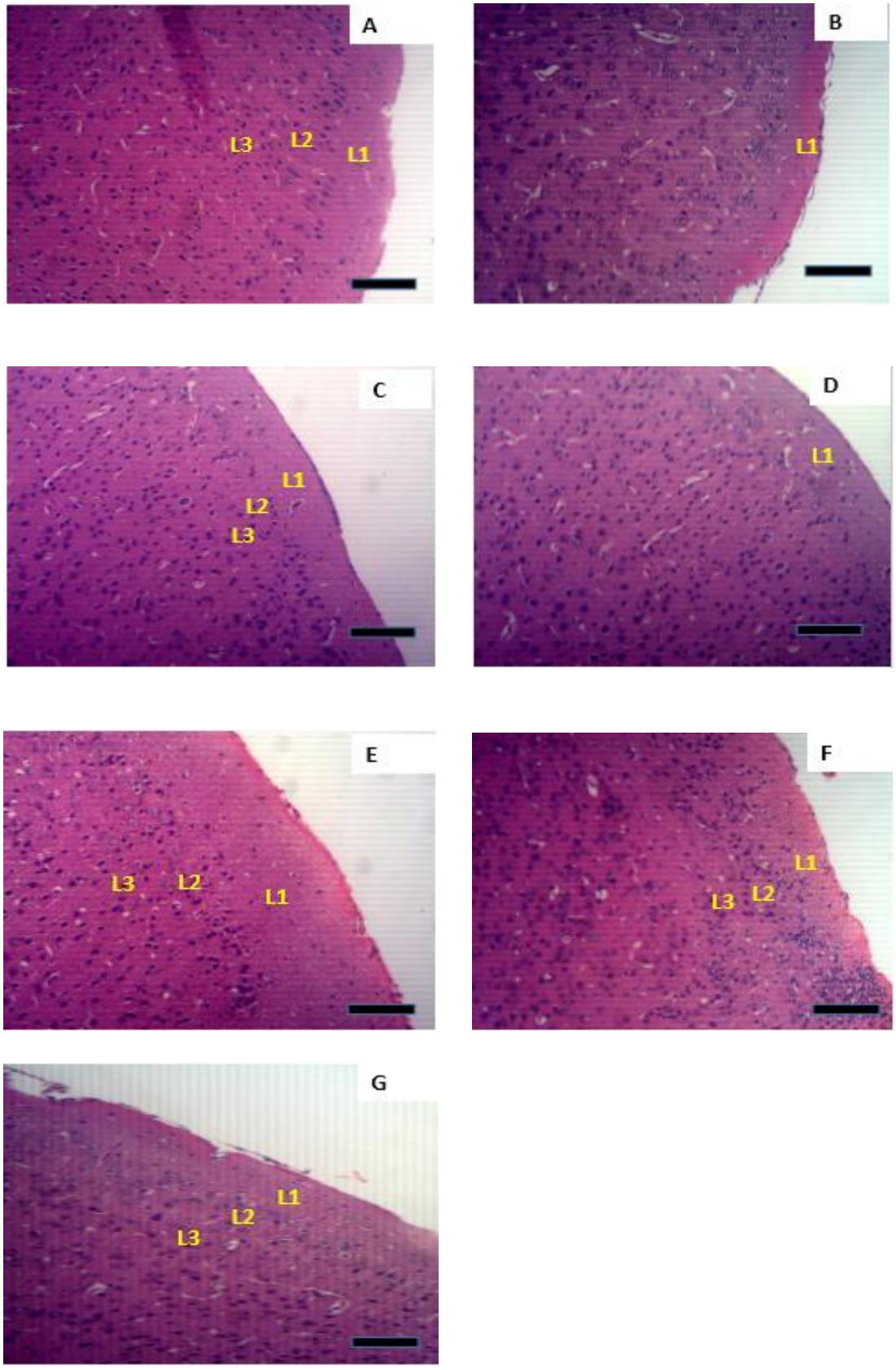

Figure 4.16 A-G

4.5.1.2 Expression of tissue cytoarchitecture using Haematoxylin and Eosin stain

The photomicrograph of the control group (Figure 4.17 A) was characterised by numerous large pyramidal neurons with very few degenerating neurons. In Pb treated group (Figure 4.17 B), there were degenerative changes characterised by numerous shrunken neurons with angular cell bodies, fragmented cytoplasm and condensed nuclei (pyknosis) within the soma. Vitexin group (Figure 4.17 C) present similar cytoarchitectural features as seen in the control group. Furthermore, Pb + Vitexin (M) and Pb + Vitexin (F) groups (Figure 4.17 D & E) shows little degenerative changes when compared with Pb treated group. Also, Vitexin pre-treated and Vitexin post-treated groups (Figure 4.17 F & G), were characterised by few degenerative changes when compared with Pb treated group.

Figure 4.17A-G: Representative photomicrographs of H&E stain in mice prefrontal cortex at higher magnification (Scale bar 45 μm). The control group (A) was characterised by numerous large pyramidal neurons (black arrows) with very few degenerating neurons (yellow arrows). In Pb treated group (B), there were degenerative changes characterised by numerous shrunken neurons with angular cell bodies, fragmented cytoplasm and condensed nuclei (pyknosis) within the soma (yellow arrows). Vitexin group (C) present similar cytoarchitectural features as seen in the control group. Furthermore, Pb + Vitexin (M) and Pb + Vitexin (F) groups (D and E) shows little degenerative changes (yellow arrows) when compared with Pb treated group. Also, Vitexin pre-treated and Vitexin post-treated groups (F and G) were characterised by few degenerative changes (yellow arrows) when compared with Pb treated group.

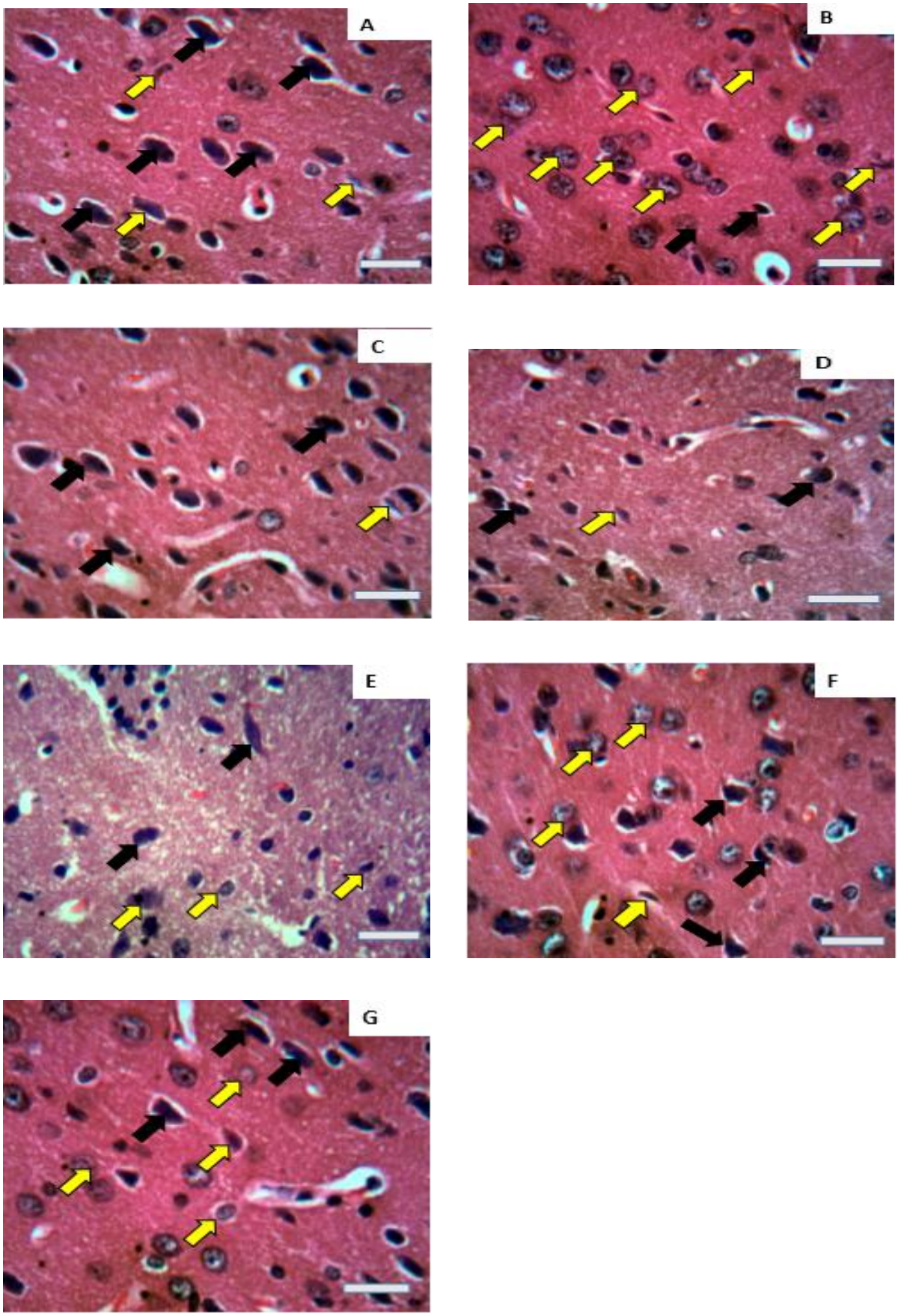

Figure 4.17 A-G

4.5.2 Histochemical observation of the prefrontal cortex

4.5.2.1 Cresyl fast violet (CFV)

The prefrontal cortex section of Vitexin group (Figure 4.18 C) stain intensely for numerous Nissl bodies with fewer chromatolytic cells observed. These observations were similar to the Control group (Figure 4.18 A). In Pb treated group (Figure 4.18 B), numerous cells were observed to have undergone chromatolysis; with many neurons staining less intensely to Nissl dye when compared with the Control group. The Pb + Vitexin (M), and Pb + Vitexin (F) groups (Figure 4.18 D & E) showed few chromatolytic cells, with the number of cells that stain intensely with Nissl dye much higher when compared with the Pb treated group (Figure 4.18 B). The photomicrograph of Vitexin post-treated group (Figure 4.18 G), showed numerous, less intensely stained cells, with high chromatolytic features, almost similar to the observation in Pb treated group.

Figure 4.18A-G: Representative photomicrographs of cresyl fast violet (CFV) stain in mice prefrontal cortex (Scale bar 45 µm). The tissue section of Vitexin group (C) stain intensely for numerous Nissl bodies (red arrows) with fewer chromatolytic cells (yellow arrows) when observation was made. These observations were similar to the Control group (A). In Pb treated group (B), numerous cells were observed to have undergone chromatolysis (yellow arrows); with many neurons staining less intensely to Nissl dye when compared with the Control group (A). The Pb + Vitexin (M), and Pb + Vitexin (F) groups (D and E) showed few chromatolytic cells (yellow arrows), with the number of cells that stain intensely with Nissl dye much higher when compared with the Pb treated group (B). The photomicrograph of Vitexin post-treated group (G), showed numerous, less intensely stained cells, with high chromatolytic features (yellow arrows), almost similar to the observation in Pb treated group.

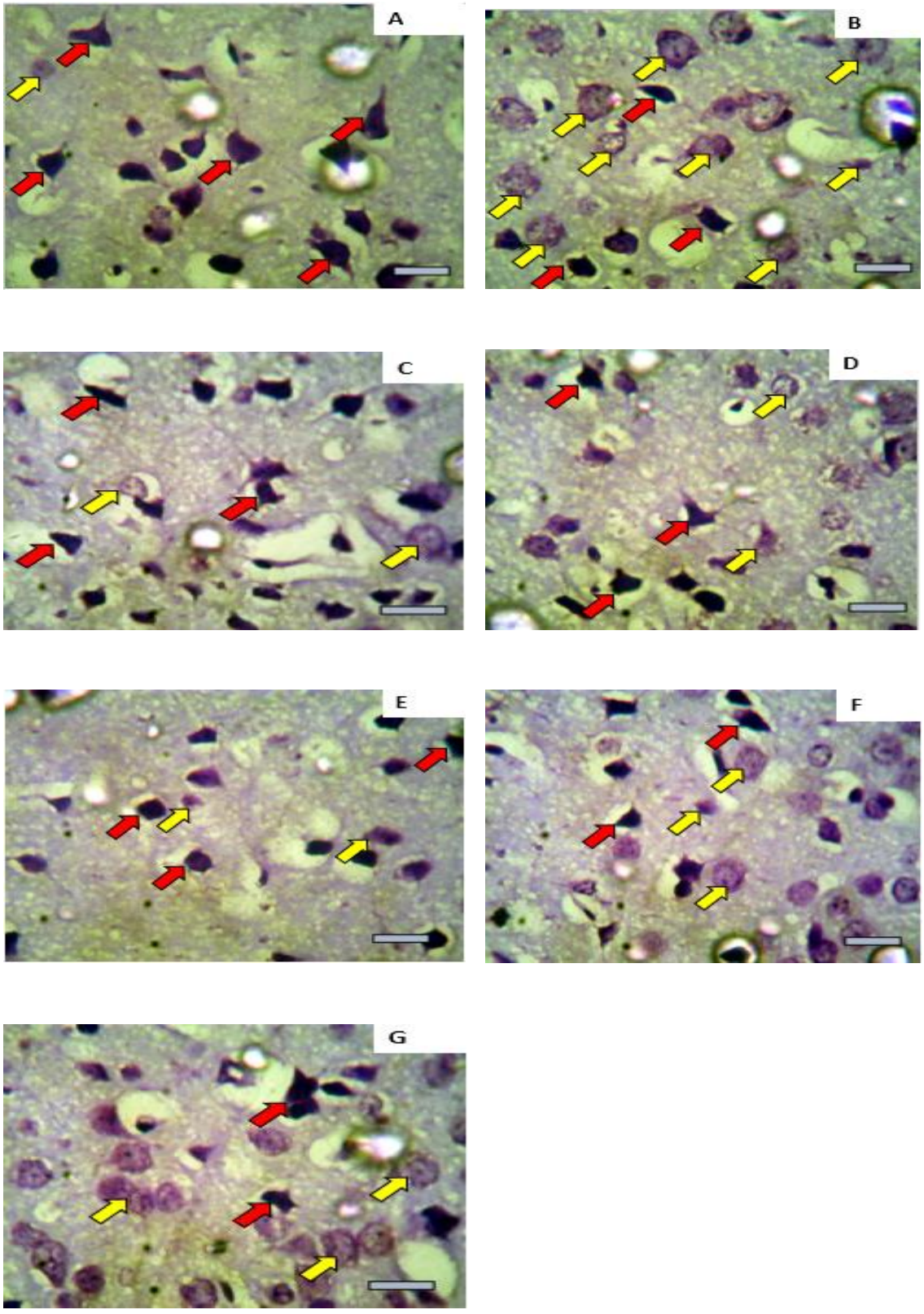

Figure 4.18 A-G

4.5.2.2 Congo red stain

Amyloid protein expression was not significant enough to draw inference from all the treated groups (Figure 4.19 B-G) as well as the control group (Figure 4.19 A).

Figure 4.19A-G: Representative photomicrographs of Congo red stain in mice prefrontal cortex (Scale bar 45 µm). Amyloid protein expression was not significant enough to draw inference from all the treated groups (B-G) as well as the control group (A).

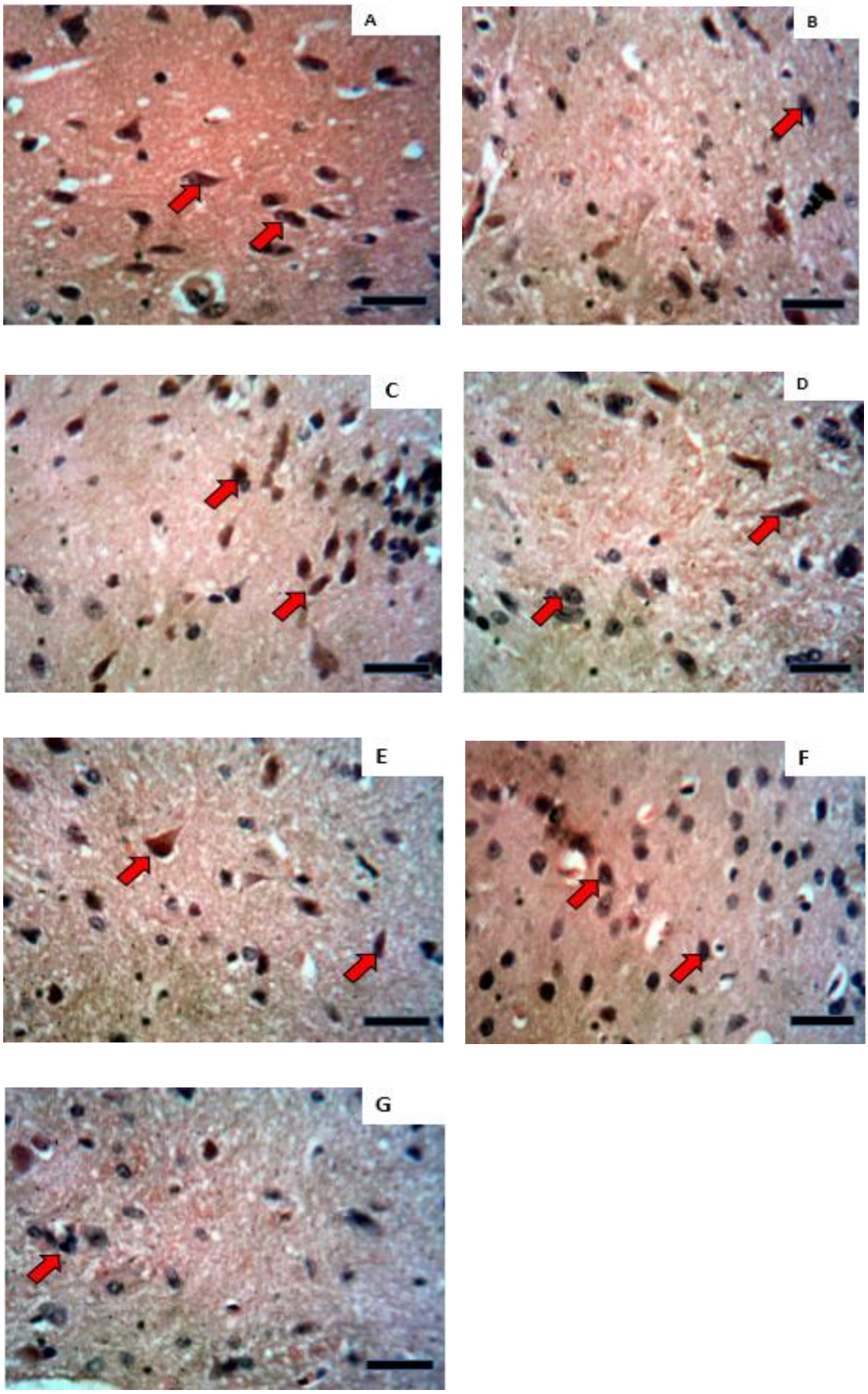

Figure 4.19 A-G

4.5.2.3 Bielchowsky stain

In Figure 4.20, senile plaques were observed in all the treated groups except the Vitexin group (Figure 4.20 C). However, the senile plaques observed, were more numerous in Pb treated (Figure 4.20 B) and Vitexin post-treated groups (Figure 4.20 G).

Figure 4.20A-G: Representative photomicrographs of Bielchowsky stain in mice prefrontal cortex (Scale bar 45 µm). Senile plaques (yellow arrows) were observed in all the treated groups except the Vitexin group (C). The senile plaques observed, were more numerous in Pb treated (B) and Vitexin post-treated groups (G).

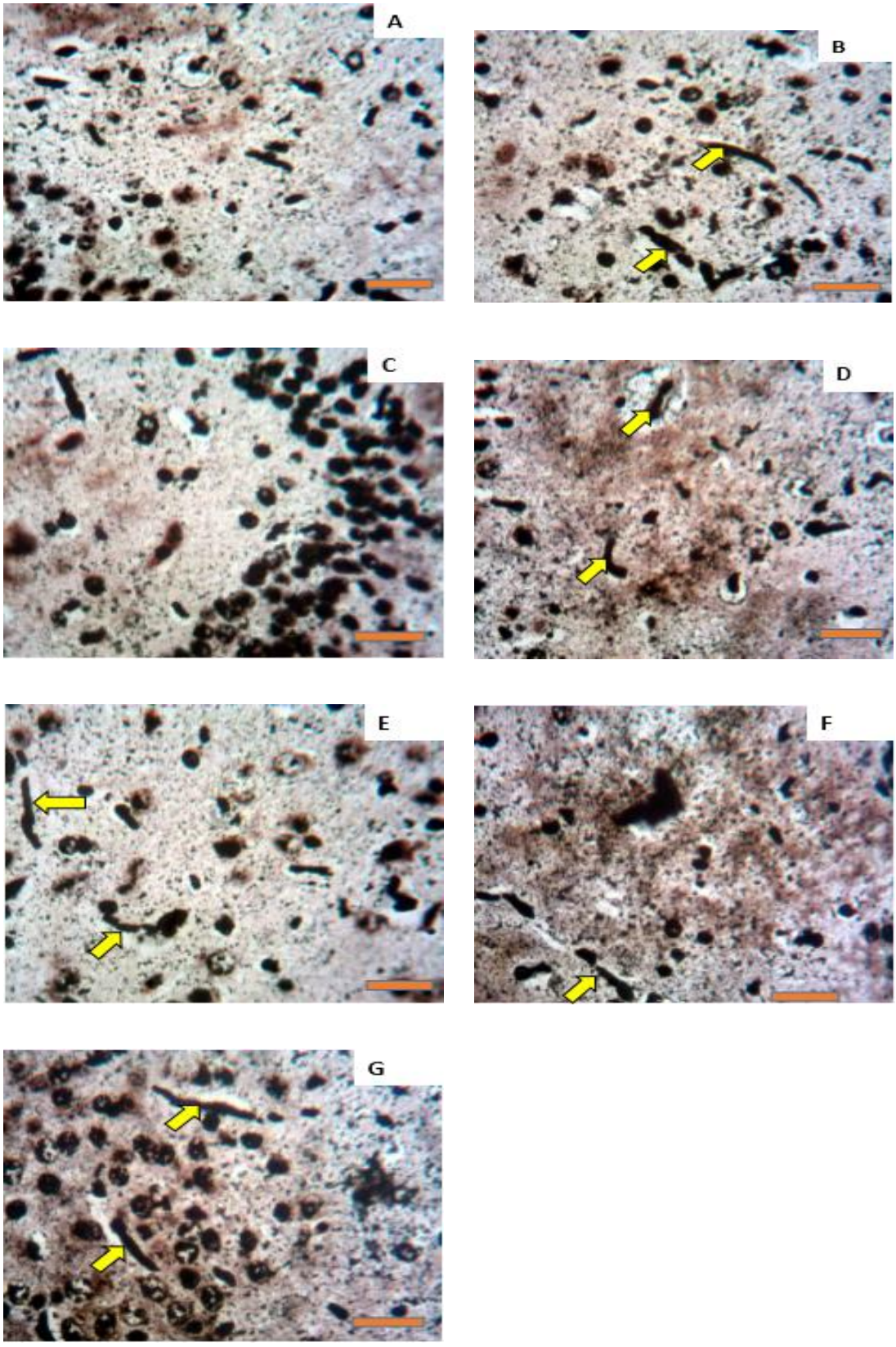

Figure 4.20 A-G

4.5.3 Immunohistochemical observation of the prefrontal cortex

4.5.3.1 Glial fibrillary acidic protein (GFAP) stain

Astrocytes immunoreactivity were not present in any of the treated groups (Figure 4.21 B-G). Likewise, the control group (Figure 4.21 A) did not express immunoreactivity despite the presence of astrocytes.

Figure 4.21A-G: Representative photomicrographs of glial fibrillary acidic protein (GFAP) stain in mice prefrontal cortex (Scale bar 45 μm). Astrocytes immunoreactivity were not present in any of the treated groups (B-G). Likewise, the control group (A) did not express immunoreactivity despite the presence of astrocytes.

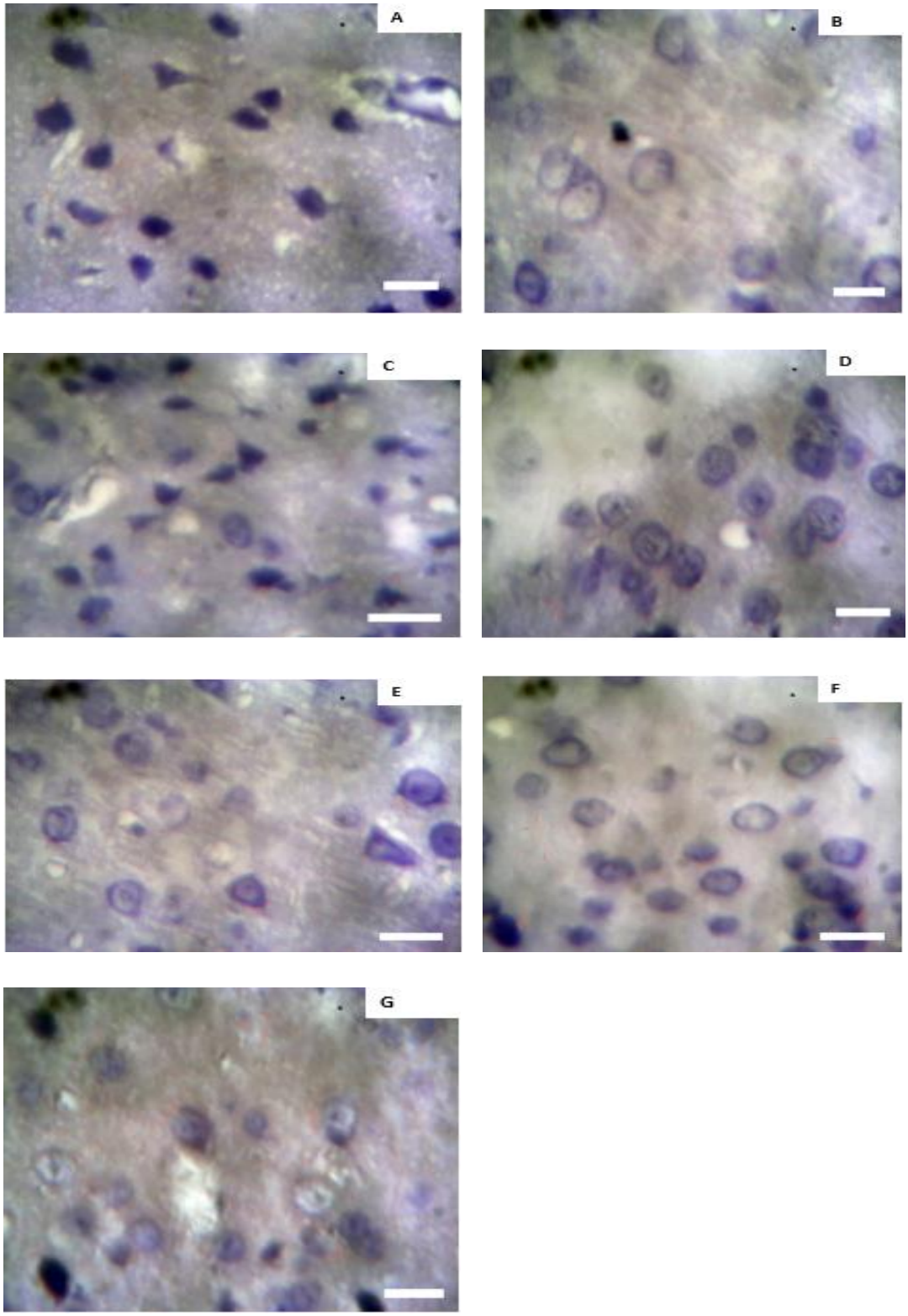

Figure 4.21 A-G

4.5.3.2 Synaptophysin stain

The synaptophysin protein expression in the control group (Figure 4.22 A), was characterised by deeply stained brown appearance in the tissue. In Pb treated group (Figure 4.22 B), low synaptophysin protein immunoreactivity was characterised by less intense brown stained appearance. Although the level of synaptophysin immunoreactivity in treated groups (Figure 4.22 D-G) were not as intense as the control group, their levels of reactivity were better than the Pb treated group (Figure 4.22 B).

Figure 4.22A-G: Representative photomicrographs of synaptophysin stain in mice prefrontal cortex (Scale bar 45 µm). The synaptophysin protein expression in the control group (A), was characterised by deeply stained brown appearance in the tissue (yellow arrows). In Pb treated group (B), low synaptophysin protein immunoreactivity was characterised by less intense brown stained appearance (blue arrows). Although the level of synaptophysin immunoreactivity in treated groups (D-G) were not as intense as the control group, their levels of reactivity (yellow arrows) were better than the Pb treated group (B).

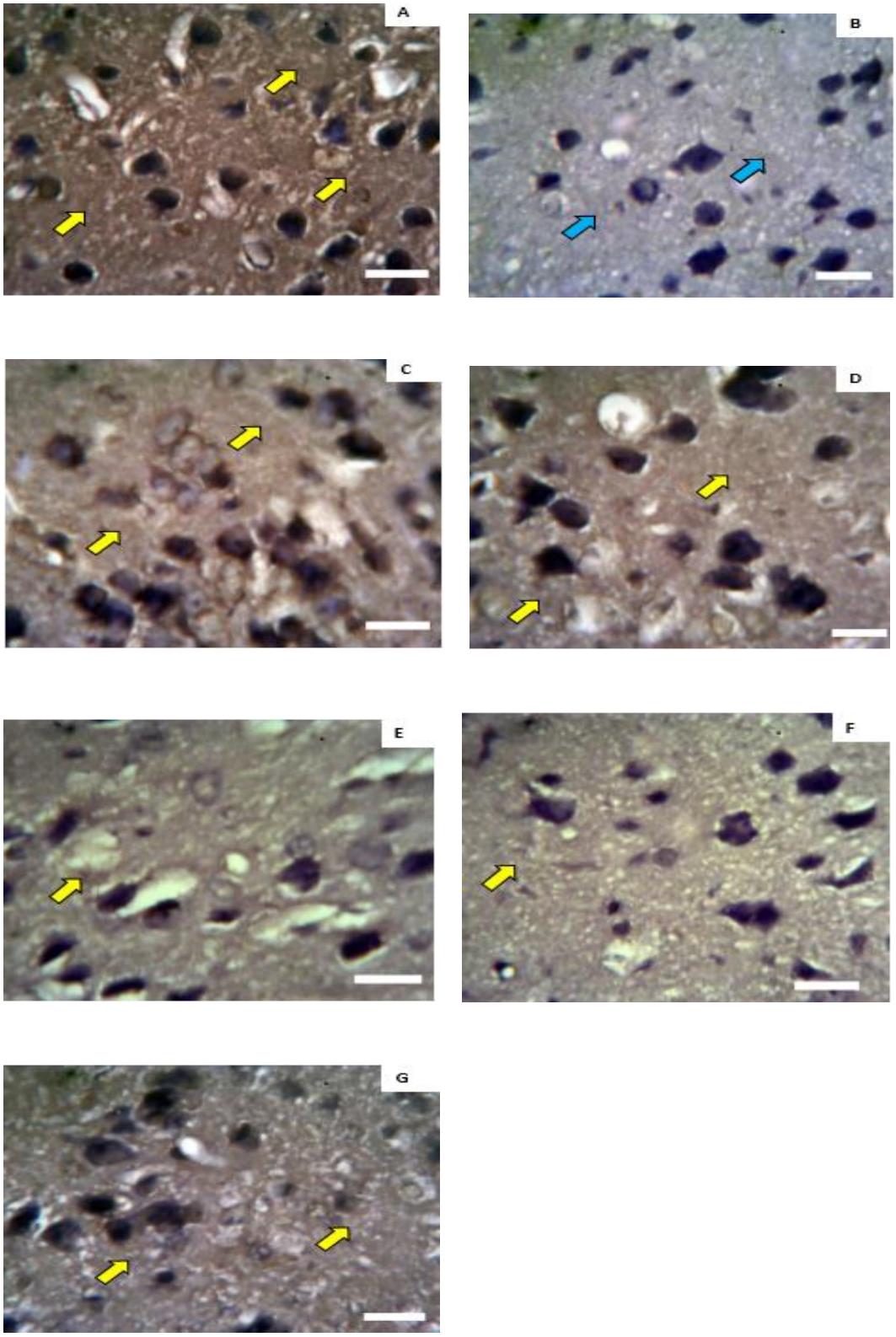

Figure 4.22 A-G

4.5.3.3 p-53 stain

In Figure 4.23 (A-G), no apparent protein- 53 expressions were found in all the treated groups (Figure 4.23 B-G), as well as the control group (Figure 4.23 A).

Figure 4.23A-G: Representative photomicrographs of P53 stain in mice prefrontal cortex (Scale bar 45 µm). Protein- 53 expression was absent in all the treated groups (B-G), as well as the control group (A).

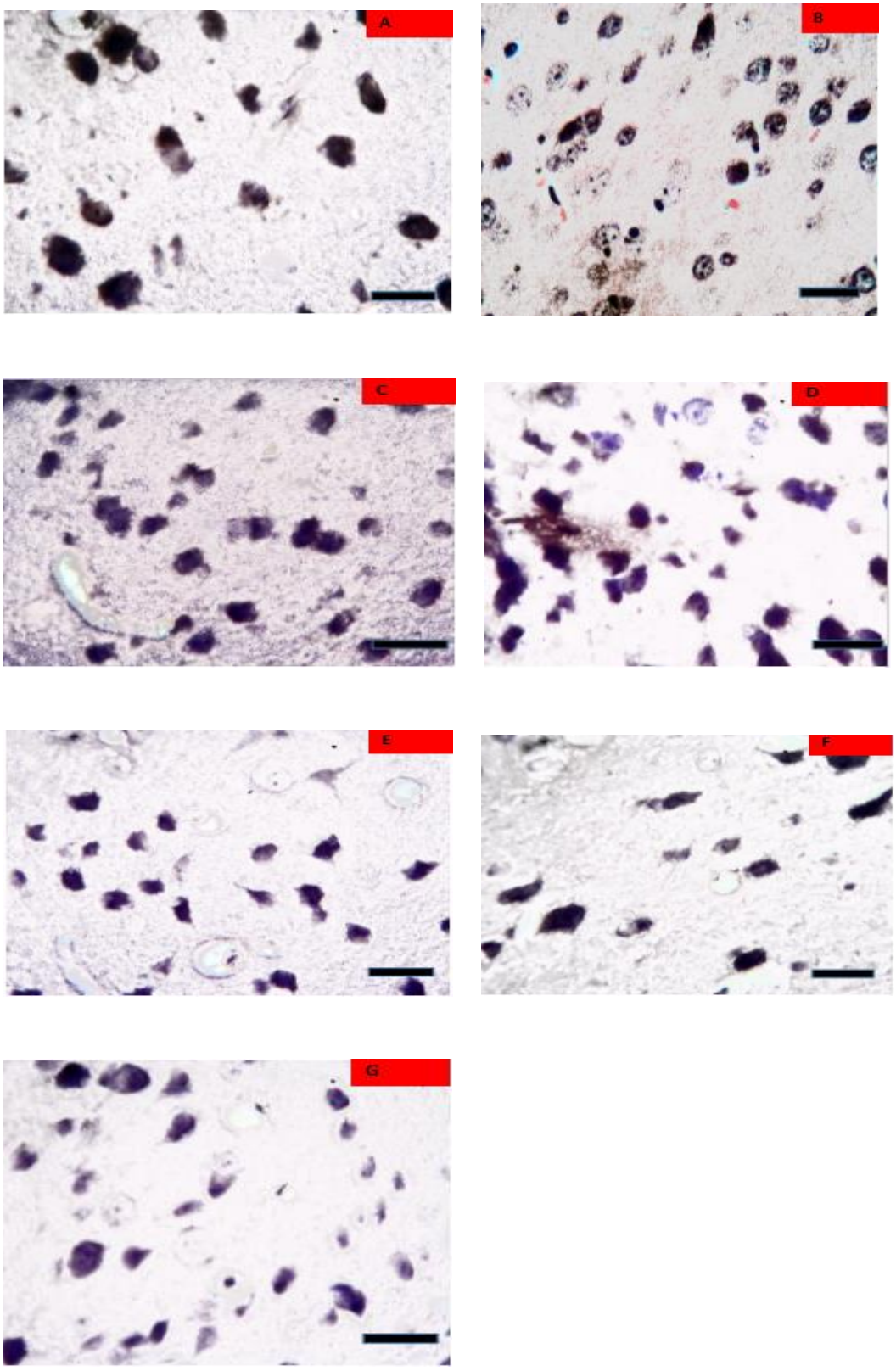

Figure 4.23 A-G

4.6 Morphometric observation of the prefrontal cortical neurons

4.6.1 Neuronal count in layer II/III of the prefrontal cortex

In all the treated groups (Figure 4.24), the number of neurons in layer II-III of the prefrontal cortex were significantly low ($p<0.05$) when compared with the control group (219±6.7). The number of normal neurons in Pb + Vitexin (M); Pb + Vitexin (F) and Vitexin pre-treated groups (184±2.3; 159±1.8; and 132±1.1 respectively) were significantly high ($p<0.05$) when comparisons were made with Pb treated group (85±2.9). Furthermore, the number of normal neurons in Pb + Vitexin (M); Pb + Vitexin (F) and Vitexin pre-treated groups (184±2.3; 159±1.8; and 132±1.1 respectively) were significantly high ($p<0.05$) when comparisons were made with Vitexin post-treated group (93±1.4). The number of normal neurons in Pb + Vitexin (M) group was not significantly different ($p>0.05$) from Pb + Vitexin (F) group when comparison was made. Additionally, the number of normal neurons in Pb treated group was not significantly different ($p>0.05$) from Vitexin post-treated group; neither was there any significant difference between Pb + Vitexin (M) group and Vitexin group.

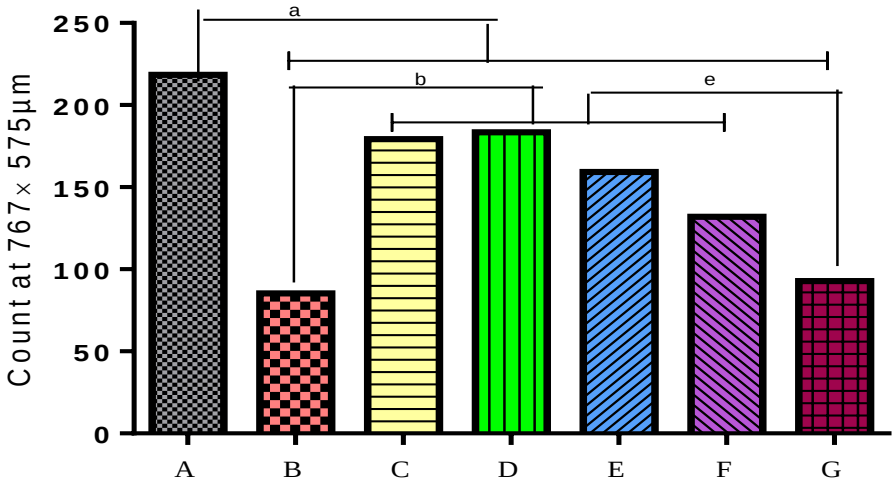

Figure 4.24: Neuron count in layer II/III.

The figure represent the number of normal neurons (not degenerating) in various groups. The coloured bars represent each group (A-G) of the experiment. The horizontal lines with superscript alphabets joining directly with the vertical lines above the groups, indicates significant difference between groups connected by the horizontal lines. [a] represent groups (B-G) that have significantly lower number of neurons than A; [b] represent groups (C-F) that has significantly higher number of neurons than B; [e] represent groups (D, E and F) that have significantly higher number of neurons than G.

Keys: A= Control; B = Lead (Pb); C =Vitexin; D = Pb + Vitexin (M); E= Pb + Vitexin (Female); F =Pre-treated with vitexin; G =Post-treated with vitexin.

4.6.2 Degenerating neuronal count in layer II/III

The number of degenerating neurons (Figure 4.25) in Pb treated group (183±4.1), was significantly high ($p<0.05$) when compared with the control group (29±1.3) as well as other treated groups. Similarly, the number of degenerating neurons in all the treated groups were significantly high ($p<0.05$) when comparisons were made with the control group (29±1.3). Furthermore, the number of degenerating neurons in Pb + Vitexin (F); Vitexin pre-treated and Vitexin post-treated groups (61±2.7; 64±2.7; and 139±4.9 respectively) were significantly high when compared with Vitexin group (45±1.8). Also, the number of degenerating neurons in Pb + Vitexin (F) group (64±2.7) was significantly low ($p<0.05$) when compared with Vitexin post-treated group (139±4.9). Conversely, there was no significant difference ($p>0.05$) in the number of degenerating neurons when comparison was made between Pb + Vitexin (M) group (57±2.2) and Pb + Vitexin (F) group (61±2.7).

Number of degenerating neurons in layer II/III

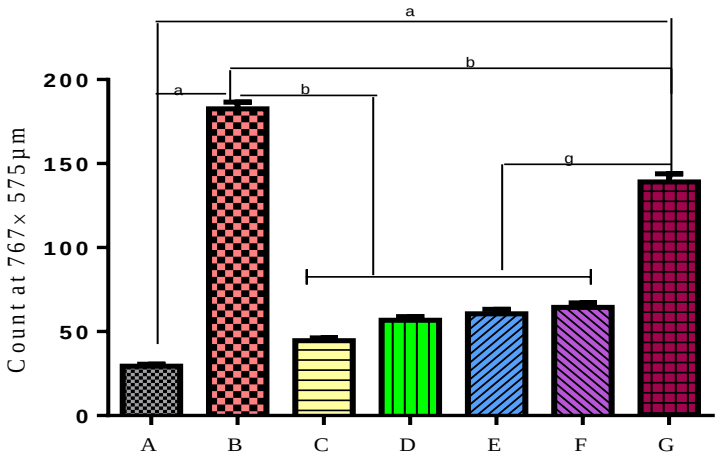

Figure 4.25: Degenerating neuron count in layer II/III.

The figure represent the number of degenerating neurons in various groups. The coloured bars represent each group (A-G) of the experiment. The horizontal lines with superscript alphabets joining directly with the vertical lines above the groups, indicates significant difference between groups connected by the horizontal lines. [a] represent groups (B-G) that have significantly higher number of neurons than A; [b] represent groups (C-G) that have significantly lower number of neurons than B; [g] represent groups (D, E and F) that have significantly lower number of neurons than G.

Keys: A= Control; B = Lead (Pb); C =Vitexin; D = Pb + Vitexin (M); E= Pb + Vitexin (Female); F =Pre-treated with vitexin; G =Post-treated with vitexin.

4.6.3 Intercellular distance between neurons

The intercellular distance between neurons in layer II-III (Figure 4.26) of the prefrontal cortex was not significantly different (p>0.05) when comparisons were made between the treated groups and the control group (72±8.5 µm). Similarly, the intercellular distance between neurons in Pb + Vitexin (M) and Pb + Vitexin (F) groups (77±7.7 µm and 83±8.3 µm respectively) were not significantly different (p>0.05) from the Pb treated group (91±10 µm). Furthermore, the intercellular distance between neurons in Vitexin pre-treated and Vitexin post-treated groups (75±8.2 µm and 81±9.2 µm respectively) were not significantly different (p>0.05) from the Pb treated group (91±10 µm).

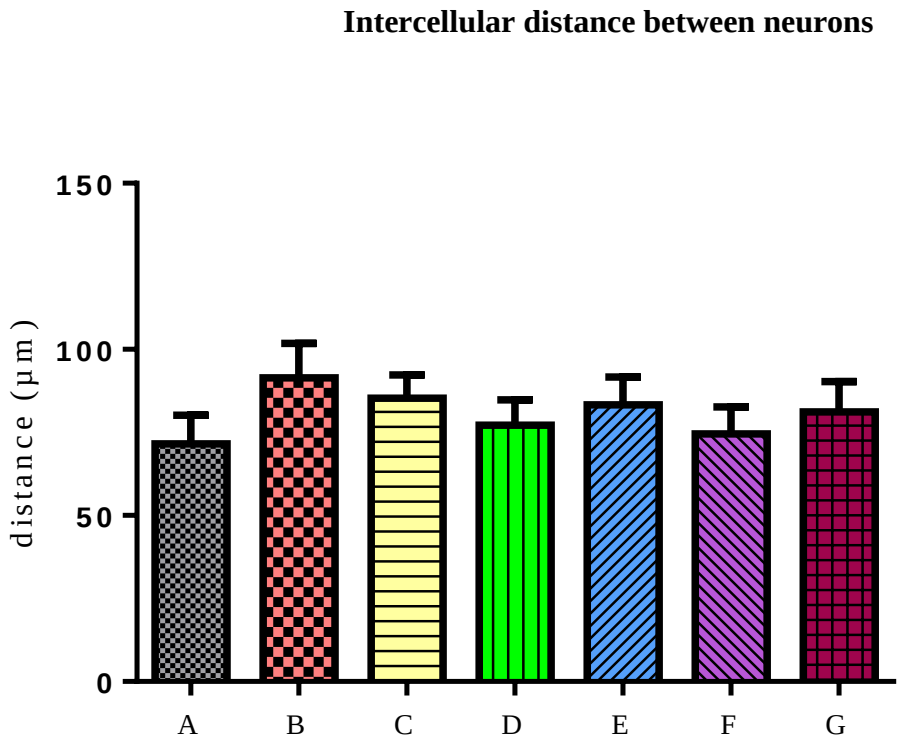

Figure 4.26: Intercellular distance between neurons.

The figure represent the mean distance between neurons of Layer II-III of the PFC. The coloured bars represent each group (A-G) of the experiment. There was no significant different in intercellular distance treated groups (B-G) when compared with A

Keys: A= Control; B = Lead (Pb); C =Vitexin; D = Pb + Vitexin (M); E= Pb + Vitexin (Female); F =Pre-treated with vitexin; G =Post-treated with vitexin.

4.6.4 Neuronal length

The neuronal lengths of neurons (Figure 4.27), in all the treated groups were not significantly different ($p>0.05$) when comparisons were made with the control group (48±2.3 µm). Similarly, neuronal lengths in Pb treated group (53±3.7 µm) were not significantly different ($p>0.05$) from those in Pb + Vitexin (M) and Pb + Vitexin (F) groups (44±1.9 µm and 38±5.4 µm respectively). Also, neuronal lengths in Pb treated group (53±3.7 µm) were not significantly different ($p>0.05$) from those in Vitexin pre-treated and Vitexin post-treated groups (45±2.8 µm and 49±3.7 µm respectively). On the other hand, the neuronal lengths in Vitexin group (60±4.5 µm) were significantly longer ($p<0.05$) when compared with those in Pb + Vitexin (M) group (44±1.9 µm) and Pb + Vitexin (F) group (38±5.4 µm).

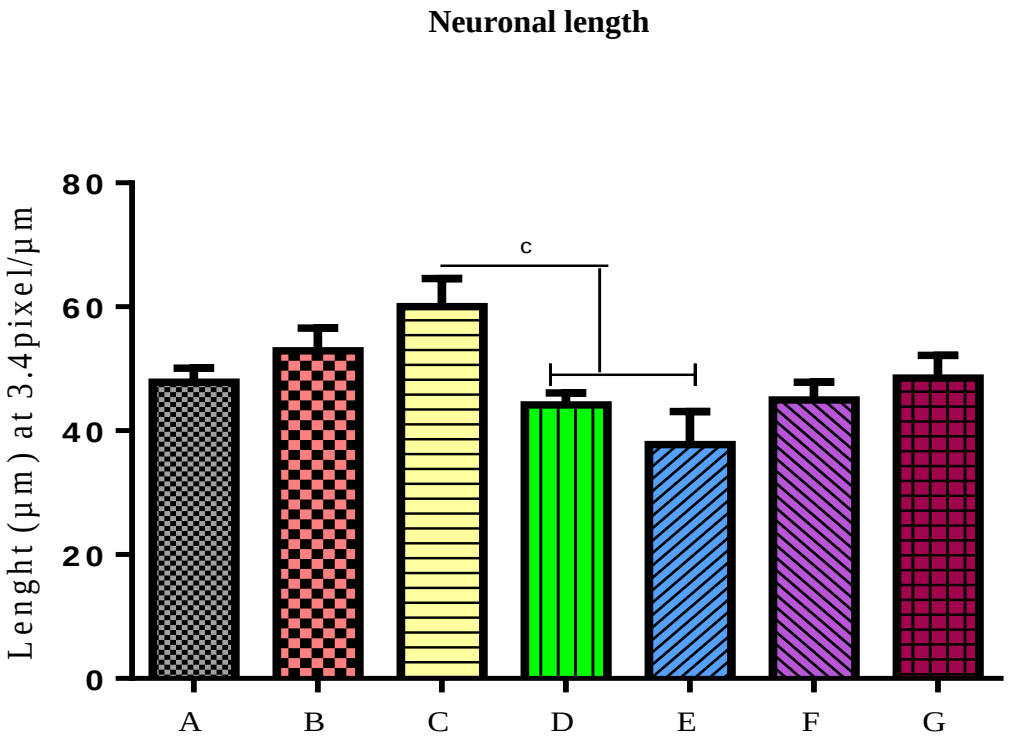

Figure 4.27: Comparison of neuronal length in layers II/III of PFC.

The figure represent the mean length of neurons in layers II/III of PFC for various groups. The coloured bars represent each group (A-G) of the experiment. The horizontal line with superscript alphabets joining directly with the vertical line above the groups, indicates significant difference between groups connected by the horizontal lines. ^{c} represent groups (D & E) that have significantly longer neurons than C.

Keys: A= Control; B = Lead (Pb); C =Vitexin; D = Pb + Vitexin (M); E= Pb + Vitexin (Female); F =Pre-treated with vitexin; G =Post-treated with vitexin.

4.6.5 Soma length of neurons

The soma length of neurons (Figure 4.28) in all the treated groups were not significantly different ($p>0.05$) from the control group (14±0.67 µm). Similarly, soma lengths in Pb treated group (16±1.1 µm) were not significantly different ($p>0.05$) from those in Pb + Vitexin (M) and Pb + Vitexin (F) groups (13±0.57 µm and 11±1.6 µm respectively). Also, soma lengths in Pb treated group (16±1.1 µm) were not significantly different ($p>0.05$) from those in Vitexin pre-treated and Vitexin post-treated groups (13±0.84 µm and 14±1.1 µm respectively). On the other hand, the soma lengths in Vitexin group (18±1.3 µm) were significantly longer ($p<0.05$) when compared with those in Pb + Vitexin (M) group (13±0.57 µm) and Pb + Vitexin (F) group (11±1.6 µm).

Soma length of neurons

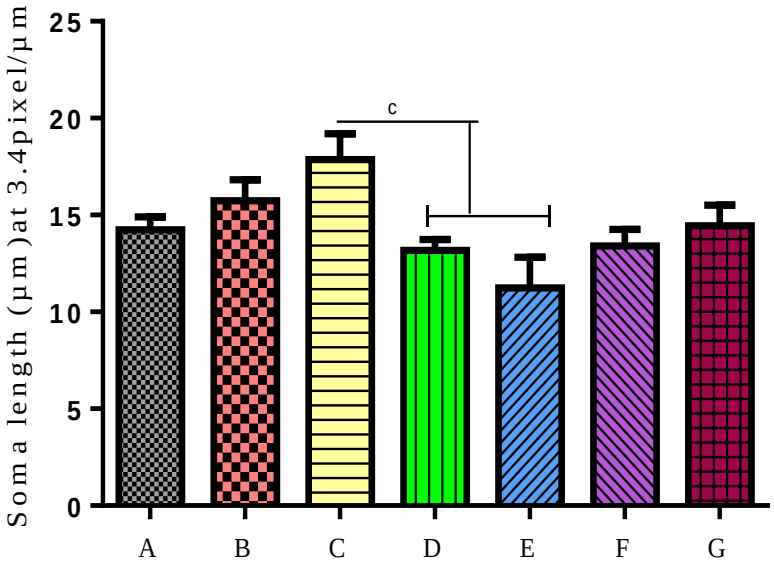

Figure 4.28: Comparison soma length of neurons in layer II/III.

The figure represent the mean soma length of neurons in layers II/III of PFC for various groups. The coloured bars represent each group (A-G) of the experiment. The horizontal line with superscript alphabets joining directly with the vertical line above the groups, indicates significant difference between groups connected by the horizontal lines. ^{c} represent groups (D & E) that have significantly larger soma than C.

Keys: A= Control; B = Lead (Pb); C =Vitexin; D = Pb + Vitexin (M); E= Pb + Vitexin (Female); F =Pre-treated with vitexin; G =Post-treated with vitexin.

4.6.6 Cross-sectional area of neurons

The cross-sectional area of neurons (Figure 4.29) in all the treated groups were not significantly different ($p>0.05$) from the control group (1284±150 μm^2). The cross-sectional area of neurons in Pb + Vitexin (M) group (918±78 μm^2) and Pb + Vitexin (F) group (958±156 μm^2) were not significantly different ($p>0.05$) from the Pb treated group (1535±222 μm^2). Similarly, the cross-sectional area of neurons in Vitexin pre-treated group (1277±202 μm^2) and Vitexin post-treated group (1078±91 μm^2) were not significantly different ($p>0.05$) from the Pb treated group (1535±222 μm^2).

Cross-sectional area of neurons

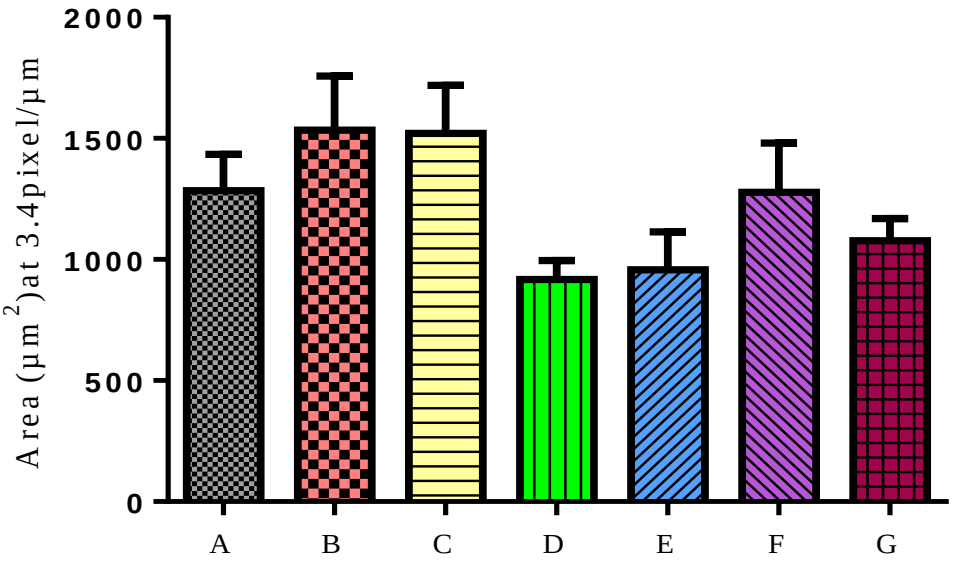

Figure 4.29: Comparison of cross sectional area of neurons in layer II/III.

The figure represent the mean cross-sectional area of neurons in Layer II-III of the PFC. The coloured bars represent each group (A-G) of the experiment. There was no significant different in intercellular distance treated groups (B-G) when compared with A

Keys: A= Control; B = Lead (Pb); C =Vitexin; D = Pb + Vitexin (M); E= Pb + Vitexin (Female); F =Pre-treated with vitexin; G =Post-treated with vitexin.

CHAPTER FIVE

DISCUSSION

5.1 Discussion

5.1.1 Body weight of mice at certain stage of development was unperturbed by both Lead and Vitexin administration

Body weight can be used to assess health status and the effects of both dietary and physical activity in animals (Shah and Bilal, 2009). The findings of this study on body weight of mice, shows general progressive weight gain with increasing age regardless of treatment administered. However, in the control group, there was a weight decrease on PND 56 when compared with PND 42. The reason for the weight loss observed could be due to loss of appetite (anorexia) and high physical activity that occurred within the period. In the Pb-treated group, the body weights of the mice were not significantly different, beginning from PND 42 until PND 63. This result is supported by earlier report of Correa *et al.* (2004) which states that, Pb acetate does not affect body weight. In this study, the body weights of mice in Pb + Vitexin (F), vitexin pre-treated, and vitexin post-treated groups were not different beginning from PND 63 until PND 68. This result could be an outcome of balance in physical activities and eating rate observed within those groups at the time of weight measurement. This result also suggest a balance in regulatory activity of the hunger centre (lateral hypothalamus), satiety centre (ventromedial hypothalamus) and metabolic rate in mice. It is also possible that vitexin may have significantly inhibited fat accumulation in 3T3-L1 adipocytes via AMPKα mediated pathway (Peng *et al.,* 2019).

5.1.2 Neither Vitexin nor Lead affects the brain weight

Brain weight can be used as an indicator to identify neurodegenerative diseases, cognitive impairments, and epilepsy (Holmes *et al.,* 2012; Budson and Solomon, 2016). It can also be an endpoint for ascertaining neurotoxicity (Bolon *et al.,* 2013). In this study, the result of brain

weight shows no significant difference when all the experimental groups were compared with the control group. This finding is supported by previous assertion, which stated that brain weight is stable throughout adulthood, with no increase in brain weight over the 10–30 month age range in mouse (Jones, 1983). Pb acetate at 100 mg/kg was reported not to have effect on brain weight (Correa *et al.,* 2004).

Similarly, when Pb treated group was compared with other experimental groups, no significant difference was found in brain weight. According to An *et al.,* (2012), Vitexin at high, medium, and low doses significantly reduced brain weight. The current study did not observe significant reduction in brain weight after Vitexin administration as earlier stated by An *et al.* (2012) probably due to variation in the age of mice, dose, and duration used in the current study. Furthermore, no significant brain weight difference was found between male and female animals in this study neither was there any significant difference between vitexin pre-treated and post-treated groups. This result implies that Vitexin at the dose administered has no sex-specific effect on brain weight. This result also implies that whether pre-treating with Vitexin or post-treating with Vitexin the brain weight would remain the same.

In this study, PFC weight was significantly low in Pb-treated group when compared with the control group. The loss of PFC weight observed, could be as a result of apoptosis and loss of frontal gray matter volume created due to exposure to Pb (Cecil *et al.,* 2008; Beckwith *et al.,* 2018). When Pb+Vitexin male treated group and Pb+Vitexin female treated group were compared with Pb treated group, only the male group showed a significant increase in PFC weight. This result suggests that concurrent treatment of Pb with Vitexin has sex disparity in PFC weight, which favours the male mice. The reason for this outcome is not fully understood but could linked to interactions of structural, neurochemical, and neuroendocrinological sex differences and factors. Furthermore, this study has shown that pre-treating or post-treating

with Vitexin has a noticeable increasing effect on the PFC weight of mice exposed to Pb. This result is due to apparent mitigation of cell and gray matter volume loss by Vitexin via its neuroprotective actions (Lima *et al.,* 2018).

5.1.3 High level of Lead in the blood is an indicator of possible neurotoxicity

Blood lead level (BLL) is the quantity of Pb in the blood which determines the level of its toxicity in the body (Klotz and Göen, 2017). Low to high BLL, particularly in children, results in neurological damage, including cognitive impairment (Sobin *et al.,* 2015; von Stackelberg *et al.,* 2015; Wani *et al.,* 2015). In this study, the blood lead level (BLL) in the Pb treated group was significantly high when compared with the control group. This result suggests that the animals treated with lead would probably suffer neuronal degeneration, cognitive impairments and other neurotoxic effects associated with high BLL (Ahmed *et al.,* 2013; Sharma *et al.,* 2015; von Stackelberg *et al.,* 2015). This study further shows a reduction in BLL in all the groups Vitexin was administered as treatment for Pb. The result implies that Vitexin can reduce BLL, probably through the activation of pathways that reduces the body's ability to absorb Pb (Thayer, 2018).

Haematological parameters, comprising red and white blood cell counts, haemoglobin concentration, platelets, and others, are commonly utilized as clinical indicators of health conditions (Pilny, 2008; Okada and Kamatani, 2012).

Findings in this study showed significantly low red blood cells (RBCs), and haemoglobins (Hb) in Pb treated group when compared with the control group. The result may be due to the toxic level of Pb, which tends to interfere with enzymatic steps in the heme synthesis pathway, which in turn diminishes RBCs count (Hsieh *et al.,* 2017). Also, an increased level of Pb was associated with a reduced level of Hb (Katavolos *et al.,* 2007). This result suggests that the animals treated with only Pb may be anaemic (Flora *et al.,* 2007b; Sobin *et al.,* 2013; Wani *et*

al., 2015) or anisocytotic. In groups where vitexin was involved in treatment, RBCs count and Hb were maintained or restored to the level of control. That outcome was probably through the activation of enzymatic steps in the heme synthesis pathway with the help of Vitexin administered. Also, this result implies that vitexin (particularly post-treating) could eliminate Pb-induced RBC loss and anaemia.

The outcome of this study further shows that the white blood cells (WBCs) were not significantly different between the control group and the experimental groups as well as within experimental groups when comparisons were made. The result of WBCs in this study suggests that all the groups have equal capacity to fight infection or respond to immune reactions equally.

5.1.4 Vitexin combats oxidative stress via up-regulation and maintenance of cell antioxidant defences

Malondialdehyde (MDA) is one of the end products of lipid peroxidation and a widely recognize oxidative stress marker (Ayala *et al.,* 2014; Tang *et al.,* 2019) which could indicate cellular damage. In this study, the MDA level in Pb treated group was significantly higher than the control, vitexin pre-treated, vitexin post-treated, and Pb+vitexin male- treated groups. This result suggests that the level of oxidative damage was higher in Pb treated group. Previous reports stated that Pb induces oxidative stress and damage through increased production of ROS and decreased activity of the antioxidant system (Gottipolu and Davuljigari, 2014; Sharma *et al.,* 2014; Andrade *et al.,* 2015). Earlier reports (Xu *et al.,* 2008; Barkur and Bairy, 2015) also observed that Pb increases the level of tissue MDA. However, the administration of Vitexin has been linked with the reduction of oxidative damage (Nurdiana *et al.,* 2018). The observation by Nurdiana *et al.,* (2018) may be the reason why the level of MDA in most groups administered Vitexin appeared low. Regarding, the Pb+vitexin female group that was not

significantly different from Pb treated group, Pb may have induced oxidative stress associated with elevated levels of lipid hydroperoxides (LPH) but not MDA (Dobrakowski *et al.*, 2017).

Superoxide dismutase (SOD), glutathione peroxidase (GPx), and catalase (CAT) are first-line defence antioxidant enzymes that dismutate superoxide radicals and reduce peroxides into harmless molecules (Ighodaro and Akinloye, 2018). In this study, the levels of SOD, GPx and CAT were significantly low in Pb treated group when compared with the control and other experimental groups (particularly vitexin pre-treated, vitexin post-treated and Pb+vitexin male-treated groups). This result suggests that Pb may have caused the reduction of SOD, GPx, and CAT in the tissues, as reported previously by Correa *et al.*, (2004). However, vitexin may have boosted the antioxidant enzyme defences of the cells to scavenge excessive ROS generated as a result of Pb toxicity (Kumar and Pandey, 2013), which in turn reduced cellular injury and apoptosis. Findings from earlier studies (An *et al.,* 2012; Nurdiana *et al.,* 2018) observed an increase in the level of SOD and GPx when vitexin was administered and a reduction of oxidative stress (Aseervatham *et al.,* 2016).

5.1.5 Energy expenditure level and signal transduction level within the cells are the same following Lead and Vitexin administration

In this study, Na^+/K^+ ATPase level in the control group was significantly higher than the Pb treated group. However, the level of the enzyme was not significantly different when comparisons were made among the experimental groups. An *et al.,* (2012) also, reports that vitexin improved the level of Na^+/K^+ ATPase in D-galactose aged mice. Since Na^+/K^+ ATPase maintains resting potential, transportation, signal transduction, energy expenditure, among other functions in the cells (Matchkov and Krivoi, 2016), the current finding suggests that energy expenditure level and other functions within the cells in all the experimental groups are at the same level.

5.1.6 Lead perturbs cholinergic system via acetylcholinesterase inhibition

Acetylcholinesterase (AChE) is a neurotransmitter that is involve in synaptic transmission of information. In the present study, the level of AChE in the Pb treated group was significantly low when compared with the control group as well as the remaining experimental groups. Chintapanti *et al.* (2018) linked reduction of AChE level to perinatal Pb exposure in rats. This present result implies that Pb will perturb the synaptic transmission and cholinergic system via acetylcholine (Ach) accumulation in the synaptic cleft with consequent (Andrade *et al.,* 2015; Gupta *et al.,* 2015; von Stackelberg *et al.,* 2015) effect on working memory. Similarly, the level of AChE was significantly low in the vitexin pre-treated group when compared with vitexin post-treated group. The result suggests that post-treating with vitexin will increase the level of AChE better than pre-treating with vitexin.

5.1.7 Lead inhibits the production of nitric oxide

Nitric oxide (NO) is a signalling molecule that is involved in different physiological functions. Significant reduction in NO level has been linked to cognitive impairment (Nava-Ruiz *et al.,* 2012). In this study, the NO level in the control group was significantly high when compared with all the experimental groups. In Pb treated group, the level of NO was significantly low when compared with Pb+vitexin concurrent treated groups as well as vitexin pre-treated group. Nava-Ruiz *et al.* (2012) stated that Pb could interfere with the production of nitric oxide via the disruption of nNOS/eNOS activities. Since the significant reduction of NO has been linked with Pb neurotoxicity and subsequently with cognitive impairment (Nava-Ruiz *et al.,* 2012), current result implies that animals in Pb treated group would suffer cognitive impairment. This evidence is seen in the behavioural results of this study. According to Guimaraes *et al.* (2015), Vitexin significantly reduced high NO. The current outcome contradicts the previous report by Guimaraes *et al.* (2015) probably because of the variation in research model.

5.1.8 Vitexin improves learning and memory impairments via modulating pro/antioxidant balance

Findings in this study from the Barnes maze test shows that mice in Pb treated group took longer time to locate the dropbox when compared with the control or any of the other experimental groups. This result suggests that animals exposed to Pb at the dose and duration (from PND 21-35) as seen in the current study, would have deficits in learning and working memory. Sprowles *et al.* (2018) also revealed that litters of rats exposed to Pb from PND 4-28 experienced impaired maze performance and consequently learning and memory disabilities. This finding supports previous studies that stated exposure to Pb at various stages of early life (prenatal or postnatal) development would impair cognition later in life (Zhang *et al.,* 2017; Rahman *et al.,* 2018). This study further shows that animals treated with only Pb had significantly low preference for new object in a novel recognition test (NOR). A similar outcome was reported by Moosavirad *et al.* (2016) in adult rats with a higher dose and longer duration of administration. The impaired working memory seen in the Pb treated group of this study may have been as a result of neuronal loss in the prefrontal cortex (Kougias *et al.,* 2018). Additionally, impairment of the working memory seen in Pb treated group could be linked with oxidative stress, disruption of signaling molecules and neurotransmitters as proven by various results of this study.

Flavonoids including vitexin have ability to conserve neuronal survival, long-term potentiation, learning and memory (Krishnaveni, 2012). The ability of vitexin to conserve neuronal survival is associated with maintaining pro/antioxidant balance which in turn reduces oxidative stress and neuronal damage that could subsequently cause learning and memory deficits. The current study observed that groups co-administered Vitexin and Pb (including pre-treating and post-treating) showed higher preference for new object than old (familiar) object. This result implies that co-administration of Pb with Vitexin (including pre-treating and post-treating) will

significantly eliminate, retrieve or improve learning and memory impairment via modulating pro/antioxidant balance (Abbasi *et al.,* 2013; Min *et al.,* 2015; Lima *et al.,* 2018; Nurdiana *et al.,* 2018).

5.1.9 Vitexin demonstrates anti-depressant ability

.Depression is one of the early symptoms of Pb neurotoxicity (Andrade *et al.,* 2015). According to Highab (2018), 100 mg/kg and 200 mg/kg doses of Pb will increase the duration of immobility in a depression test. The outcome of the current study shows longer immobility time in Pb treated group when compared with the control group as well as groups vitexin was involved in treating. De- Souza *et al.,* (2005) reported depressive-like behavior in female rats and not in male mice, as seen in this study. The current result implies that sex and animal type are key factors that influence depressive-like behaviours linked to Pb neurotoxicity.

Vitexin has been reported to possess anti-depressant properties according to Can *et al.,* (2013). The result of Can *et al.,* (2013) was probably the reason behind the shorter immobility time in Vitexin treated group when compared with the control as well as groups in this study. The anti-depressant action of Vitexin may have interceded via increase in catecholamine levels in the synaptic cleft as well as through interactions with the serotonergic 5-HT_{1A}, noradrenergic α_2, and dopaminergic D_1, D_2, and D_3 receptors (Can *et al.,* 2013). Also, anti-depressant action of Vitexin may have acted through suppression of oxidative- nitroxative stress (Hritcu *et al.,* 2017).

5.1.10 Vitexin exhibits anxiolytic capability

The current study shows that Pb exposure in Pb treated group resulted in a significant increase in anxiety-like behaviour. However, when Vitexin was administered (alone, concurrently, or pre-treated), there was a significant decrease in anxiety-like behaviour in the animals. The present study support previous *in vivo* studies that also observed increase in anxiety and

reduction of open-field activity after Pb exposure in early stages of life (including early postnatal) (Soeiro *et al.,* 2007; Reckziegel *et al.,* 2011; Flores-Montoya & Sobin, 2015; Chintapanti *et al.,* 2018; Sprowles *et al.,* 2018). However, most of the previous works cited were based on chronic administration rather than subchronic, as seen in this study. This observation implies that even at subchronic dose, Pb will promote an anxiety-like effect in mice. Vitexin has previously been identified as a possible anxiolytic agent (Soulimani *et al.,* 1997). The finding by Soulimani *et al.,* (1997) could be the reason behind the reduced anxiety-like behaviour observed in groups where Vitexin administered (either co-administered with Pb, pre-treated, or post-treated).

5.1.11 Lead neurotoxicity initiates poor motor coordination while Vitexin´s response was ineffective

Delay in motor development and minor motor deficits are part of the early symptoms of intellectual disability (APA, 2013). The general finding from two different tests in this study shows that in Pb treated group, the animals displayed poor motor coordination (hanging test) and staggered movement that appeared ataxia-like. An earlier study suggests that perinatal Pb exposure reduced locomotor activity in adult rats (Chintapanti *et al.,* 2018); while other studies reported a spontaneous reduction of locomotor activity for 24 hours and beyond following acute Pb administration (Correa *et al.,* 2004; Reckziegel *et al.,* 2011). Although there was an improvement in motor coordination in various groups that vitexin was administered, the improvement was marginal and not different from Pb-treated group in the current study. This result suggests that Pb exposure in young mice would cause deficits in motor coordination and cannot be ameliorated with Vitexin.

5.1.12 Lead induces loss of neurons particularly in layer II-III of the prefrontal cortex

Layer II-III of the prefrontal cortex comprises of pyramidal neurons and in mice these layers are often difficult to distinguish hence the use of "layer II-III" (Van Eden and Uylings, 1985). Layer II-III of the prefrontal cortex mediates communication across cortical regions and provide insights into mechanism involved in higher cognitive functions (Nathalie *et al.,* 2009; Song *et al.,* 2012). Intrinsic connections of Layer II-III of the prefrontal cortex are important in special cognitive processing in the prefrontal cortex (Kritzer and Goldman-Rakic, 1995; Petanjek *et al.,* 2019).

The histomorphological observation of H&E stain in the Pb-treated group of this study showed degenerative changes that were characterised by numerous pyknotic neurons with fragmented cytoplasm and condensed nuclei within the soma. The number of degenerating neurons in layer II-III of this group was also very high. Previous studies also reported that, chronic Pb exposure was the basis for brain degeneration, disorganization of cell layers, and neuronal loss (Deveci, 2006; Baranowska-Bosiacka *et al.,* 2013; Highab, 2018; Kougias *et al.,* 2018). Loss of neurons is one of the primary reasons behind cognitive impairment, especially in layer II-III of PFC, which has been linked to cognitive functions (Kritzer and Goldman-Rakic, 1995; Song *et al.,* 2012; Petanjek *et al.,* 2019). The loss of neurons could be the reason behind the deficits in working memory, and other neurobehavioural impairments seen in Pb treated group of this study.

In groups where Vitexin was administered in the current study, the cellular layers of the PFC were generally distinct with better cytoarchitectural features and reduced degenerative changes, when compared with Pb treated group. Also, the number of degenerating neurons in layer II-III of PFC in Pb + Vitexin treated and Vitexin pre-treated groups were lower when compared with the Pb treated group. This result implies that Vitexin administration protects the PFC from

Pb- induced damage and cell loss during critical developmental stage. This is done by up-regulating the activities of antioxidant enzyme defences of the cells in other to combat ROS and by extension apoptosis caused by Pb toxicity (An *et al.,* 2012; Lima *et al.,* 2018). Additionally, Vitexin may have protected the neurons from damage through modulating mitogen-activated protein kinase and apoptosis signaling pathways (Wang *et al.,* 2015). Previous studies also noted that pre-treatment with Vitexin protects cells from damage and enhance their recovery from atrophy (Yang *et al.,* 2014; Min *et al.,* 2017).

Chromatolysis is the dissolution of Nissl bodies present in neurons in response to toxicity and other factors (Bradley *et al.,* 2018). The present study shows that, in Pb treated group, the tissue had numerous cells that have undergone chromatolysis with many more staining less intensely to Nissl dye. Since Nissl staining intensity indicates the health state of the neuron (van der Ham and Ruotolo, 2017), this result suggests that the neurons in the Pb treated group were not healthy. Consequently, resulting in high level of apoptosis in the group. This result also suggests that Pb exposure in young mice would result in chromatolysis or other forms of degeneration in adulthood, probably due to the release of Pb that has been stored in the bone or teeth at the peak of exposure (von Stackelberg *et al.,* 2015).

Generally, in Vitexin administered groups (alone, concurrent, and pre-treated), the number of cells that stain intensely for Nissl bodies were much higher with fewer chromatolytic cells when compared with Pb treated group. This result implies that, there were healthier and normal neurons in Vitexin administered groups (alone, concurrent, and pre-treated) than Pb treated group. This result also buttresses earlier suggestion that Vitexin may have protected the neurons from damage by up-regulating the activities of antioxidant enzyme defences of the cells to counteract ROS generated due to Pb exposure (An *et al.,* 2012; Wang *et al.,* 2015; Lima *et al.,* 2018). An earlier study by Min *et al.* (2015) suggested that 5 minutes pre-treatment with

Vitexin provided neuroprotection (seen using Nissl stain) but post-treatment after 3 hours did not offer protection. The finding of Min *et al.* (2015) could be the reason behind the similar cytoarchitecture seen in Vitexin post-treated group and Pb treated group in this study.

5.1.13 Amyloid protein was absent in both Lead and Vitexin-treated mice

The presence of amyloid beta (Aβ) peptide in the prefrontal cortex (PFC) disrupts PFC activity and its long-range interactions throughout the brain (Flores-Martinez and Pena-Ortega, 2017). In this study, the amyloid protein expression via Congo red staining technique was not significant enough to draw inference from all the groups. The reason for this result could be due to small amyloid deposits within the tissues. This result implies that, the deposits of amyloid beta (Aβ) peptide in all the groups were not high enough to disrupt PFC activity and its long-range interactions throughout the brain.

Senile plaques are extracellular deposits of amyloid beta in the grey matter of the brain (Purves *et al.,* 2012). These plagues can be stained for histological examination using Bielschowsky's silver technique (Bancroft and Gamble, 2008). The presence of senile plaques is a neuropathological indication of neurodegenerative diseases, including those linked to memory. In the present study, senile plaques were numerous in Pb treated group as well as Vitexin post-treated group. Although senile plaques were present in other Vitexin administered groups (concurrent and pre-treated), its deposits were not as much as those found in the Pb treated group. A study by Basha *et al.* (2005) noted that Pb administration in rats from PND 1 until 20 increased *APP* mRNA expression in cortical brain tissue before returning to basal levels after one year. *APP* later resurged at 20 months of age in company of elevated Aβ without Pb exposure. This present finding supports the work of Basha *et al.* (2005) and suggests that early-life Pb exposure will have long-term effects on amyloidogenesis in adulthood. The pathway used by Vitexin to significantly reduce amyloidogenesis in this work is not fully understood,

but it is suspected to have activated an anti-aggregation process against Aβ protein in the tissues thereby rendering them less potent (Malar *et al.,* 2017).

5.1.14 Mice devoid of GFAP can still develop normal histological architecture

Glial fibrillary acidic protein (GFAP) is an intermediate filament protein that is expressed in numerous cells of the central nervous system (CNS), particularly astrocytes (Jäkel and Dimou, 2017). GFAP plays vital roles in the CNS, such as cell communication, proper functioning of the blood-brain barrier, mitosis, repairs, among other functions (Sofroniew, 2005; Brenner, 2014; Jäkel and Dimou, 2017;). In this present study, it was observed that astrocyte immunoreactivity was absent in all the experimental groups, including Pb treated group. This result is contrary to earlier reports that observed hypertrophic immunoreactive astrocytes and astrogliogenesis in the frontal cortex and other brain structures of chronic Pb- treated animals (Sansar *et al.,* 2011; Liu *et al.,* 2015). The reason for this present result is not fully understood, but it is possible that the mice used for this experiment lack intermediate filament protein or were experiencing late onset of intermediate filament protein due to mutation (Liedtke *et al.,* 1996). Since the study of intermediate filament protein mutation was beyond the scope of this present study, this theory about the late onset of intermediate filament protein being the reason behind the absence of GFAP could not be proven further. Interestingly, mice that are devoid of GFAP can still develop normally with no abnormalities in the histological architecture (Gomi *et al.,* 1995; Pekny *et al.,* 1995; Brenner, 2014).

5.1.15 Synaptophysin protein was poorly expressed in Lead-treated animals

Synaptophysin is a major synaptic vesicle glycoprotein that is found in neuroendocrine cells and almost all neurons (McMahon *et al.,* 1996). Synaptophysin is use as a marker to quantify synapses. Lately, studies have shown, that knockout of synaptophysin protein in mice results to impaired novel object recognition, reduced spatial learning and other behavioural changes

(Schmitt *et al.,* 2009). The current study, observed that, Pb treated group had a very low synaptophysin immunoreactivity, which was in contrast to what was observed in the control group. Although the level of synaptophysin immunoreactivity in vitexin administered groups (alone, concurrent, pre-treated, and post-treated), were not at the same level as the control, their level of reactivity was much better than Pb treated group. Yu *et al.* (2016), also observed that alterations in synaptic protein induced by Pb exposure in early life plays a key role in subsequent intellectual impairments such as deficits in spatial learning and memory at later ages. The inference made by Yu *et al.* (2016), support the current inference that states that mice in Pb-treated group will have deficits in learning and memory due to major loss of synaptophysin. This inference was further proven by the learning and memory deficits seen in Pb treated group during the behavioural tests of the current study (Figure 4.8 and Figure 4.4.1.2). This result further suggests that, Vitexin administration can maintain or restore the level of synaptophysin protein after Pb toxicity. This is probably done through the activation of pathways that prevent the breakdown of synaptophysin protein in the synaptic vesicles (Cohen and Ziv, 2017).

5.1.16 p53 expression was absent in Lead and Vitexin- treated mice

Protein 53 (P53) is one of the essential proteins in cells, and it is produced from the P53 gene. In collaboration with other related proteins, P53 regulates, cell cycle, apoptosis, and developmental differentiation, among other functions (Jazvinscak *et al.,* 2018). Impairment of P53 expression results in various disorders and neurodegeneration (Engel *et al.,* 2010; Stanga *et al.,* 2010). In this study, P53 expression was not noticeable in all of the groups. The reason for this result is not fully known, but the P53 gene may have mutated hence the absence of P53 expression in the tissues. Additionally, P53 may have failed to bind target DNA sequences that promotes or represses the expression of genes that mediate p53-dependent functions (Jazvinscak *et al.,* 2018). Since P53 was not noticeable in this study, its functions may have

been taken over by related proteins such as P63 and P73 (Jazvinscak *et al.,* 2018). This could be the reason why no deficit was noticed due to the absence of P53.

5.1.17 Neither Lead nor Vitexin affects cross-sectional area and intercellular distance between neurons

The size, shape of dendrites, axons, and even neurons are strong determinants of neuronal information processing (Mohan *et al.,* 2015). Interneuronal distance is one of the factors that determine general information processing capacity of neurons and also one of the factors that link brain traits with the degree of intelligence among mammals (Ursula, 2016). Results from this study shows that, the cross-sectional area of neurons and the intercellular distance between neurons in layer III were not different among the groups. This result suggests that Pb or Vitexin administration at the dose and duration used in this study will not affect the cross-sectional area of neurons and intercellular distance. The result also suggests that neuronal information processing capacity of the neurons, in all the groups, are probably at the same level.

5.2 Conclusion

Vitexin administration attenuated Pb-induced deficits in working memory and improved anxiety, depression, and motor behaviours in male and female mice. Neither pre-treating nor post-treating with Vitexin offers better result on working memory, anxiety and depression.

Administration of Vitexin decreased blood Pb level and procalcitonin level, while it also increased the level of RBC, Hb, PLT, and RDW. The WBC was unaffected by Vitexin administration, while the haematological results were generally not influenced by gender.

Vitexin administration attenuated Pb-induced neuronal, histomorphological, and synaptophysin protein damage in either male or female mice. Pre-treating or post-treating with Vitexin to a less significant extent produced similar results. Astrocytes immunoreactivity and amyloid protein expression were absent in the groups.

Vitexin reduced oxidative stress via up-regulation of antioxidant enzyme activities (SOD, GPx, and CAT) against ROS. Also, Vitexin administration increased the level of AChE as well as NO in the PFC. However, the level of Na^+/K^+ ATPase was unaffected by Vitexin administration.

The number of neurons remained high when Vitexin was co-administered with Pb. However, the cross-sectional area, and intercellular distance of neurons were not affected.

Vitexin co-administration with Pb increased prefrontal cortical weight but not overall brain weight.

5.3 Contribution to knowledge

According to many previous studies, Pb neurotoxicity promotes neurodegeneration in all parts of the brain including the prefrontal cortex. This study went further to add that neurodegeneration is more common in layer II-III of mice prefrontal cortex.

Prior to this study, there were arguments for and against the possibility of acute Pb exposure being able to cause neurotoxicity. From the outcome of this study, it can now be added to the existing body of knowledge that acute Pb administration at 100 mg/kg can indeed cause neurotoxicity in mice.

Prior to this study, the potency of Vitexin as an antioxidant, capable of combating oxidative stress was in doubt when compared, with other well established flavonoids that also have antioxidant potential. This study, has added to the existing knowledge that, Vitexin at minimum dose of 1 mg/kg (ip) has the antioxidant potency to combat oxidative stress caused by Pb in mice.

This study also added to knowledge by reporting that, Vitexin co-administration with Pb has an incremental influence on prefrontal cortical weight but not on the overall brain weight of mice. Furthermore, this study added to the existing knowledge by reporting that, co-administering Vitexin with Pb will cause, decrease in neuronal length but administering only Vitexin in mice leads to increase in neuronal length.

In addition to knowledge, this study showed that effects of Vitexin in mice at the dose administered is mostly not dimorphic in nature. Finally, Vitexin co-administration with Pb attenuates deficit in working memory and also mitigates anxiety, depression, and motor behaviours in mice.

5.4 Recommendations

Further research still needs to be carried out using electrophysiological techniques to provide insights into electrical properties involved in higher intellectual functions, anxiety, and depression in mice exposed to Pb and Vitexin treatment.

A different research model such as monkey or other primates is recommended for a similar study to generate a better research data that could be replicated in clinical trials in future.

The basis for GFAP null reactivity seen in this study is recommended for further study, particularly from the approach of delayed onset of intermediate filament protein expression.

The exact mechanism or transporter used by Vitexin to transverse the blood brain barrier requires more clarity.

The reason behind Vitexin neuroprotective effect on PFC tissue over a long period after its administration has stopped deserves more answers.

The study recommends that, Vitexin be explored further as an agent that protects the PFC from Pb-induced neurodegeneration.

REFERENCES

Aartsma-Rus, A., van Putten, M. (2014). Assessing functional performance in the mdx mouse model. *Journal of Visualized Experiments,* (85). doi: 10.3791/51303

Abadin A (2007). Toxicological Profile for Lead: Chemical And Physical Information. Retrieved from https://www.ncbi.nlm.nih.gov/books/NBK158769/ on 13 May, 2017.

Abbasi, E., Nassiri-Asl, M., Sheikhi, M., Shafiee, M. (2013). Effects of vitexin on scopolamine-induced memory impairment in rats. *Chinese Journal Physiology*, *56*(3), 184-189.

Afifi, A.K., Bergman, R.A. (2005). *Functional Neuroanatomy: Text and Atlas. 2nd Edition. Baltimore*: McGraw-Hill Education, 251.

Ahmed, M. B., Ahmed, M. I., Meki, A. R., Abdraboh, N. (2013). Neurotoxic effect of lead on rats: Relationship to Apoptosis. *International Journal of Health Sciences, 7*(2), 192-199.

Ahur, V.M., Anika, S.M., Onyeyili, P.A. (2018). Age-sex dimorphisms in the estimation of median lethal dose of lead diacetate in rabbits using up-and-down procedure (Arithmetic method). *Sokoto Journal of Veterinary Sciences,* 16 (4): 64 - 72.

Ajumobi, O. O., Tsofo, A. Y., Matthias, A., Mabel, K., Anagbogu, I. N., Mohammed, A., Nsubuga, P. (2014). High concentration of blood lead levels among young children in Bagega community, Zamfara - Nigeria and the potential risk factor. *Pan African Medical Journal, 18* (Suppl 1), 4-14.

An, F., Yang, G., Tian, J., Wang, S. (2012). Antioxidant effects of the orientin and vitexin in Trollius chinensis Bunge in D-galactose-aged mice. *Neural Regeneration Research, 7*(33), 2565-2575.

Anderson, D. W., Mettil, W., Schneider, J. S. (2016). Effects of low level lead exposure on associative learning and memory in the rat: Influences of sex and developmental timing of exposure. *Toxicology Letter, 246*, 57-64.

Andrade, V. M., Mateus, M. L., Batoréu, M. C., Aschner, M., Marreilha dos Santos, A. P. (2015). Lead, Arsenic, and Manganese Metal Mixture Exposures: Focus on Biomarkers of Effect. *Biological Trace Element Research, 166*(1), 13-23.

Antonio-García, M. T., Massó-Gonzalez, E. L. (2008). Toxic effects of perinatal lead exposure on the brain of rats: Involvement of oxidative stress and the beneficial role of antioxidants. *Food and Chemical Toxicology, 46*(6), 2089-2095.

Arredondo, F., Echeverry, C., Blasina, F., Vaamonde, L., Díaz, M., Rivera, F., Dajas, F. (2015). Flavones and flavonols in brain and disease: Facts and Pitfalls. In R. R. Watson & V. R. Preedy (Eds.), *Bioactive Nutraceuticals and Dietary Supplements in Neurological and Brain Disease.* San Diego: Academic Press, 229-236.

Aseervatham, G. S., Suryakala, U., Doulethunisha, Sundaram, S., Bose, P. C., Sivasudha, T. (2016). Expression pattern of NMDA receptors reveals antiepileptic potential of apigenin 8-C-glucoside and chlorogenic acid in pilocarpine induced epileptic mice. *Biomedicine and Pharmacotherapy, 82*, 54-64.

Ashraf, M. S., Abdel-Razik, H. F., Hany, M. F. (2017). Protectivce effects of Vitamin C on hematological and biochemical parameters of intoxicated male albino rats with Lead and Cadmium. *Middle East Journal of Applied Sciences,* 7 (1): 57-67.

Aungst, B. J., Dolce, J. A., Fung, H. (1981). The effect of dose on the disposition of lead in rats after intravenous and oral administration. *Toxicology and Applied Pharmacology, 61*(1), 48-57.

Aungst, Bruce J., Dolce, James A., Fung, Ho-Leung. (1981). The effect of dose on the disposition of lead in rats after intravenous and oral administration. *Toxicology and Applied Pharmacology, 61*(1), 48-57.

Ayala, A., Muñoz, M.F., Argüelles. S. (2014). Lipid Peroxidation: Production, Metabolism, and Signaling Mechanisms of Malondialdehyde and 4-Hydroxy-2-Nonenal. *Oxidative Medicine and Cellular Longevity*, *2014*, 31. doi.org/10.1155/2014/36043 8

Balez, R., Steiner, N., Engel, M., Munoz, S. S., Lum, J. S., Wu, Y., Ooi, L. (2016). Neuroprotective effects of apigenin against inflammation, neuronal excitability and apoptosis in an induced pluripotent stem cell model of Alzheimer's disease. *Scientific Reports, 6*, 31450. doi: 10.1038/srep31450.

Bancroft, J.D., Gamble, M. (2008). Theory and practice of histological techniques. Sixth edtion, London: Churchill Livingstone, 121-392.

Baranowska-Bosiacka, I., Struzynska, L., Gutowska, I., Machalinska, A., Kolasa, A., Klos, P., Chlubek, D. (2013). Perinatal exposure to lead induces morphological, ultrastructural and molecular alterations in the hippocampus. *Toxicology, 303,* 187-200.

Barkur, R. R., Bairy, L. K. (2015). Assessment of oxidative stress in hippocampus, cerebellum and frontal cortex in rat pups exposed to lead (Pb) during specific periods of initial brain development. *Biological Trace Element Research, 164*(2), 212-218.

Barkur, R. R., Bairy, L. K. (2016). Histological study on hippocampus, amygdala and cerebellum following low lead exposure during prenatal and postnatal brain development in rats. *Toxicology and Industrial Health, 32*(6), 1052-1063.

Barkur, R. R., Rao, M. S., Bairy, L. K. (2011). Low lead exposure during foetal and early postnatal life impairs passive avoidance learning in adulthood in rats. *Arhiv za Higijenu Radai Toksikologiju, 62*(2), 147-153.

Bartrem, C., Tirima, S., von Lindern, I., von Braun, M., Worrell, M. C., Mohammad Anka, S., Moller, G. (2014). Unknown risk: co-exposure to lead and other heavy metals among children living in small-scale mining communities in Zamfara State, Nigeria. *International Journal of Environvironmental Health Research, 24*(4), 304-319.

Basha, M. R., Wei, W., Bakheet, S. A., Benitez, N., Siddiqi, H. K., Ge, Y. W., Zawia, N. H. (2005). The fetal basis of amyloidogenesis: exposure to lead and latent overexpression of amyloid precursor protein and beta-amyloid in the aging brain. *Journal of Neuroscience, 25*(4), 823-829.

Beckwith, T. J., Dietrich, K. N., Wright, J. P., Altaye, M., Cecil, K. M. (2018). Reduced regional volumes associated with total psychopathy scores in an adult population with childhood lead exposure. *Neurotoxicology, 67*, 1-26.

Bedell, S., Wells, J., Liu, Q., Breivogel, C. (2019). Vitexin as an active ingredient in passion flower with potential as an agent for nicotine cessation: vitexin antagonism of the

expression of nicotine locomotor sensitization in rats. *Pharmaceutical Biology, 57*, 8-12.

Bolon, B., Butt, M.T., Garman, R.H., Dorman, D.C. (2013). Nervous System. In W. M. Haschek, C. G. Rousseaux & M. A. Wallig (Eds.), *Haschek and Rousseaux's Handbook of Toxicologic Pathology.* 3rd Edition; Boston: Academic Press, 2005-2093

Bradley, A., Bertrand, L., Rao, D.B., Greg Hall, D., Sharma, A.K. (2018). Chapter 13 - Brain. In A. W. Suttie (Ed.), *Boorman's Pathology of the Rat (Second Edition)* (pp. 191-215). Boston: Academic Press.

Brenner, M. (2014). Role of GFAP in CNS injuries. *Neuroscience Letter, 565*, 7-13.

Budson, A. E., Solomon, P. R. (2016). Chapter 4 - Alzheimer's Disease Dementia and Mild Cognitive Impairment Due to Alzheimer's Disease. In A. E. Budson & P. R. Solomon (Eds.), *Memory Loss, Alzheimer's Disease, and Dementia. 2nd Edition,* London: Elsevier, 47-69.

Can, A., Dao, D. T., Terrillion, C. E., Piantadosi, S. C., Bhat, S., & Gould, T. D. (2012). The tail suspension test. *Journal of visualized experiments : JoVE*(59), e3769-e3769.

Can, O. D., Demir Ozkay, U., Ucel, U. I. (2013). Anti-depressant-like effect of vitexin in BALB/c mice and evidence for the involvement of monoaminergic mechanisms. *European Journal Pharmacology, 699*(1-3), 250-257.

Carter, R. J., Morton, J., Dunnett, S. B. (2001). Motor coordination and balance in rodents. *Current Protocols in Neuroscience, Chapter 8*, Unit 8, Pg 12.

Cecil, K. M., Brubaker, C. J., Adler, C. M., Dietrich, K. N., Altaye, M., Egelhoff, J. C., Lanphear, B. P. (2008). Decreased brain volume in adults with childhood lead exposure. *PLoS Medicine, 5*(5), e112. Doi:10.1371/journal.pmed.0050112

Chetty, C. S., Reddy, G. R., Murthy, K. S., Johnson, J., Sajwan, K., Desaiah, D. (2001). Perinatal lead exposure alters the expression of neuronal nitric oxide synthase in rat brain. *International Journal Toxicology*, 20(3), 113–120.

Chintapanti, S., Pratap, R. K., Sreenivasula R. P. (2018). Behavioral and neurochemical consequences of perinatal exposure to lead in adult male Wistar rats: protective effect by Centella asiatica. *Environmental Science and Pollution Research International, 25*(13), 13173-13185.

Choi, J. S., Nurul, I., Yousof, A., Kim, Eon Ji, Kim, Young, M., Jung, H. A. (2014). Effects of C-glycosylation on anti-diabetic, anti-Alzheimer's disease and anti-inflammatory potential of apigenin. *Food and Chemical Toxicology, 64*, 27-33.

Cohen, L. D., Ziv, N. E. (2017). Recent insights of synaptic protein degradation. *F1000Research*, 6, 675. Doi: 10.12688/f1000research.10599.1

Correa, M., Roig-Navarro, A. F., Aragon, C. M. (2004). Motor behavior and brain enzymatic changes after acute lead intoxication on different strains of mice. *Life Sciences, 74*(16), 2009-2021.

Daneman, R., Prat, A. (2015). The blood–brain barrier. *Cold Spring Harbor perspectives in biology* **7** (1), a020412. Doi:10.1101/cshperspect.a020412

Defelipe, J. (2011). The evolution of the brain, the human nature of cortical circuits, and intellectual creativity. *Frontiers in Neuroanatomy, 5*, 29. Doi:10.3389/fnana.2011.00029

Deveci, E. (2006). Ultrastructural effects of lead acetate on brain of rats. *Toxicology and Industrial Health, 22*(10), 419-422.

Dobrakowski, M., Boroń, M., Birkner, E., Kasperczyk, A., Chwalińska, E., Lisowska, G., Kasperczyk, S. (2017). The Effect of a Short-Term Exposure to Lead on the Levels of Essential Metal Ions, Selected Proteins Related to Them, and Oxidative Stress Parameters in Humans. *Oxidative Medicine and Cellular Longevity, 9*, 8763793. Doi:10.1155/2017/8763793

Dooyema, C. A., Neri, A., Lo, Y., Durant, J., Dargan, P. I., Swarthout, T., Brown, M. J. (2012). Outbreak of fatal childhood lead poisoning related to artisanal gold mining in northwestern Nigeria, 2010. *Environmental health perspectives, 120*(4), 601-607.

Ellison, J. W., Rosenfeld, J. A., Shaffer, L. G. (2013). Genetic basis of intellectual disability. *Annual Review of Medicine, 64*, 441-450.

Ellman, G. L., Courtney, K. D., Andres, V., Featherstone, R. M. (1961). A new and rapid colorimetric determination of acetylcholinesterase activity. *Biochemical Pharmacology, 7*(2), 88-95.

Elston, G. N., Oga, T., Fujita, I. (2009). Spinogenesis and pruning scales across functional hierarchies. *The Journal of Neuroscience, 29*(10), 3271-3275.

Engel, T., Tanaka, K., Jimenez-Mateos, E. M., Caballero-Caballero, A., Prehn, J. H., Henshall, D. C. (2010). Loss of p53 results in protracted electrographic seizures and development

of an aggravated epileptic phenotype following status epilepticus. *Cell Death and Disease, 1*, e79.

Faria, A., Mateus, N., Calhau, C. (2012). Flavonoid transport across blood-brain barrier: Implication for their direct neuroprotective actions. *Nutrition and Aging*. 1: 89 – 97.

Flora, G., Gupta, D., Tiwari, A. (2012). Toxicity of lead: A review with recent updates. *Interdisciplinary toxicology, 5*(2), 47-58.

Flora, S. J., Saxena, G., Gautam, P., Kaur, P., Gill, K. D. (2007a). Response of lead-induced oxidative stress and alterations in biogenic amines in different rat brain regions to combined administration of DMSA and MiADMSA. *Chemico- Biological Interactions, 170*(3), 209-220.

Flora, S. J., Saxena, G., Mehta, A. (2007b). Reversal of lead-induced neuronal apoptosis by chelation treatment in rats: role of reactive oxygen species and intracellular $Ca^{(2+)}$. *Journal of Pharmacology Experimental and Therapeutics, 322*(1), 108-116.

Flores-Martinez, E., Pena-Ortega, F. (2017). Amyloid beta Peptide-Induced Changes in Prefrontal Cortex Activity and Its Response to Hippocampal Input. *International Journal of Peptides*, 9, 16-26

Flores-Montoya, M. G., Alvarez, J. M., Sobin, C. (2015). Olfactory recognition memory is disrupted in young mice with chronic low-level lead exposure. *Toxicology Letter, 236*(1), 69-74.

Flores-Montoya, M. G., Sobin, C. (2015). Early chronic lead exposure reduces exploratory activity in young C57BL/6J mice. *Journal of Applied Toxicology, 35*(7), 759-765.

Franklin, K. B. J., Chudasama, Y. (2012). Prefrontal Cortex. In C. Watson, G. Paxinos & L. Puelles (Eds.), *The Mouse Nervous System*. San Diego: Academic Press, 727-735.

Funahashi, S. (2017). Working Memory in the Prefrontal Cortex. *Brain Science, 7*(5). doi: 10.3390/brainsci7050049

Fuster, J. M. (2008). Chapter Two - Anatomy of the Prefrontal Cortex. In J. M. Fuster (Ed.), *The Prefrontal Cortex. 4th Edition,* San Diego: Academic Press, 7-58.

Gage, G. J., Kipke, D. R., Shain, W. (2012). Whole Animal Perfusion Fixation for Rodents. *Journal of Visualized Experiment,* 65, e3564.

Global Burden of Disease Study, Collaborators. (2015). Global, regional, and national incidence, prevalence, and years lived with disability for 301 acute and chronic diseases and injuries in 188 countries, 1990-2013: a systematic analysis for the Global Burden of Disease Study 2013. *Lancet (London, England), 386,* 743-800.

Goldman-Rakic, P. S. (1995). Cellular basis of working memory. *Neuron, 14*(3), 477-485.

Goldman-Rakic, P. S., Bates, J. F., Chafee, M. V. (1992). The prefrontal cortex and internally generated motor acts. *Current Opinion in Neurobiology, 2*(6), 830-835.

Goldstein, G.W. (1993). Evidence that lead acts as a calcium substitute in second messenger metabolism. *Neurotoxicology*. 14:97–101.

Gomi, H., Yokoyama, T., Fujimoto, K., Ikeda, T., Katoh, A., Itoh, T., Itohara, S. (1995). Mice devoid of the glial fibrillary acidic protein develop normally and are susceptible to scrapie prions. *Neuron, 14*(1), 29-41.

Gottipolu, R. R., Davuljigari, C. B. (2014). Perinatal exposure to lead: reduction in alterations of brain mitochondrial antioxidant system with calcium supplement. *Biology of Trace Element Research, 162*(1-3), 270-277.

Guan, L. P., Liu, B. Y. (2016). Antidepressant-like effects and mechanisms of flavonoids and related analogues. *European Journal of Medicine and Chemistry, 121*, 47-57.

Guidotti, T. L., Ragain, L. (2007). Protecting children from toxic exposure: three strategies. *Pediatric Clinical North America, 54*(2), 227-235.

Guimaraes, C. C., Oliveira, D. D., Valdevite, M., Saltoratto, A. L., Pereira, S. I., Franca, C., Pereira, P. S. (2015). The glycosylated flavonoids vitexin, isovitexin, and quercetrin isolated from Serjania erecta Radlk (Sapindaceae) leaves protect PC12 cells against amyloid-beta25-35 peptide-induced toxicity. *Food Chemistry and Toxicology, 86*, 88-94.

Gupta, V. K., Pal, R., Siddiqi, N. J., Sharma, B. (2015). Acetylcholinesterase from Human Erythrocytes as a Surrogate Biomarker of Lead Induced Neurotoxicity. *Enzyme Research, 2015*, 370705. Doi: 10.1155/201/370705

Hafez, N. H., Tahoun, N. S. (2011). Diagnostic value of p53 and Ki67 immunostaining for distinguishing benign from malignant serous effusions. *Journal of Egyptian National Cancer Institute*, 23(4), 155-162.

Hallen, I. P., Jonsson, S., Karlsson, M. O., Oskarsson, A. (1996). Toxicokinetics of lead in lactating and nonlactating mice. *Toxicology and Applied Pharmacology, 136*(2), 342-347.

Hallen, I. P., Jonsson, S., Karlsson, M. O., Oskarsson, A. (1996). Toxicokinetics of lead in lactating and nonlactating mice. *Toxicology and Applied Pharmacology, 136*(2), 342-347.

He, M., Min, J. W., Kong, W. L., He, X. H., Li, J. X., Peng, B. W. (2016). A review on the pharmacological effects of vitexin and isovitexin. *Fitoterapia, 115*, 74-85.

Heydari, A., Norouzzadeh, A., Khoshbaten, A., Asgari, A., Ghasemi, A., Najafi, S. Badalzadeh, R. (2006). Effects of short-term and subchronic lead poisoning on nitric oxide metabolites and vascular responsiveness in rat. *Toxicology Letter, 166*(1), 88-94.

Highab, S. M., Magaji, R. A., Muhammad, B. Y. (2018). Effect of Lead Poisoning and Antidepressant Drug on the Cerebral Cortex of the Wister Rats. *Acta Scientific Pharmaceutical Sciences, 2*(5), 16-21.

Holmes, G. L., Milh, M. D., Dulac, O. (2012). Maturation of the human brain and epilepsy. In H. Stefan & W. H. Theodore (Eds.), *Handbook of Clinical Neurology*, 107, 135-143.

Hritcu, L., Ionita, R., Postu, P. A., Gupta, G. K., Turkez, H., Lima, T. C., de Sousa, D. P. (2017). Antidepressant Flavonoids and Their Relationship with Oxidative Stress. *Oxidative Medicine and Cellular Longevity, 2017*, 5762172. Doi: 10.1155/2017/5762172

Hsieh, N-H., Chung, S-H., Chen, S-C., Chen, W-Y., Cheng, Y-H., Lin, Y-J., Liao, C-M. (2017). Anemia risk in relation to lead exposure in lead-related manufacturing. *BMC Public Health, 17*(1), 389. Doi: 10.1186/s12889-017-4315-7

Hu, M., Li, F., Wang, W. (2018). Vitexin protects dopaminergic neurons in MPTP-induced Parkinson's disease through PI3K/Akt signaling pathway. *Drug Design, Development and Therapy, 12*, 565-573.

Huang, T-N., Hsueh, Y-Ping. (2014). Novel Object Recognition for Studying Memory in Mice. *Bio-protocol, 4*(19), e1249. Doi: 10.21769/BioProtoc.1249

Ighodaro, O. M., Akinloye, O. A. (2018). First line defence antioxidants-superoxide dismutase (SOD), catalase (CAT) and glutathione peroxidase (GPX): Their fundamental role in the entire antioxidant defence grid. *Alexandria Journal of Medicine, 54*(4), 287-293.

Jäkel, S., Dimou, L. (2017). Glial Cells and Their Function in the Adult Brain: A Journey through the History of Their Ablation. *Frontiers in Cellular Neuroscience, 11*, 24. Doi: 3389/fncel.2017.00024

Jazvinscak J. M., Slade, N., Hof, P. R., Simic, G. (2018). The interactions of p53 with tau and Ass as potential therapeutic targets for Alzheimer's disease. *Progress in Neurobiology, 168*, 104-127.

Jiang, J., Dai, J., Cui, H. (2018). Vitexin reverses the autophagy dysfunction to attenuate MCAO-induced cerebral ischemic stroke via mTOR/Ulk1 pathway. *Biomedical Pharmacotherapy, 99*, 583-590.

Jones, D. G. (1983). Development, Maturation, and Aging of Synapses. In S. Fedoroff & L. Hertz (Eds.), *Advances in Cellular Neurobiology*, 4, 163-222.

Jusko, T. A., Henderson, C. R., Lanphear, B. P., Cory-Slechta, D. A., Parsons, P. J., Canfield, R. L. (2008). Blood lead concentrations < 10 microg/dL and child intelligence at 6 years of age. *Environmental Health Perspective, 116*(2), 243-248.

Kabeer, A., Muhammad, M.M., Danmaigoro, A., Abdul, R. E., Abubakar, M. Z. (2019). Therapeutic potential of curcumin against lead-induced toxicity: A review. *Biomedical Research and Therapy,* 6 (3):3053-3066.

Katavolos, P., Staempfli, S., Sears, W., Gancz, A. Y., Smith, D. A., Bienzle, D. (2007). The effect of lead poisoning on hematologic and biochemical values in trumpeter swans and Canada geese. *Veterinary Clinical Pathology*, *36*(4), 341-347.

Kim, H. C., Jang, T. W., Chae, H. J., Choi, W. J., Ha, M. N., Ye, B. J., Hong, Y. S. (2015). Evaluation and management of lead exposure. *Annals of Occupational and Environmental Medicine*, *27*, 30.

Klotz, K., Göen, T. (2017). Human Biomonitoring of Lead Exposure *Lead – Its Effects on Environment and Health,* 17. Doi:10.1515/9783110434330-006

Kokras, N., Dalla, C. (2014). Sex differences in animal models of psychiatric disorders. *British journal of pharmacology, 171*(20), 4595-4619.

Kolb, B., Mychasiuk, R., Muhammad, A., Li, Y., Frost, D. O., Gibb, R. (2012). Experience and the developing prefrontal cortex. *Proceedings of the National Academy of Science U. S. A., 109* (2), 17186-17193.

Komada, M., Takao, K., Miyakawa, T. (2008). Elevated plus maze for mice. *Journal of visualized experiments*, 22, 1088. Doi: 10.3791/1088

Kougias, D. G., Sellinger, E. P., Willing, J., Juraska, J. M. (2018). Perinatal exposure to an environmentally relevant mixture of phthalates results in a lower number of neurons and synapses in the medial prefrontal cortex and decreased cognitive flexibility in adult

male and female rats. *Journal of Neuroscience*, 38(31), 6864-6872. doi: 10.1523/jneurosci.0607-18.2018

Kraeuter, A. K., Guest, P. C., Sarnyai, Z. (2019). The Y-Maze for Assessment of Spatial Working and Reference Memory in Mice. *Methods in Molecular Biology, 1916*, 105-111.

Krishnaveni, M. (2012). Flavonoids in enhancing memory function. *Journal of Pharmacy Research*, 5, 3870-3874

Kritzer, M. F., Goldman-Rakic, P. S. (1995). Intrinsic circuit organization of the major layers and sublayers of the dorsolateral prefrontal cortex in the rhesus monkey. *Journal of Complementary Neurology, 359*(1), 131-143.

Kroon, T., van Hugte, E., van Linge, L., Mansvelder, H. D., Meredith, R. M. (2019). Early postnatal development of pyramidal neurons across layers of the mouse medial prefrontal cortex. *Scientific Reports, 9*(1), 5037. Doi:10.1038/s41598-019-41661-9

Kumar, S., Pandey, A. K. (2013). Chemistry and Biological Activities of Flavonoids: An Overview. *The Scientific World Journal, 2013*, 16. Doi: 10.1155/2013/162750

Lanphear, B. P., Hornung, R., Khoury, J., Yolton, K., Baghurst, P., Bellinger, D. C., Roberts, R. (2005). Low-level environmental lead exposure and children's intellectual function: an international pooled analysis. *Environmental Health Perspectives, 113*(7), 894-899.

Lentz, M. R., Westmoreland, S.V., Greco, J. B., Fuller, R. A., Ratai, E. M., He, J., Sehgal, P., Halpern, E.F., Lackner, A. A., Masliah, E., Gonzalez, G. (2005). Quantitative neuropathologic correlates of changes in ratio of N-accetylaspartate to the creatine in Macaque brain. *Radiology*, 235, 461-468.

Li, N., Liu, X., Zhang, P., Qiao, M., Li, H., Li, X., Yu, Z. (2015). The effects of early life lead exposure on the expression of interleukin (IL) 1beta, IL-6, and glial fibrillary acidic protein in the hippocampus of mouse pups. *Human Experimental Toxicology, 34*(4), 357-363.

Lima, L. K. F., Pereira, S. K. S., Junior, R.D.S.S., Santos, F.P.D.S., Nascimento, A. S., Feitosa, C. M., Rai, M. (2018). A Brief Review on the Neuroprotective Mechanisms of Vitexin. *Biomed Research International, 2018,* 4785089. Doi: 10.1155.2018/4785089

Liu, J. T., Chen, B. Y., Zhang, J. Q., Kuang, F., & Chen, L. W. (2015). Lead exposure induced microgliosis and astrogliosis in hippocampus of young mice potentially by triggering TLR4-MyD88-NFkappaB signaling cascades. *Toxicology Letter, 239*(2), 97-107.

Liu, J., Li, L., Wang, Y., Yan, C., Liu, X (2013). Impact of low blood lead concentrations on iq and school performance in Chinese children. *PLoS One* 8 (5), e65230. Doi: 10.1371/journal.pone.0065230

Lyu, Z., Cao, J., Wang, J., Lian, H. (2018). Protective effect of vitexin reduces sevoflurane-induced neuronal apoptosis through HIF-1α, VEGF and p38 MAPK signaling pathway in vitro and in newborn rats. *Experimental and Therapy Medicine, 15*(3), 3117-3123.

Mahmoud, Y. I., Sayed, S. S. (2016). Effects of L-cysteine on lead acetate induced neurotoxicity in albino mice. *Biotechnic and Histochemistry, 91*(5), 327-332.

Malar, D. S., Suryanarayanan, V., Prasanth, M. I., Singh, S. K., Balamurugan, K., Devi, K. P. (2018). Vitexin inhibits Abeta25-35 induced toxicity in Neuro-2a cells by augmenting Nrf-2/HO-1 dependent antioxidant pathway and regulating lipid homeostasis by the activation of LXR-alpha. *Toxicology In Vitro, 50,* 160-171.

Markham, J. A., Morris, J. R., Juraska, J. M. (2007). Neuron number decreases in the rat ventral, but not dorsal, medial prefrontal cortex between adolescence and adulthood. *Neuroscience, 144*(3), 961-968.

Mason, L. H., Harp, J. P., Han, D. Y. (2014). Lead neurotoxicity: neuropsychological effects of lead toxicity. *Biomedl Research International, 2014*, 840547. Doi: 10.1155/2014/840547

Matchkov, V. V., Krivoi, I. I. (2016). Specialized Functional Diversity and Interactions of the Na,K-ATPase. *Frontiers in Physiology, 7*(179). doi: 10.3389/fphys.2016.00179

Mazumdar, M., Bellinger, D. C., Gregas, M., Abanilla, K., Bacic, J., Needleman, H. L. (2011). Low-level environmental lead exposure in childhood and adult intellectual function: a follow-up study. *Environmental Health, 10*, 24. Doi: 10.1186/1476-069X-10-24.

McMahon, H. T., Bolshakov, V. Y., Janz, R., Hammer, R.E., Siegelbaum, S. A., Sudhof, T. C. (1996). Synaptophysin, a major synaptic protein is not essential for neurotransmitter release. *Proceedings of the National Academy of Science, U.S.A*, 93(10), 4760-4764.

Meija, J., Coplen, B., Berglund, M., Brand, W. A., De Bièvre, P., Gröning, M., Holden, N. E., Irrgeher, J., Loss, R. D., Walczyk, T., Prohaska, T. (2016). Atomic weights of the elements 2013 (IUPAC Technical Report), *Pure and Applied Chemistry*, 88(3), 265-291.

Meng, H., Larson, S. K., Gao, R., Qiao, X. (2007). BDNF transgene improves ataxic and motor behaviors in stargazer mice. *Brain Research, 1160*, 47-57.

Min, J. W., Kong, W. L., Han, S., Bsoul, N., Liu, W. H., He, X. H., Peng, B. W. (2017). Vitexin protects against hypoxic-ischemic injury via inhibiting Ca2+/Calmodulin-dependent

protein kinase II and apoptosis signaling in the neonatal mouse brain. *Oncotarget, 8*(15), 25513-25524.

Min, J-W., Hu, J-J., He, M., Sanchez, R. M., Huang, W-X., Liu, Y-Q., Peng, B-W. (2015). Vitexin reduces hypoxia–ischemia neonatal brain injury by the inhibition of HIF-1alpha in a rat pup model. *Neuropharmacology, 99*, 38-50.

Miyake, A., Shah, P. (1999). Models of working memory: Mechanisms of active maintenance and executive control: Cambridge University Press.

Mohan, H., Verhoog, M. B., Doreswamy, K. K., Eyal, G., Aardse, R., Lodder, B. N., de Kock, C. P. J. (2015). Dendritic and Axonal Architecture of Individual Pyramidal Neurons across Layers of Adult Human Neocortex. *Cerebral Cortex, 25*(12), 4839-4853.

Moosavirad, S. A., Rabbani, M., Sharifzadeh, M., Hosseini-Sharifabad, A. (2016). Protective effect of vitamin C, vitamin B12 and omega-3 on lead-induced memory impairment in rat. *Research in Pharmaceutical Science, 11*(5), 390-396.

Muralidhara, K. G. (2015). Dietary Supplements as Cognitive Enhancers: The Role of Flavonoid-Rich Foods and their Relevance in Age-Related Neurodegeneration. In R. R. Watson & V. R. Preedy (Eds.), *Bioactive Nutraceuticals and Dietary Supplements in Neurological and Brain Disease*. San Diego, Academic Press, 281-290.

Nabavi, S. F., Khan, H., D'Onofrio, G., Samec, D., Shirooie, S., Dehpour, A. R., Sobarzo-Sanchez, E. (2018). Apigenin as neuroprotective agent: Of mice and men. *Pharmacology Research, 128*, 359-365.

Narayanan, R. T., Udvary, D., Oberlaender, M. (2017). Cell Type-Specific Structural Organization of the Six Layers in Rat Barrel Cortex. *Frontiers in neuroanatomy, 11*, 91-91.

Nathalie, M. G., Madhurima, B., Vidita, A. V., Evelyn, K. L. (2009). Layer II-III of the prefrontal cortex: Inhibition by the serotonin 5-HT_{1A} receptor in development and stress. *Journal of Neuroscience*, 29 (32): 10094-10103.

Nava-Ruiz, C., Mendez-Armenta, M., Rios, C. (2012). Lead neurotoxicity: effects on brain nitric oxide synthase. *Journal of Molecular Histology*, *43*(5), 553-563.

Neal, A. P., Worley, P. F., Guilarte, T. R. (2011). Lead exposure during synaptogenesis alters NMDA receptor targeting via NMDA receptor inhibition. *Neurotoxicology, 32*(2), 281-289.

Noske, R., Cornelius, F., Clarke, Ronald, J. (2010). Investigation of the enzymatic activity of the Na+,K+-ATPase via isothermal titration microcalorimetry. *Biochimica et Biophysica Acta (BBA) - Bioenergetics, 1797*(8), 1540-1545.

NRC (National Research Council) (2008). Guide for the care and use of laboratory animals. Eight edition, Washington D.C, The National Academies Press, 11-40.

Nurdiana, S., Goh, Y. M., Hafandi, A., Dom, S. M., Nur Syimal'ain, A., Noor Syaffinaz, N. M., Ebrahimi, M. (2018). Improvement of spatial learning and memory, cortical gyrification patterns and brain oxidative stress markers in diabetic rats treated with Ficus deltoidea leaf extract and vitexin. *Journal of Traditional and Complementary Medine, 8*(1), 190-202.

Ogunseitan, O., Oladele, A., Smith T. (2007). The cost of environmental lead (Pb) poisoning in Nigeria *African Journal of Environmental Science and Technology, 1*(2), 027-036.

Okada, Y., Kamatani, Y. (2012). Common genetic factors for hematological traits in humans. *Journal of Human Genetics, 57*(3), 161-169.

Olajide, O.J., Akinola, O. (2016). Sodium azide-induced degenerative changes in the dorsolateral prefrontal cortex of rats: Attenuating mechanisms of kolaviron. *European Journal of Anatomy,* 20 (1): 47-64.

Oliveira, D. R., Zamberlam, C. R., Gaiardo, R. B., Rego, G. M., Cerutti, J. M., Cavalheiro, A. J., Cerutti, S. M. (2014). Flavones from Erythrina falcata are modulators of fear memory. *BMC Complement and Alternative Medicine, 14*, 288. Doi:10.1186/1472-6882-14-288

Panche, A. N., Diwan, A. D., Chandra, S. R. (2016). Flavonoids: an overview. *Journal of nutritional science, 5*, e47. Doi: 10.1017/jns.2016.41

Parasuraman, S., Raveendran, R., Kesavan, R. (2010). Blood sample collection in small laboratory animals. *Journal of pharmacology & pharmacotherapeutics, 1*(2), 87-93.

Paxinos, G., Franklin, K. B. J.(2007). The Mouse Brain in Stereotaxic Coordinates. 3rd edition, Amsterdam; Boston: Elsevier.

Pekny, M., Levéen, P., Pekna, M., Eliasson, C., Berthold, C. H., Westermark, B., Betsholtz, C. (1995). Mice lacking glial fibrillary acidic protein display astrocytes devoid of intermediate filaments but develop and reproduce normally. *EMBO Journal, 14*(8), 1590-1598.

Peng, Y., Sun, Q., Xu, W., He, Y., Jin, W., Yuan, L., Gao, R. (2019). Vitexin ameliorates high fat diet-induced obesity in male C57BL/6J mice via the AMPKalpha-mediated pathway. *Food Function, 10*(4), 1940-1947.

Petanjek, Z., Judaš, M., Šimić, G., Rašin, M., Roko, U., Harry, B. M., Rakic, P., Kostović, I. (2011). Extraordinary neoteny of synaptic spines in the human prefrontal cortex. *Proceedings of the National Academy of Sciences, 108*(32), 13281-13286.

Petanjek, Z., Sedmak, D., Džaja, D., Hladnik, A., Rašin, M. R., Jovanov-Milosevic, N., Jovanov-Milosevic, N. (2019). The Protracted Maturation of Associative Layer IIIC Pyramidal Neurons in the Human Prefrontal Cortex During Childhood: A Major Role in Cognitive Development and Selective Alteration in Autism. *Frontier in Psychiatry, 10*, 122.

Pilny, A. A. (2008). Clinical hematology of rodent species. *Veterinary Clinics of North America: Exotic Animal Practice, 11*(3), 523-533.

Pomierny-Chamioło, L., Moniczewski, A., Wydra, K., Suder, A., Filip, M. (2013). Oxidative stress biomarkers in some rat brain structures and peripheral organs underwent cocaine. *Neurotoxicity Research, 23*(1), 92-102. doi: 10.1007/s12640-012-9335-6

Popović, N., Pajović, S.B., Stojiljković, V (2017). Prefrontal catecholaminergic turnover and antioxidant defense system of chronically stressed rats. *Folia Biologica*, 65(1), 43–54.

Popović, N., Stojiljković, V., Pejić, S., Todorović, A., Pavlović, I., Gavrilović, L., Pajović, S. B (2019). Modulation of Hippocampal Antioxidant Defense System in Chronically Stressed Rats by Lithium. *Oxidative Medicine and Cellular Longevity, 2019*, 8745376. doi: 10.1155/2019/8745376

Prabhakar, M., Bano, H., Kumar, I., Shamsi, M., Khan, S. (1981). Pharmacological Investigations on Vitexin. *Planta Medica,* 43(12), 396–403.

Purves, D., Augustine, G. J., Fitzpatrick, D., Hall, W. C., LaMantia, A-S., White, L. E. (2012). Neuroscience. Sunderland, Massachusetts: Sinauer Associates, Inc. ISBN: 0878936467

Rădulescu, A., Lundgren, S. (2019). A pharmacokinetic model of lead absorption and calcium competitive dynamics. *Scientific Reports, 9*(1), 14225. Doi: 10.1038/s41598-019-50654-7

Rahman, A., Rao, M. S., Khan, K. M. (2018). Intraventricular infusion of quinolinic acid impairs spatial learning and memory in young rats: a novel mechanism of lead-induced neurotoxicity. *Journal of Neuroinflammation, 15*(1), 263. Doi: 10.1186/s12974-018-1306-2

Reckziegel, P., Dias, V. T., Benvegnu, D., Boufleur, N., Silva Barcelos, R. C., Segat, H. J., Burger, M. E. (2011). Locomotor damage and brain oxidative stress induced by lead exposure are attenuated by gallic acid treatment. *Toxicology Letter, 203*(1), 74-81.

Ricart-Jané, D., Llobera, M., and López-Tejero, M. D. (2002). Anticoagulants and other preanalytical factors interfere in plasma nitrate/nitrite quantification by the Griess method. *Nitric Oxide, 6*(2), 178-185.

Rosa, S. I. G., Rios-Santos, F., Balogun, S. O., Martins, D. T. (2016). Vitexin reduces neutrophil migration to inflammatory focus by down-regulating pro-inflammatory mediators via inhibition of p38, ERK1/2 and JNK pathway. *Phytomedicine, 23*(1), 9-17.

Rosenfeld, C. S., Ferguson, S. A. (2014). Barnes maze testing strategies with small and large rodent models. *Journal Visualized Experiment,* 84, e51194.

Ruan, S.Y., Gu, Z. (1999). Toxic effects of lead on the blood brain barrier in rats. *Journal of Occupational Health.* 41:39–42

Sanders, T., Liu, Y., Buchner, V., Tchounwou, P.B. (2009). Neurotoxic effects and biomarkers of lead exposure: a review. *Review on Environmental Health*, 24 (1): 15-45.

Sansar, W., Ahboucha, S., Gamrani, H. (2011). Chronic lead intoxication affects glial and neural systems and induces hypoactivity in adult rat. *Acta Histochemical, 113*(6), 601-607.

Satsix. (2010). Mouse Brain Anatomy Retrieved 11 October, 2019, from https://m.blog.naver.com

Saxena, D. K., Lal, B., Murthy, R. C., Chandra, S. V. (1984). Lead induced histochemical changes in the testes of rats. *Industrial Health,* 22, 255-260.

Schmitt, U., Tanimoto, N., Seeliger, M., Schaeffel, F., Leube, R. E. (2009). Detection of behavioral alterations and learning deficits in mice lacking synaptophysin. *Neuroscience*, *162*(2), 234-243.

Schneider, J. S., Anderson, D. W., Kidd, S. K., Sobolewski, M., Cory-Slechta, D. A. (2016). Sex-dependent effects of lead and prenatal stress on post-translational histone modifications in frontal cortex and hippocampus in the early postnatal brain. *Neurotoxicology*, *54*, 65-71.

Schneider, Jay S., Lidsky, T. I. (2003). Lead neurotoxicity in children: basic mechanisms and clinical correlates. *Brain, 126*(1), 5-19.

Schubert, D., Martens, G. J. M., Kolk, S. M. (2015). Molecular underpinnings of prefrontal cortex development in rodents provide insights into the etiology of neurodevelopmental disorders. *Molecular psychiatry, 20*(7), 795-809.

Schwartz, J., Landrigan, P. J., Baker, E. L. Jr., Orenstein, W. A. & Lindern, I. H. V. (1990). Lead-induced anemia: dose-response relationships and evidence for a threshold. *American journal of public health* 80 (2), 165–168.

Seibenhener, M. L., Wooten, M. C. (2015). Use of the Open Field Maze to measure locomotor and anxiety-like behavior in mice. *Journal Visualized Experiment,* 96, e52434. Doi: 10.3791/52434

Semple, B. D., Blomgren, K. G., Kayleen, Ferriero, D. M., Noble-Haeusslein, L. J. (2013). Brain development in rodents and humans: Identifying benchmarks of maturation and vulnerability to injury across species. *Progress in neurobiology, 106-107*, 1-16. Doi: 10.1016/j.pneurobio.2013.04.001

Shah, A. H., Bilal, R. (2009). Body Composition, its Significance and Models for Assessment. *Pakistan Journal of Nutrition, 8, 198-202.*

Sharma, B., Singh, S., Siddiqi, N. J. (2014). Biomedical implications of heavy metals induced imbalances in redox systems. *Biomed Research International, 2014*, 640754. Doi: 10.1155/2014/640754

Sharma, P., Chambial, S., Shukla, K. K. (2015). Lead and neurotoxicity. *Indian Journal of Clinical Biochemistry, 30*(1), 1-2.

Sheeja, M. D., Beema, S. R., Karutha, P. S., Pandima, D. K. (2017). Cholinesterase inhibitory, anti-amyloidogenic and neuroprotective effect of the medicinal plant Grewia tiliaefolia - An in vitro and in silico study. *Pharmacceutical Biology, 55*(1), 381-393.

Singh, G., Singh, V., Sobolewski, M., Cory-Slechta, D. A., Schneider, J. S. (2018). Sex-Dependent Effects of Developmental Lead Exposure on the Brain. *Front Genet, 9*, 89. Doi: 10.3389/fgene.2018.00089

Sobin, C., Flores-Montoya, M. G., Gutierrez, Marisela, Parisi, Natali., Schaub, T. (2015). δ-Aminolevulinic acid dehydratase single nucleotide polymorphism 2 (ALAD2) and peptide transporter haplotype differently influence neurobehavior in low-level lead exposed children. *Neurotoxicology and teratology, 47*, 137-145.

Sobin, C., Montoya, M. G., Parisi, N., Schaub, T., Cervantes, M., Armijos, R. X. (2013). Microglial disruption in young mice with early chronic lead exposure. *Toxicology Letter, 220*(1), 44-52.

Soeiro, A. C., Gouvea, T. S., Moreira, E. G. (2007). Behavioral effects induced by subchronic exposure to Pb and their reversion are concentration and gender dependent. *Human Experimental Toxicology, 26*(9), 733-739.

Sofroniew, M. V. (2005). Reactive astrocytes in neural repair and protection. *Neuroscientist, 11*(5), 400-407.

Song, D., Opris, I., Chan, R. H., Marmarelis, V. Z., Hampson, R. E., Deadwyler, S. A., Berger, T. W. (2012). Functional connectivity between Layer 2/3 and Layer 5 neurons in prefrontal cortex of nonhuman primates during a delayed match-to-sample task.

Conference Proceeding of IEEE Engineering in Medicine and Biology Society, 2012, 2555-2558.

Soulimani, R., Younos, C., Jarmouni, S., Bousta, D., Misslin, R., Mortier, F. (1997). Behavioural effects of Passiflora incarnata L. and its indole alkaloid and flavonoid derivatives and maltol in the mouse. *Journal of Ethnopharmacology, 57*(1), 11-20.

Souza, S. F., Goncalves, G., Komatsu, F., Queiroz, C. A., Almeida, A. A., Moreira, E. G. (2005). Developmental lead exposure induces depressive-like behavior in female rats. *Drug and Chemical Toxicology, 28*(1), 67-77.

Sprowles, J. L. N., Amos-Kroohs, R. M., Braun, A. A., Sugimoto, C., Vorhees, C. V., Williams, M. T. (2018). Developmental manganese, lead, and barren cage exposure have adverse long-term neurocognitive, behavioral and monoamine effects in Sprague-Dawley rats. *Neurotoxicology and Teratology, 67*, 50-64.

Stanga, S., Lanni, C., Govoni, S., Uberti, D., D'Orazi, G., Racchi, M. (2010). Unfolded p53 in the pathogenesis of Alzheimer's disease: is HIPK2 the link? *Aging, 2*(9), 545-554.

Stangle, D. E., Smith, D. R., Beaudin, S. A., Strawderman, M. S., Levitsky, D. A., Strupp, B. J. (2007). Succimer chelation improves learning, attention, and arousal regulation in lead-exposed rats but produces lasting cognitive impairment in the absence of lead exposure. *Environmental Health Perspectives, 115*(2), 201-209.

Struzynska, L., Walski, M., Gadamski, R., Dabrow-ska-Bouta, B., Rafalowska, U. (1997). Lead-induced abnormalities in blood-brain barrier permeability in experimental chronic toxicity. *Molecular and Chemical Neuropathology,* 31(3): 207–224.

Sun, L., Zhou, X. L., Yi, H. P., Jiang, S. J., Yuan, H. (2014). Lead-induced morphological changes and amyloid precursor protein accumulation in adult rat hippocampus. *Biotechnic and Histochemistry, 89*(7), 513-517.

Tang, Q., Su, Y-W., Xian, C. J. (2019). Determining Oxidative Damage by Lipid Peroxidation Assay in Rat Serum. *Bio-protocol, 9*(12), e3263. Doi:10.21769/BioProtoc.3263

Tena, A., Peru, E., Martinetti, L. E., Cano, J. C., Loyola Baltazar, C. D., Wagler, A. E., Fenelon, K. (2019). Long-term consequences of early postnatal lead exposure on hippocampal synaptic activity in adult mice. *Brain and Behaviour, 9*(8), e01307. Doi: 10.1002/brb3.1307

Thangarajan, S., Vedagiri, A., Somasundaram, S., Sakthimanogaran, R., Murugesan, M. (2018). Neuroprotective effect of morin on lead acetate- induced apoptosis by preventing cytochrome c translocation via regulation of Bax/Bcl-2 ratio. *Neurotoxicology and Teratology, 66*, 35-45.

Thayer, B. (2018). How to Fight Lead Exposure with Nutrition *Preventing Illness.* https://www.eatright.org/health/wellness/preventing-illness/how-to-fight-lead-exposure-with-nutrition. Retrieved on 24 October, 2018.

Tsujimoto, S. (2008). The prefrontal cortex: functional neural development during early childhood. *Neuroscientist, 14*(4), 345-358.

Ukeda, H., Kawana, D., Maeda, S., and Sawamura, M (1999). Spectrophotometric Assay for Superoxide Dismutase Based on the Reduction of Highly Water-soluble Tetrazolium Salts by Xanthine-Xanthine Oxidase. *Bioscience, Biotechnology and Biochemistry,* 63:3, 485-488. Doi: 10.1271/bbb.63.48

Ursula, R., Dicke, G. (2016). Neuronal factors determining high intelligence. *Philosophical Transactions of the Royal Society B, 371*(1685), 20150180. Doi: 10.1098/rstb.2015.0180

Van De Werd, H. J., Rajkowska, G., Evers, P., Uylings, H. B. (2010). Cytoarchitectonic and chemoarchitectonic characterization of the prefrontal cortical areas in the mouse. *Brain Structure and Function, 214*(4), 339-353.

Van De Werd, H. J., Uylings, H. B. (2014). Comparison of (stereotactic) parcellations in mouse prefrontal cortex. *Brain Structure and Function, 219*(2), 433-459.

Van der Ham, I. J. M., Ruotolo, F. (2017). On Inter- and Intrahemispheric Differences in Visuospatial Perception. In A. Postma & I. J. M. van der Ham (Eds.), *Neuropsychology of Space.* San Diego, Academic Press, 35-76.

Van Eden, C. G., Kros, J. M., Uylings, H. B. (1990). The development of the rat prefrontal cortex. Its size and development of connections with thalamus, spinal cord and other cortical areas. *Progress in Brain Research, 85*, 169-183.

Van Eden, C. G., Uylings, H. B. (1985). Cytoarchitectonic development of the prefrontal cortex in the rat. *Journal of Complementary Neurology, 241*(3), 253-267.

von Stackelberg, K., Guzy, E., Chu, Tian., Claus Henn, B. (2015). Exposure to Mixtures of Metals and Neurodevelopmental Outcomes: A Multidisciplinary Review Using an Adverse Outcome Pathway Framework. *Risk analysis : an official publication of the Society for Risk Analysis, 35*(6), 971-1016.

Wang, Y., Zhen, Y., Wu, X., Jiang, Q., Li, X., Chen, Z., Dong, L. (2015). Vitexin protects brain against ischemia/reperfusion injury via modulating mitogen-activated protein kinase and apoptosis signaling in mice. *Phytomedicine, 22*(3), 379-384.

Wani, A. L., Ara, A., Usmani, J. A. (2015). Lead toxicity: a review. *Interdisciplinary Toxicology, 8*(2), 55-64.

Weston, H. I., Weston, D. D., Allen, J. L., Cory-Slechta, D. A. (2014). Sex-dependent impacts of low-level lead exposure and prenatal stress on impulsive choice behavior and associated biochemical and neurochemical manifestations. *Neurotoxicology, 44*, 169-183.

WHO. (2018). Lead poisoning and health. *Newsroom/Fact Sheets.* https://www.who.int/news-room/fact-sheets/detail/lead-poisoning-and-health. Retrieved on 20 September, 2019.

Xu, J. L., Ling-jun, W. C., Wang, X, F., Wen-yu, X. L. (2008). Lead induces oxidative stress, DNA damage and alteration of p53, Bax and Bcl-2 expressions in mice. *Food and Chemical Toxicology, 46*(5), 1488-1494.

Yan, C., Liu, H., Lin, L. (2013). Simultaneous determination of vitexin and isovitexin in rat plasma after oral administration of *Santalum album L.* leave extract by liquid chromatography tandem mass spectrometry. *Biomedical Chromatography*, 27 (2): 228–232.

Yang, L., Yang, Z. M., Zhang, N., Tian, Z., Liu, S. B., Zhao, M. G. (2014). Neuroprotective effects of vitexin by inhibition of NMDA receptors in primary cultures of mouse cerebral cortical neurons. *Molecular and Cellular Biochemistry, 386*(1-2), 251-258.

Yin, J., Qu, J., Zhang, W., Lu, D., Gao, Y., Ying, X., Kang, T. (2014). Tissue distribution comparison between healthy and fatty liver rats after oral administration of hawthorn leaf ex-tract, *Biomedical Chromatography,* 28 (5): 637–647.

Yu, H., Liao, Y., Li, T., Cui, Y., Wang, G., Zhao, F., Jin, Y. (2016). Alterations of Synaptic Proteins in the Hippocampus of Mouse Offspring Induced by Developmental Lead Exposure. *Molecular Neurobiology, 53*(10), 6786-6798

Zhai, Q., Yang, L., Zhao, J., Zhang, H., Tian, F., Chen, W. (2018). Protective Effects of Dietary Supplements Containing Probiotics, Micronutrients, and Plant Extracts Against Lead Toxicity in Mice. *Frontier in Microbiology, 9,* 2134. Doi: 10.3389/fmicb.2018.02134

Zhang, L., Tu, R., Wang, Y., Hu, Y., Li, X., Cheng, X., Huang, H. (2017). Early-Life Exposure to Lead Induces Cognitive Impairment in Elder Mice Targeting SIRT1 Phosphorylation and Oxidative Alterations. *Frontier in Physiology, 8,* 446. Doi: 10.3389/fphys.2017.00446

Zhu, Q. M., Li-Na, L. C., Sun, Y., Jiang, B., Zhang, W., Li, J. (2016). Antinociceptive effects of vitexin in a mouse model of postoperative pain. *Scientific Reports, 6,* 19266. Doi: 10.1038/srep19266

APPENDIX I: Preparation of fixatives and other related solutions

Preparation of phosphate buffered saline (PBS)

Reagents required

1. Sodium chloride (NaCl)
2. Potassium chloride (KCl)
3. Sodium di-hydrogen orthophosphate (Na_2HPO_4)
4. Potasium di-hydrogen orthophosphate (KH_2PO_4)
5. Hydrochloric Acid

All reagents were purchased from Sigma Aldrich, MO, U.S.A through their distributor Bristol Scientific Co., Lagos, Nigeria.

Procedure

For 1 litre of 1X PBS

1. 8 g of NaCl was added to 800 ml of distilled water.
2. While stirring the solution, the following compounds were added:

   0.2 g of KCl;

   1.44 g of Na_2HPO_4; and

   0.24 g of KH_2PO_4.

3. The pH of the solution was adjusted to 7.4 with HCl (using pipette and pH meter).
4. Distilled water added to make a total volume of 1 litre.

The solution was then stored at 4°C temperature.

Preparation of 4% paraformaldehyde

1. For 1 Litre of 4% paraformaldehyde, 800 mL of PBS in a glass beaker was heated while stirring to approximately 60 °C.
2. 40 g of paraformaldehyde powder was added to the heated PBS solution while stirring.
3. The pH of the solution was raised by adding (drop wise) 1 N NaOH from a pipette until the solution clears.
4. Once the paraformaldehyde was dissolved, the solution was cooled and filtered.
5. The pH was rechecked and adjusted with small amounts of dilute HCl to approximately 6.9 using pH meter.
6. The 4% PFA solution was then stored at 4°C temperature until use (within a week).

Preparation of 0.25 M of sucrose solution

85.5 g of sucrose powder was added to 342 ml of distilled water. Thereafter, the solution was stirred and stored until use at 4°C in a Refrigerator (LG; S. Korea)

APPENDIX II: Tissue processing technique

Fixation: This process was carried out to preserve tissue integrity and prevent autolysis by using fixative. In this study, the fixative used was 4% paraformaldehyde (4% PFA), and the type of fixation used was perfusion fixation. Tissues were also post-fixed in 4% PFA for 24 hours for proper fixing.

Dehydration: The process was carried out to remove water from the tissue because effective wax impregnation of tissue would be difficult to accomplish in the presence of water. The dehydration process in this study was done using ascending grades of alcohol.

i. 50% alcohol..... 1 hour
ii. 70% alcohol..... 1 hour
iii. 90% alcohol..... 1 hour
iv. Two changes of absolute alcohol..... 1 hour each

The preparation of different percentages of alcohol used:

50% alcohol

i. Absolute alcohol..... 50ml
ii. Distilled water..... 50ml

70% alcohol

i. Absolute alcohol..... 70ml
ii. Distilled water..... 30ml

90% alcohol

i. Absolute alcohol..... 90ml

ii. Distilled water..... 10ml

Absolute 100% of alcohol

Clearing: This process was used to replace dehydrating fluid (i.e., alcohol) with a clearing fluid (xylene) because alcohol cannot mix with the embedding medium (paraffin wax). The choice of xylene for clearing in this study was based on its ability to mix with the embedding medium (paraffin wax).

The clearing process used is as follows:

i. Xylene I..... 1 hour
ii. Xylene II..... 1 hour

Infiltration (Impregnation): Molten paraffin wax (at 56˚C) was used for filtration. Infiltration was done twice (for 1 hour each) to remove the clearing agent before embedding.

Embedding: In this process, tissues were placed in the embedding cassettes in a coronal orientation using forceps. The cassettes were subsequently filled with molten wax and cooled to solidify in tap water at room temperature. Embedding tissues in wax provides solidity and support the tissues require to allow for sectioning.

Trimming: The base of each tissue was trimmed to remove excess wax and to expose the embedded tissue using a microtome knife.

Sectioning: Rotatory microtome (Reichert-Jung, Model: 2030) was used to section tissue blocks. The tissue blocks were initially clamped on to a microtome chuck; the microtome was adjusted to 5 µm, and the microtome knife was placed at 45˚ to the block.

Floating: The ribbons produced from sectioning were floated on a water bath (at 35˚C) to straighten folded sections.

Mounting: Egg albumen was smeared on clean glass slides. The slides were then used to pick sections from the water bath.

Drying: The slides were appropriately arranged and allowed to dry overnight. Finally, each slide was labelled and kept in slide rack, awaiting staining.

APPENDIX III: Tissue staining techniques

1. Haematoxylin and Eosin staining technique

Reagents and solutions:

1% Acid Alcohol Solution (for differentiation):

Hydrochloric acid ----------	1 ml
70% ethanol ----------	100 ml

0.2% Ammonia Water Solution (Bluing):

Ammonium hydroxide (concentrated) -----	2 ml
Distilled water ----------	1000 ml

Eosin Y Solution:

Eosin Y Stock Solution (1%):

Eosin Y ----------	10 g
Distilled water ----------	200 ml
95% Ethanol ----------	800 ml

Mix to dissolve and store at room temperature.

Eosin Y Working Solution (0.25%):

Eosin Y stock solution ----------	250 ml
80% Ethanol ----------	750 ml
Glacial acetic acid (concentrated) -----	5 ml

Mix well and store at room temperature.

Haematoxylin Solution (Harris):

Potassium alum ----------	100 g
Distilled water ----------	1000 ml

The potassium alum was dissolved in distilled water by heating. 50 ml of 10% alcoholic haematoxylin solution was added and heated to boiling point for 1 minute. The solution was

removed from heat, while 2.5 g of mercuric oxide was slowly added. The solution was heated until it became dark purple in colour. Thereafter, the solution was cooled in a water bath and 20 ml of concentrated glacial acetic acid was added.

Procedure:

1. Sections were deparafinized in xylene for 10 minutes (×2).
2. Sections were rehydrated in:

   100% alcohol for 5 minutes (×2);

   95% alcohol for 2 minutes; and

   70% alcohol for 2 minutes.
3. Sections were washed briefly in distilled water and stained in Harris haematoxylin solution for 8 minutes.
4. Thereafter, Sections were washed in running tap water for 5 minutes, and differentiated in 1% acid alcohol for 30 seconds.
5. After washing in tap water for 1 minute, sections underwent Bluing process (in 0.2% ammonia water) for 1 minute.
6. After bluing, sections were washed in tap water for 5 minutes, and rinsed in 95% alcohol (10 dips).
7. Sections were then counterstained in eosin Y solution for 30 seconds.
8. Thereafter, sections were dehydrated by:

   95% alcohol 5 min (×2); and

   100% alcohol for 5 minutes (×2).
9. Sections were cleared in xylene for 5 minutes (×2), and then mounted with two drops of DPX (Dibutylphythalate-in-xylene).

2. **Cresyl fast violet staining technique**

Reagent and Solution:

0.1% Cresyl violet solution:

Cresyl echt violet ---------- 0.1 g

Distilled water ---------- 100 ml

Procedure:

1. Sections were deparaffinised in xylene for 10 minutes (×2).
2. Sections were rehydrated in:

   100% alcohol for 5 minutes (×2);

   95% alcohol for 3 minutes; and

   70% for 3 minutes.
3. Sections were rinsed briefly in distilled water and stained in 0.1% cresyl violet solution for 10 minutes.
4. The sections were rinsed in distilled water and then differentiated in 95% ethyl alcohol for 20 minutes.
5. Sections were then dehydrated by:

   95% alcohol 5 min (×2); and

   100% alcohol for 5 minutes (×2).
6. Finally, sections were cleared in xylene for 5 minutes (×2) and mounted with two drops of DPX (Dibutylphythalate-in-xylene).

3. Congo red staining technique (Highman's)

Reagents and Solutions:

0.5% Congo red in 50% alcohol:

Congo red ---------- 0.5 g

50% Alcohol ---------- 100 ml

1% Sodium Hydroxide:

Sodium hydroxide ---------- 1 g

Distilled water ---------- 100 ml

Alkaline Alcohol Solution:

1% Sodium hydroxide ---------- 1 ml

50% alcohol ---------- 100 ml

Haematoxylin Solution:

Potassium alum ---------- 100 g

Distilled water ---------- 1000 ml

Procedure:

1. Sections were deparafinized in xylene for 10 minutes (×2).
2. Sections were rehydrated in:

   100% alcohol for 5 minutes (×2);

   95% alcohol for 2 minutes; and

   70% alcohol for 2 minutes.
3. Sections were rinsed briefly in distilled water and stained in Congo red solution for 20 minutes.
4. After a brief rinse in distilled water, sections were differentiated in alkaline alcohol solution (10 dips).

5. Sections were then:

   rinsed in tap water for 1 minute; counterstained in haematoxylin solution for 30 seconds; and rinsed in tap water for 2 minutes.

6. Sections were then dehydrated by:

   95% alcohol for 5 minutes; and

   100% alcohol, 3 minutes (×2).

7. Sections were cleared in xylene for 3 minutes (×2) before mounting with two drops of DPX (Dibutylphythalate-in-xylene).

4. Bielschowsky's silver staining technique

Reagents and Solutions:

10% Silver Nitrate Stock Solution:

Silver nitrate ----------	5 g
Distilled water ----------	50 ml

1% Ammonium Hydroxide Solution:

Ammonium hydroxide concentrated ----------	1 ml
Distilled water ----------	100 ml

Developer Stock Solution:

40% Formaldehyde ----------	20 ml
Citric acid (trisodium dihydrate) -----	0.5 g
Nitric acid, concentrated ----------	2 drops
Distilled water ----------	100 ml

Developer Working Solution (Prepared immediately before use):

Developer Stock Solution ----------	8 drops
Ammonium hydroxide concentrated ---------	8 drops
Distilled water ----------	50 ml

5% Sodium Thiosulfate (HYPO):

Sodium Thiosulfate ---------- 5 g

Distilled water ---------- 100 ml

Procedure:

1. Sections were deparafinized in xylene for 10 minutes (×2).
2. Sections were rehydrated in:

   100% alcohol for 5 minutes (×2);

   95% alcohol for 2 minutes; and

   70% alcohol for 2 minutes.
3. Sections were then:

   washed with distilled water for 1 minute (×3);

   immersed in 10% silver nitrate solution (40 ºC) for 15 minutes staining; and

   washed again in distilled water for 1 minute (×3).
4. Concentrated ammonium hydroxide was added to the silver nitrate solution in droplets until the precipitate formed was clear.
5. Sections were again immersed in ammonium silver solution (40 ºC) and stained for 30 minutes.
6. Unwashed sections from ammonium silver solution were immersed directly in the developer working solution for 1 minute.
7. Sections were immersed in 1% ammonium hydroxide solution for 1 minute to stop the silver reaction.
8. Sections were then, washed in distilled water for 1 minute (×3), before immersing in 5% sodium thiosulfate solution for 5 minutes.
9. Thereafter, sections were washed in distilled water for 1 minute (×3).
10. Sections were then dehydrated by:

95% alcohol for 3 minutes; and

100% alcohol, 2 minutes (×2).

8. Sections were cleared in xylene for 5 minutes (×2) before mounting with two drops of DPX (Dibutylphythalate-in-xylene).

Glial fibrillary acidic protein (GFAP) staining technique

Reagents and Solutions

Citrate Buffer (10mM Citric Acid, 0.05% Tween 20, pH 6.0):

Citric acid (anhydrous) ---------- 1.92 g

Distilled water ---------- 1000 ml

It was stirred to dissolve, and pH adjusted to 6.0 with 1N NaOH. Thereafter, 0.5 ml of Tween 20 was added and stirred properly.

Peroxidase Blocking Solution (3% H_2O_2 in PBS):

30% H_2O_2 ---------- 10 ml

1X PBS ---------- 90 ml

Anti-GFAP antibody (polyclonal to GFAP)

Host species ---------- Goat

Specificity reaction---------- Mouse, rats, human and zebrafish

Concentration used ---------- 4 µg/ml

Primary antibody dilution buffer

5%BSA

0.5% Triton X-100

0.05% sodium azide

0.01M PBS, pH 7.3

Dilution---------- 1:500

Secondary Antibody Dilution Buffer:

0.01M PBS, pH 7.2

0.05% Tween 20

To make 1000 ml of the buffer, 0.5 ml of Tween 20 was added to 1000 ml, 0.01M PBS, pH 7.2

Diaminobenzidine tetrahydrochloride (DAB) solution

3, 3 DAB---------- 0.1g in distilled water

10N HCl---------- 4 drops

The solution was stirred until DAB was completely dissolved to give brownish colour.

Procedure

1. Sections were deparafinized in xylene for 5 minutes (×2).
2. Sections were rehydrated in:

   100% alcohol for 3 minutes (×2);

   95% alcohol for 1 minutes (×2); and

   70% alcohol for 1 minutes (×2).
3. Protein cross-linkages, masking antigenic sites on the tissues were removed by heating the tissues in citrate buffer (pH 6) at 95 °C for 20 minutes (antigens retrieval).
4. Sections were then washed in PBS for 20 minutes (×2).
5. Endogenous peroxidase blocking was done using 3% H_2O_2 in PBS for 10 minutes, before washing with PBS (×2).
6. Sections were immerse in 5% bovine serum albumin (BSA) for 20 minutes
7. Anti GFAP primary antibody (1:500) in 5% BSA, 0.5% Triton X-100, and 0.01M PBS was incubated with the sections for 60 minutes at 37°C.
8. Sections were washed four times in 6 minutes with PBS.

9. Subsequently, a secondary biotinylated antibody (diluted in 0.01M PBS, 0.05% Tween 20) was incubated with the sections at room temperature for 45 minutes.
10. Sections were then washed 3 times in 5 minutes with PBS.
11. 3′3 diaminobenzidine tetrachloride (DAB) was incubated with the sections for 5 minutes.
12. Sections were rinsed with four changes of distilled water and counterstained with haematoxylin for 5 minutes.
13. Sections were rinsed in running tap water for 5 minutes.
14. Sections were then dehydrated by:

    95% alcohol for 3 minutes; and

    100% alcohol, 2 minutes (×2).

9. Samples were then cleared in 2 changes of xylene (10 dips each) before mounting with two drops of DPX (Dibutylphythalate-in-xylene).

5. Synaptophysin staining technique

Reagents and Solutions

Citrate Buffer (10 mM Citric Acid, 0.05% Tween 20, pH 6.0):

Citric acid (anhydrous) ----------	1.92 g
Distilled water ----------	1000 ml

The solution was stirred, while the pH was adjusted to 6.0 with 1N NaOH. Afterwards, 0.5 ml of Tween 20 was added to the solution and stirred properly.

Peroxidase Blocking Solution (3% H_2O_2 in PBS):

30% H_2O_2 ----------	10 ml
1X PBS ----------	90 ml

Primary antibody dilution buffer

5% BSA

0.5% Triton X-100

0.01M PBS, pH 7.3

3, 3´ Diaminobenzidine tetrahydrochloride (DAB)-peroxidase solution (pH 7.2)

1% DAB---------- 250µl

0.3% H_2O_2---------- 250µl

PBS ---------- 5ml

The solution was stirred until DAB was completely dissolved to give brownish colour.

Procedure

1. Sections were deparafinized in xylene for 5 minutes (×2).
2. Sections were rehydrated in:

   100% alcohol for 3 minutes (×2);

   95% alcohol for 1 minutes (×2);

   70% alcohol for 1 minutes (×2); and

   rinsed in distilled water for 3 minutes.
3. Protein cross-linkages, masking antigenic sites on the tissues were removed by heating the tissues in citrate buffer (pH 6) at 95 °C for 20 minutes (antigen retrieval).
4. Sections were then washed in PBS for 10 minutes (×2).
5. Endogenous peroxidase blocking was done using 3% H_2O_2 in PBS for 10 minutes, before washing with PBS (×2).
6. 5% of bovine serum albumin (BSA for 20 min) was used to reduce non-specific protein reactions.
7. The anti-synaptophysin antibody was diluted (1:1000; 5% BSA, 0.5% Triton X-100, and 0.01M PBS) before incubating with the sections at 4 °C overnight.

8. Sections were rinsed 3 times in 5 minutes with PBS before incubating in biotinylated goat antimouse (1:250; 5% BSA, 0.5% Triton X-100 and 0.01M) for 1 h at room temperature.
9. Sections were then, rinsed 4 times in 6 minutes with PBS.
10. Sections were exposed to 3′3′ DAB in 0.01% H_2O_2 for 10 minutes.
11. Sections were rinsed with four changes of distilled water and counterstained with haematoxylin for 5 minutes.
12. Sections were rinsed in running tap water for 5 minutes.
13. Sections were then, dehydrated by:

    95% alcohol for 2 minutes; and

    100% alcohol, 2 minutes (×2).
14. Samples were cleared in 2 changes of xylene (10 dips each) before mounting with two drops of DPX (Dibutylphythalate-in-xylene).

6. p53 staining techniques

Reagents and Solutions

Citrate Buffer (10mM Citric Acid, 0.05% Tween 20, pH 6.0):

Citric acid (anhydrous) ----------	1.92 g
Distilled water ----------	1000 ml

It was mixed to dissolve, while the pH was adjusted to 6.0 with 1N NaOH. After that, 0.5 ml of Tween 20 was added and mixed properly.

Peroxidase Blocking Solution (3% H_2O_2 in PBS):

30% H_2O_2 ----------	10 ml
1X PBS ----------	90 ml

Anti-P53 mouse monoclonal antibody

Primary antibody dilution buffer

1% BSA

0.5% Triton X-100

0.01M PBS, pH 7.3

Procedure

1. Sections were deparafinized in xylene for 5 minutes (×2).
2. Sections were rehydrated in:

   100% alcohol for 3 minutes (×2);

   95% alcohol for 1 minutes (×2);

   70% alcohol for 1 minutes (×2); and

   rinsed in distilled water for 3 minutes.
3. Protein cross-linkages, masking antigenic sites on the tissues were removed by heating the tissues in citrate buffer (pH 6) at 95 °C for 20 minutes (antigen retrieval).
4. Sections were then washed in PBS for 10 minutes (×2).
5. Endogenous peroxidase blocking was done using 3% H_2O_2 in PBS for 10 minutes, before washing with PBS (×2).
6. 5% of bovine serum albumin (BSA for 20 min) was used to reduce non-specific protein reactions.
7. Anti p53 antibody was diluted (1:200; in 1% BSA, 0.5% Triton X-100 and 0.01M) prior to incubating with sections at room temperature (1 h).
8. Sections were rinsed 2 times in 3 minutes in PBS before incubating in biotinylated secondary antibody for 30 minutes at room temperature.
9. Sections were then, rinsed 4 times in 6 minutes with PBS and, counterstained with Haematoxylin solution for 30 seconds.
10. Sections were then, dehydrated by:

    95% alcohol for 2 minutes; and

100% alcohol, 2 minutes (×2).

11. Samples were cleared in 2 changes of xylene (10 dips each) before mounting with two drops of DPX (Dibutylphythalate-in-xylene).

PUBLICATIONS

1. Nathaniel Amedu and Gabriel Omotoso (2020). Lead acetate- induced neurodegenerative changes in the dorsolateral prefrontal cortex of mice: the role of Vitexin. *Environmental Analysis Health and Toxicology,* 35(1), e2020001. Doi: 10.5620/eaht.e2020001
2. Nathaniel Amedu and Gabriel Omotoso (2020). Evaluating the role of vitexin on hematologic and oxidative stress markers in lead-induced toxicity in mice. *Toxicology and Environmental Health Sciences,* 12 (3), 257-263. Doi: 10.1007/s13530-020-00039-5
3. Nathaniel Amedu and Gabriel Omotoso (2020). Influence of Vitexin on ataxia- like condition initiated by Lead exposure in mice. *Toxicology and Environmental Health Sciences,* 12(4), 305-313. Doi: 10.1007/s13530-020-00041-x